



Controlling the structure and properties of toughened and reinforced isotactic polypropylene

Shi-Wei Wang

► To cite this version:

Shi-Wei Wang. Controlling the structure and properties of toughened and reinforced isotactic polypropylene. Food and Nutrition. Université de Lorraine, 2012. English. NNT : 2012LORR0231 . tel-01749412

HAL Id: tel-01749412

<https://hal.univ-lorraine.fr/tel-01749412>

Submitted on 29 Mar 2018

HAL is a multi-disciplinary open access archive for the deposit and dissemination of scientific research documents, whether they are published or not. The documents may come from teaching and research institutions in France or abroad, or from public or private research centers.

L'archive ouverte pluridisciplinaire **HAL**, est destinée au dépôt et à la diffusion de documents scientifiques de niveau recherche, publiés ou non, émanant des établissements d'enseignement et de recherche français ou étrangers, des laboratoires publics ou privés.



AVERTISSEMENT

Ce document est le fruit d'un long travail approuvé par le jury de soutenance et mis à disposition de l'ensemble de la communauté universitaire élargie.

Il est soumis à la propriété intellectuelle de l'auteur. Ceci implique une obligation de citation et de référencement lors de l'utilisation de ce document.

D'autre part, toute contrefaçon, plagiat, reproduction illicite encourt une poursuite pénale.

Contact : ddoc-theses-contact@univ-lorraine.fr

LIENS

Code de la Propriété Intellectuelle. articles L 122. 4

Code de la Propriété Intellectuelle. articles L 335.2- L 335.10

http://www.cfcopies.com/V2/leg/leg_droi.php

<http://www.culture.gouv.fr/culture/infos-pratiques/droits/protection.htm>



en co-tutelle avec l'Université de Sichuan

Ecole Nationale Supérieure des
Industries Chimiques
(ENSIC)

Ecole Doctorale : Ressources Procédés
Produits Environnement (RP2E)

Laboratoire Réactions et Génie des Procédés
(LRGP-CNRS UPR 3349)

**Controlling the structure and properties of toughened
and reinforced isotactic polypropylene**
**Contrôle des structures et des propriétés d'un
polypropylène isotactique.**

THESE

présentée en vue de l'obtention du

DOCTORAT DE L'INSTITUT NATIONAL POLYTECHNIQUE DE LORRAINE

Spécialité : Génie des Procédés et des Produits

par

Shi-Wei WANG

Soutenue le 12 avril 2012

Composition du jury:

Rapporteurs :	Michel BOUQUEY	Maître des Conférences à l'Université de Strasbourg, France
	Xiao-Bo LIU	Professeur à l'Université des Sciences et Technologie Electroniques, Chine
Examinateurs :	Guo-Hua HU	Professeur à l'Université de Lorraine et membre de l'IUF, France
	Ming-Bo YANG	Professeur à l'Université de Sichuan, Chine

TITRE

Contrôle des structures et des propriétés d'un polypropylène isotactique

RESUME

En tant que polymère de grande diffusion, les applications du polypropylène isotactique (PP) sont limitées par sa faible résistance au choc. D'après la relation structure – propriétés, sa résistance au choc peut être améliorée en contrôlant sa structure. Dans ces travaux, différents types d'agents nucléants ont été utilisés pour promouvoir la formation des cristaux de type bêta et de mélanges de deux PP de masses molaires différentes. Les propriétés mécaniques, le comportement à la rupture, et la morphologie cristalline ont été étudiés. Les influences du type et de la teneur en peroxyde et agent nucléant sur la morphologie cristalline et les propriétés mécaniques ont aussi été explorées. Un agent nucléant supporté sur des nanotubes de carbone multi-parois (MWCNT) a été utilisé pour modifier la structure cristalline du PP, ce qui a permis d'augmenter sa résistance au choc 7 fois comparée à celle du PP vierge et 3 fois comparée à celle du PP cristallisé en phase bêta. Cette importante augmentation en résistance au choc peut être attribuée à la formation des trans-cristaux de type bêta qui est favorisée par l'agent nucléant supporté sur les MWCNT.

MOTS-CLES

Polypropylène, agent nucléant, polypropylène à rhéologie contrôlée, résistance au choc.

TITLE

Controlling the structure and properties of toughened isotactic polypropylene

ABSTRACT

As a commodity polymer, the applications of isotactic polypropylene (PP) are limited by its low impact strength. Based on the structure-property relationship, its impact strength could be improved by controlling its structure. In this study, different kinds of nucleating agents were used to promote the formation of beta crystals of PP as well as mixtures of two PPs of different molar masses. The mechanical properties, fracture behaviour, and crystalline morphology were investigated. The effects of the type and content of the peroxide and nucleating agent on the crystalline structure and mechanical properties of the PP were also explored. A multi-walled carbon nanotube (MWCNT) supported nucleating agent was introduced to modify the crystalline structure of PP and the impact strength of the resulting PP was 7 times that of the pure PP and more than 3 times that of β nucleated PP. The large increase in the impact strength was attributed to the formation of beta transcrystalline morphology which was promoted by the MWCT supported nucleating agent.

KEY WORDS

Polypropylene, nucleating agent, controlled rheology polypropylene, impact resistance.

Table of contents

Table of contents.....	I
Chapter 1 Introduction.....	1
1.1 Motivation and objectives	1
1.2 overview of thesis.....	3
Chapter 2 Experimental	6
2.1 Materials	6
2.1.1 Materials for chapter 3.....	6
2.1.2 Materials for chapter 4.....	6
2.1.3 Materials for chapter 5.....	6
2.1.4 Materials for chapter 6.....	7
2.1.5 Materials for chapter 7.....	7
2.1.6 Materials for chapter 8.....	7
2.2 Sample preparation	8
2.2.1 Preparations of samples for chapter 3.....	8
2.2.2 Preparations of samples for chapter 4.....	9
2.2.3 Preparations of samples for chapter 5.....	9
2.2.4 Preparations of samples for chapter 6.....	9
2.2.5 Preparations of samples for chapter 7.....	10
2.2.6 Preparations of samples for chapter 8.....	11
2.3 characterization	12
2.3.1 Differential Scanning Calorimetry (DSC) analysis.....	12
2.3.2 Wide-angle X-ray diffraction (WAXD) analysis	13
2.3.3 Mechanical Properties analysis	13
2.3.4 MFR analysis	13
2.3.5 Capillary rheology analysis	13
2.3.6 Dynamic rheological analysis (DRA).....	13
2.3.7 X-ray photoelectron spectroscopy (XPS).....	14
2.3.8 Fourier-transform infrared spectroscopy analysis (FTIR).....	14
2.3.9 Scanning electron microscopy analysis (SEM).....	14
2.3.10 polarized light microscopy analysis (PLM)	14
2.3.11 Dynamic mechanical thermal analysis	15
Chapter 3 Effect of alpha and beta nucleating agents on the fracture behavior of polypropylene-co-ethylene (CPP)	16
3.1 Introduction	16
3.2 Results and discussion.....	18
3.2.1 Load-displacement curve	18
3.2.2 Fracture parameters.....	19
3.3 Conclusions	26
3.4 References.....	27
Chapter 4 Structure and properties of peroxide induced controlled rheology polypropylene	29
4.1. Introduction	29
4.2. Results and discussion.....	30

4.2.1 Effect of different peroxides on the capillary rheology properties of peroxides induced polypropylenes	30
4.2.2 Effect of different peroxides on the MFR and mechanical properties of peroxides induced polypropylenes	32
4.2.3 Effect of different peroxides on the crystallize and dynamic rheology properties of peroxides induced polypropylenes.....	33
4.3. Conclusions	36
4.4 References.....	37
Chapter 5 Crystalline Morphology of β Nucleated Controlled Rheology Polypropylene	38
5.1. Introduction	38
5.2. Results and discussion.....	39
5.2.1 Effect of NAs on the Crystalline Morphology of CRPPs	39
5.2.2 Effect of DCP and TMB-5 content on the crystalline morphology of CRPPs.....	42
5.3. Conclusions	47
5.4 References.....	47
Chapter 6 The enhanced nucleating ability of carbon nanotube supported β nucleating agent in isotactic polypropylene	50
6.1. Introduction	50
6.2. Results and Discussion.....	53
6.2.1 Surface analysis	53
6.2.2 Mechanical properties.....	54
6.2.3 Morphology observation	55
6.2.4 Melting and crystallization behaviours	57
6.3. Conclusions	59
6.4 References.....	59
Chapter 7 Superior mechanical properties in carbon nanotube modified polypropylene composites through formation of a beta transcrystalline structure.....	61
7.1. Introduction	61
7.2 Results and discussion.....	65
7.2.1 Crystalline morphology development in micro-composites.....	65
7.2.2 Crystalline structure validation.	67
7.2.3 Crystalline morphology in injection samples.....	69
7.2.4 Relationship between crystalline morphology and mechanical properties.....	71
7.3 Conclusion	71
7.4 References.....	71
Chapter 8 Effect of filler on the structure and properties of polypropylene blends	73
8.1 Introduction	73
8.2 Results and discussions	73
8.2.1. The selection of the isotactic polypropylenes proportion.....	73
8.2.2. The selection of processing parameters	76
8.2.3. The structure and properties of beta nucleating agent modified polypropylene blends .	80
8.2.4. The structure and properties of carbon nanotube modified polypropylene blends	84
8.2.5. The structure and properties of beta nucleating agent supported carbon nanotube modified polypropylene blends	89

8.3 Conclusion	93
8.4 References.....	94
Chapter 9 conclusion.....	95
Acknowledgements.....	98
List of articles published during the thesis	99

Chapter 1 Introduction

1.1 Motivation and objectives

Polypropylene is one of the most important general used plastic materials. It is polymerized by propylene monomer and has many advantages such as a light weight, heat resistance, and good corrosion resistance. It was been widely used in many fields especially the motorcar, construction and home applications. However, compared with other materials, polypropylene also have some weak points, such as the impact resistance and high melt viscoelasticity, which will limit its applications and processing.

For polypropylene, the most urgent work needed to be addressed is its low impact resistance, which significantly limits its applications in structural and engineering material fields. Based on the structure and property relationships, it is necessary to modify the structure of polypropylene to increase its impact resistance and enlarge its application. Like other crystalline polymers, the crystallization process of polypropylene also contains two parts, which are the nucleation process and the growth of the nuclei. In the first process, the molecular chain of polymers regular stack into thermal stable and large enough nuclei, then the nuclei growth into a spherulite stage and finally start the growth process. The way of nucleation is divided into two parts consider of the existence of heterogeneous nuclei, homogeneous nucleation and heterogeneous nucleation. Homogeneous nucleation refers to the process of the spontaneous formation of nuclei for the PP melt under the decrease temperature. In such a process, the number of the nuclei is very small, and with a slow crystallization process, so the final crystal size is very large and the crystallization efficiency is very low. In contrary, the existence of solid impurities in the polypropylene melt act as the starting point in heterogeneous nucleation, and it can adsorbs the polypropylene molecules on its surface to form the nuclei. Obviously, the heterogeneous process provide more nuclei in the crystallization process, and speed up the crystallization rate as well as reduce the spherulite size, improving the crystallinity and crystallization temperature in case of constant spherulite growth rate, and finally give many new performance to polypropylene material. Therefore, the heterogeneous nucleation is the theoretical basis of the polypropylene crystallization modification.

There are different levels of polypropylene structure since the existence of asymmetric carbon atoms in the main chain of polypropylene. So, unlike the crystallization process of inorganic crystals, only part of the polymer molecular can be stack into the crystal cell.

While the crystalline morphology can be changed as a result of the change in molecular conformation or the accumulation, and form several different crystal type, the so called homogeneous polycrystalline phenomenon. Addition of nucleation agent in polypropylene melt can get the fine grain spherulites structure, increase the number of crystal nuclei within the system, make ceramics in number and decrease in the number of spherulites, and finally improve the physical and mechanical properties of polypropylene. Isotactic polypropylene has many crystal structures and the most common one is the stable alpha phase, it can be formed under the normal processing condition. Alpha crystalline morphology has a coarse grain between the spherulites, and the grains will makes the cracks caused by external force developed along it during the deformation of the materials, finally causes the brittle fracture of the materials. The internal arrangement of beta form crystal is evacuate and the interface between spherulites is much fuzzy than alpha form crystal, so it gives a good impact absorption for the deformation of polypropylene matrix.

Generally, there are four methods to induce the beta crystal in iPP matrix: (1) select the appropriate melting and crystallization temperature; (2) select the temperature trandient method; (3) select the shear direction; (4) adding beta nucleating agent. Among them, using beta nucleating agent gives a high content of beta crystal and has been considered to be the best method

Rheological property gives a significant effect on the polymer material processing. As is well known that polypropylene has good processing and performance, while it has a high molecular weight and wide molecular weight distribution because of the traditional Zigeler-Natta catalyst used in the synthesis process, and result in the high viscoelastic during processing, which will limits its processing.

There are two methods to modify the rheological properties of polypropylene. One is the in suit modification, which refers to the modification during the synthesis process; the other is the after suit modification, which refers to the blending of two different molecular weight polymers or introduce the peroxide to promoting the degradation of synthetic polypropylene. The later one has many advantages such as the easy performing and low cost and is wildly used in the control of polypropylene molecular weight and distribution. The final product obtained by this way is called controlled rheology polypropylene.

This work is mainly deal with the toughness of polypropylene, by way of introducing the beta nucleating agent into the iPP matrix. Then the type of nucleating agent was changed and the matrix was modified by way of degradation and melting blending. To

avoid the reduction of yield strength of iPP as a result of the beta crystal modification; a new method was used that is by supporting nucleating agent on the fiber surface. By this method, the toughness of iPP matrix improved more than seven times compared with the pure iPP, while the stiffness lose not so much. The mechanism of the increase of mechanical properties was also explored.

1.2 overview of thesis

A brief overview of this thesis is as follow.

Chapter 2 describes the main experiments in this study

In Chapter 3, a new method called the essential work of fracture (EWF) method was introduced to the polypropylene matrix to evaluate its fracture behaviors. The specific essential work of fracture values of CPPs incorporated with α NA of different amount were all lower than that of pure CPP, while the specific non-essential work of fracture was the highest at relative low α NA loading (0.1wt%), and then decreased with further increasing amount of α NA. Similar trend of variation was observed with increasing amount of β NA in CPP and it was found that the variation of K_β for β NA nucleated CPP versus NA content accorded well with the essential work of fracture versus NA content, which indicated that the addition of β NA could lead to effectively increased β crystal content and consequently improved fracture resistance of CPP

In Chapter 4, the structure and properties of controlled rheology polypropylene were explored by way of using three different peroxides, namely 2,5-dimethyl-2,5-di(2-ethylhexanoylperoxy) hexane (DMDEHPH), Dicumyl peroxide (DCP) and Benzoyl peroxide (BPO). The results indicated that the CRPP prepared using DMDEHPH exhibited a significant increase in viscosity with shear rate decreasing, especially in the low shear rate region and the shear stress was also higher than DCP and BPO induced iPP in the low shear rate range. The notched impact strength and the tensile elastic modulus of DMDEHPH induced CRPP were also higher than the other two peroxides induced CRPP. The melting and crystallization properties, dynamic rheological properties were also studied.

The main point in Chapter 5 is a series of beta nucleated controlled rheology polypropylenes (CRPPs), which were prepared through reactive extrusion of polypropylene (PP) and dicumyl peroxide (DCP). Differential scanning calorimetry (DSC) and wide-angle x-ray diffraction (WAXD) were used to evaluate the ability of three different kinds of

nucleating agents (NAs), E3B, WBG-II and TMB-5, to induce β -crystals in the CRPPs. The results indicate that TMB-5 shows the best nucleation effect and can induce the highest relative content of β -crystals. For the effect of DCP content on the β crystal of CRPP, it was found that with 0.3wt% TMB-5 incorporated, the critical DCP content was emerged at 0.1wt%. For the effect of NA content on the β crystal of CRPPs, the total β crystallinity index and relative β crystal content were found to reach a maximum value at a content of 0.5 wt% β NA, with a 0.1wt% DCP content incorporated.

The effect of the fiber supported nucleating agent on the mechanical properties and morphology of isotactic polypropylene were investigated in Chapter 6. The fiber and nucleating agent refers to the multi-wall carbon nanotubes and calcium pimelate respectively. The composites of isotactic polypropylene and multi-wall carbon nanotube supported β nucleating agent exhibited 7 times over that of pure isotactic polypropylene and more than 3 times over that of β nucleated isotactic polypropylene in impact toughness. Results obtained from SEM, differential scanning calorimetry and wide-angle X-ray diffraction verified the enhanced nucleating ability of the multi-wall carbon nanotube supported β nucleating agent, which greatly improved the impact toughness without significantly deteriorating the strength and stiffness of the polypropylene composites.

In Chapter 7, the mechanism of superior impact resistance of fiber supported beta nucleating agent modified isotactic polypropylene was explored. That is the formation of beta transcrystalline morphology in the interfacial region of isotactic polypropylene/fiber composites. The result is verified in beta nucleating agent supported single fiber filled isotactic polypropylene micro-composites by the polarized light microscopy. Also, in the beta nucleating agent supported carbon nanotube modified isotactic polypropylene injection molded samples, a certain number of interphase beta transcrystallinity formed in the adjacent region of carbon nanotubes. Further more, the interfacial beta transcrystalline morphology is related to the mechanical properties of the isotactic polypropylene injection molded samples, and gives a convectively evidence for the seven times improvement of the sample's impact resistance. This work gives a new perspective for the toughening of polymer and polymer composites.

In chapter 8, effect of filler (such as β NA, carbon nanotube, and β NA supported carbon nanotube) on the structure and properties of polypropylene blends was explored. Based on the melting and cooling behaviours, dynamic mechanical and rheological properties analysis, the suitable aproportion for the iPP blends is 50wt%:50wt%, the

suitable processing parameters is 200°C and the screw speed is 200rpm. The beta nucleating agent can successfully induce beta crystal in modified iPP blends and the turning point of the properties appears at the content of 0.5wt%. Carbon nanotube mainly induce alpha crystal in modified iPP blends, and for the properties of carbon nanotube modified iPP blends, there is no turning point because of its dominant alpha crystalline morphology. The β NA supported carbon nanotube shows good induction ability than the single β NA or single carbon nanotube, there is also a turning point exist at the content of 0.5wt%.

Chapter 2 Experimental

2.1 Materials

2.1.1 Materials for chapter 3

The CPP (K8303) , was a granular material of propylene-block-ethylene copolymer produced by Beijing Yanshan Petrochemical Co, Ltd (PR China), with 17.8 mole percent (mol %) of ethylene and a melt flow rate of 1.39g/10 min (measured at 230 °C and 2.16 kg). Two kinds of NAs were used. α NA Millad 3988, a kind of dibenzylidene sorbitol derivatives, was produced by Milliken Chemical Europe NV. β NA WBG- II , a kind of rare earth organic complexes, was produced by Guangdong Winner Functional Materials Co, Ltd (PR China)

2.1.2 Materials for chapter 4

The iPP with a melt flow rate (MFR) of 2.16 g/10 min (ASTM D1238, 230 °C, 2.16 kg), trademark F401, was purchased from LanZhou petroleum chemical corporation, P. R. China. The 2, 5-dimethyl-2, 5-di (2-ethylhexanoylperoxy) hexane (DMDEHPH) was purchased from Jiangsu Qiangsheng chemical Corporation, P. R. China. Dicumyl peroxide (DCP) was purchased from China National Medicine (Group) Shanghai Chemical Reagent Corporation, P. R. China. Benzoyl peroxide (BOP) was from Chengdu Kelong chemical reagent Company, P. R. China. The half time of the three kinds of peroxides is different, being 17min, 9min and 0.2min, respectively, for DMDEHPH, DCP and BPO at 150 °C. This means that the activity sequence of peroxides is BPO>DCP >DMDEHPH.

2.1.3 Materials for chapter 5

The polypropylene used in this chapter was isotactic PP (F401), a homopolymer resin with a melt flow rate of 2.16 g/10 min (ASTM D1238, 230 °C, and 2.16 kg) from LanGang Petroleum Chemical Co, Ltd (PR China). Dicumyl peroxide (DCP) was obtained from China National Medicine (Group) Shanghai Chemical Reagent Corporation, whose half-life time is about 0.25min at 200 °C. Three types of β NAs, E3B, WBG-II and TMB-5, were

supplied by Jiangsu Gaoyou Auxiliary Agent Factory (PR China), Guangdong Winner Functional Materials Co (PR China), and Shanxi Provincial Institute of Chemical Industry (PR China), respectively. Structurally, E3B is a commercial red pigment, WBG-II being a rare earth organic complex, and TMB-5 a kind of amidating agent.

2.1.4 Materials for chapter 6

A commercial grade iPP, T30S, with a melt flow rate of MFR=2.3g/10min (ASTM D1238, 2300C, and 2.16kg load) from LanZhou petroleum Chemical Co, Ltd. (PR China), was used in the chapter. The MWCNTs with a diameter of about 8nm and the length of about 10-30 μ m, synthesized from methane by way of catalytically chemical vapor deposition, was supplied by Chengdu Institute of Organic Chemistry, Chinese Academy of Science. The received MWCNTs were chemically treated and hydroxy groups were attached to the tube wall. The β NA was a compound prepared with pimelic acid and calcium stearate of the same molar ratio, which assured that the calcium stearate can only react with one of the carboxyl group of pimelic acid.

2.1.5 Materials for chapter 7

The commercial grade iPP, T30S, with a melt flow rate of MFR=2.3g/10min (ASTM D1238, 230 $^{\circ}$ C, and 2.16Kg load) from LanZhou petroleum Chemical Co, Ltd. (PR China), was used in the chapter. A short cut ribbon-like polyacrylonitrile-based CF, T300, purchased from NanTong SuTong Carbon Fiber Corporation (PR China), was used in the micro-composite preparation. The Multi-wall Carbon nanotube (MWCNT) with a diameter of about 8nm and the length of about 10-30 μ m, synthesized from methane by way of catalytically chemical vapor deposition, was supplied by Chengdu Institute of Organic Chemistry, Chinese Academy of Science. The received MWCNTs were chemically treated and 5.58wt% of hydroxy groups attached to the tube wall.

2.1.6 Materials for chapter 8

The two polypropylenes 3060 (MFI 3 g/10 min) and 11079 (MFI 60 g/10 min) with different molecular weight and molecular weight distribution used in this chapter were kindly supplied by TOTAL petrochemicals and made in E.U. The Multi-wall Carbon nanotube (MWCNT) was supplied by Chengdu Institute of Organic Chemistry, Chinese

Academy of Science. The β NA was a compound prepared with pimelic acid and calcium stearate of the same molar ratio.

2.2 Sample preparation

2.2.1 Preparations of samples for chapter 3

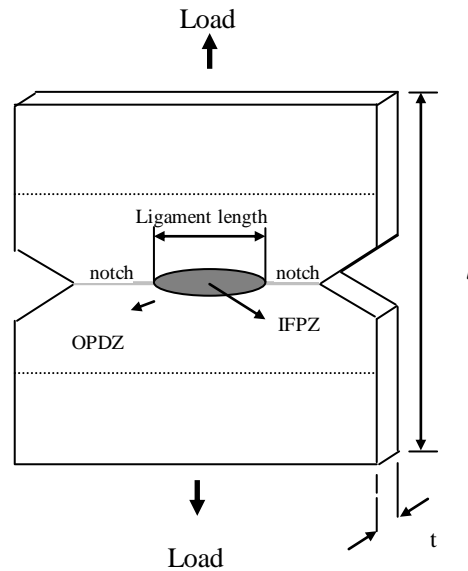


Figure. 2-1 DDENT sample used for EWF test

To compare the effect of α and β NAs on the fracture performance of nucleated CPP, the weight percentage of both NAs was set as 0, 0.1wt%, 0.3 wt % and 0.5 wt %. The CPP resin and NAs at preselected mass ratio was melting blended in an SHJ-20 co-rotating twin-screw extruder made by Nanjing Giant Electromechanical Co. Ltd (PR China). The barrel temperature was set in the range of 180-225⁰C. The extrudate was pelletized after extrusion and, after drying to remove the attached moisture during extrusion and pelletizing, the pellets were injected into both dumb-bell and rectangular shaped samples of 4 mm thickness on a PS40E5ASE (Nissei) precise injection molding machine. The temperature profile was 180-225⁰C from the feeding zone to the nozzle, and both the injection and holding pressures were 50.0 MPa. Then the rectangle samples were compression-molded into sheets of about 0.5 mm thickness at 200⁰C and 10 MPa. The DDENT specimens (length×width=100×35 mm) shown in Fig.2.1 were cut from the compression-molded sheets. The sharp pre-cracks on both sides of the specimens were made perpendicularly to the tensile direction with a fresh razor blade. The ligament lengths and the thickness were measured before the test using a microscope and a vernier caliper, respectively.

2.2.2 Preparations of samples for chapter 4

iPP and peroxide were melting mixed in a twin screw extruder (SHJ-20, Nanjing Giant Company, P. R. China) with a peroxide content of 0.03wt%. The temperatures were set at 170 to 210 °C from the hopper to die. The extruded threads were pelletized and then dried to remove the attached moisture at room temperature for 24h. The dried pellets were then injection molded into a dumbbell-shaped tensile specimens, using an injection molding machine (PS40E5ASE, Nissei, Japan) with a temperature profile of 180 to 225 °C from the hopper to nozzle. The rectangle specimens, with the thickness of about 0.5mm, were compression molded at the temperature of 200 °C and the pressure of 10Mpa.

2.2.3 Preparations of samples for chapter 5

Firstly, for the evaluation of the effectiveness in inducing β crystals of different NAs, the β NAs were mixed with PP pellets at a fixed content of 0.3wt% with 0.1wt% DCP incorporated. The reactive extrusion of the mixtures was performed on an SJ-20AX25 single-screw extruder with a temperature profile of 180 to 230 °C. The extruded threads were pelletized and then dried to remove the attached moisture at room temperature. Then the dried pellets were injected into a dumbbell-shaped mold, using an injection molding machine (PS40E5ASE, Nissei, Japan) with a temperature profile of 180 to 225 °C from the hopper to die.

For the evaluation of the effect of DCP and NA content on the crystalline morphology of CRPPs, the reactive extrusion of NA nucleated CRPPs were carried out on the same extruder. Different grades of CRPPs were prepared under the same temperature profile (180 to 230 °C). The DCP contents were set as 0.05wt%, 0.1wt%, 0.15wt%, 0.2wt% and the NA contents were set as 0.1wt%, 0.3wt%, 0.5wt%, 0.7wt%. DCP, NA and PP were premixed with set proportions and filled into the hopper at the same time. The extruded thread was pelletized and dried, and the obtained pellets were then injection molded using the same injection molding machine with a temperature profile of 180 to 225 °C from the hopper to die.

2.2.4 Preparations of samples for chapter 6

The β NA and MWCNTs were first dispersed in an ethanol suspension using a VCF-1500 ultrasonic irradiation instrument (Sonic & Materials, Inc., USA). Then the

chemical supporting process of β NA onto MWCNT surface was performed in a three necked bottle at about 80 °C for 1h with a stirring rate of 1000 r/min, followed by filtering, washing and drying. Some of the final powder was taken to perform the surface analysis.

To achieve a good dispersion of β NA, MWCNTs and MWCNT supported β NA in the matrix iPP, a two-step process was employed to prepare the materials. Namely, master batches were firstly prepared through melt compounding of β NA, MWCNT and MWCNT supported β NA with iPP resin in an internal mixer at a barrel temperature of 200 °C and an apparent shear rate of 30r/min for 5min. Secondly, all the master batches were melt compounded with iPP resins in an SHJ-20 co-rotating twin-screw extruder with a screw diameter of 25 mm, a length/diameter ratio of 23, and a temperature profile of 190, 210, 230, and 225 °C from the feeding zone to the die. The extrudates were then pelletized. The pellets were dried and injection-molded into dumb-bell tensile samples and impact samples on a PS40E5ASE precise injection-molding machine, with a temperature profile of 190, 210, 230, and 225 °C from the feeding zone to the nozzle. Both the injection pressure and the holding pressure were 37.4 MPa. The resultant samples, used for testing and characterization, were named as Sample P (pure iPP), Sample C (MWCNT filled iPP), Sample N (β NA nucleated iPP), Sample 1, 3 and 5 (MWCNT supported β NA filled iPP with different filling content). The detailed compositions of the samples were listed in Table 2.1.

Table.2.1 The composition used for preparation of iPP (Sample P), iPP/MWCNTs (Sample C), β NA nucleated iPP (Sample N) and MWCNT supported β NA modified iPP composites (Sample 1, 3, 5) samples.

Sample	Ingredients	MWCNTs (wt.-%)	β NA (wt.-%)	iPP(wt.-%)
P	iPP	-	-	100
C	iPP/MWCNTs	0.10	-	99.9
N	iPP/ β NA	-	0.25	99.75
1	iPP/ MWCNT supported β NA	0.1	0.25	99.65
3	iPP/ MWCNT supported β NA	0.3	0.75	98.95
5	iPP/ MWCNT supported β NA	0.5	1.25	98.25

2.2.5 Preparations of samples for chapter 7

The compound beta nucleating agent used in this work was prepared according to the procedure proposed before. The iPP/single fiber micro-composites were prepared as follows. First of all, the single carbon fiber was supported by beta nucleating agent

according to our previous work in 2.2.4. A single beta nucleating agent supported carbon fiber was placed between two pieces of iPP sheets on a glass slide. Then the glass slide was fixed on the hot-stage, and covered by another glass slide which prevents the molten iPP from adhering to the upper plate of the hot-stage. Using the heat-controlle, the temperature was first raised up to 200 °C over a period of 3 min to erase the previous thermal history of the sample. When the iPP melted, it surrounded the whole portion of the fiber located under the upper slide. After that it was cooled to the room temperature, the micro-composites were successfully prepared. The beta nucleating agent supported MWCNT modified iPP samples were prepared using the same procedure as described in 2.2.4.

2.2.6 Preparations of samples for chapter 8

Table.2.2 The different proportion of two iPP samples.

Samples	A	B	Notes
1	100	0	The number shows the weight percent of single iPP in the two iPP blends.
2	90	10	
3	70	30	
4	50	50	
5	30	70	
6	10	90	
7	0	100	

Table.2.3 The processing parameters used in the experiment.of different iPP blends.

No.	Parameter	Extruded temperature (°C)	Screw speed (r/min)
1		180	50
2		180	60
3		180	70
4		200	50
5		200	60
6		200	70
7		220	50
8		220	60
9		220	70

For our research, the samples with different proportion are listed in Table 1. Sample A and B have the same molecular weight distribution. A stands for the high molecule weight isotactic polypropylene 3060 (MFI 3 g/10 min), B stands for the low molecule weight isotactic polypropylene 11079 (MFI 60 g/10 min). First of all, all the samples were extruded by the mini extruder, and then injected into the mould. The parameters were set as

follow according to the orthogonal design.

Table.2.4 The different content of beta nucleating agent modified iPP samples.

Sample	iPP	Beta nucleating agent	Notes
B1	99.9wt%	0.1wt%	The beta nucleating agent is a compound of pimelic acid and calcium stearate
B2	99.7wt%	0.3wt%	
B3	99.5wt%	0.5wt%	
B4	99.3wt%	0.7wt%	

Table.2.5 The different content of carbon nanotubes modified iPP samples.

Sample	iPP	carbon nanotubes	Notes
C1	99.9wt%	0.1wt%	The carbon nanotube is a mult walled carbon nanotube made by Chemical vapor deposition method.
C2	99.7wt%	0.3wt%	
C3	99.5wt%	0.5wt%	
C4	99.3wt%	0.7wt%	

Table.2.6 The different content of beta nucleating agent supported carbon nanotube modified iPP samples.

Sample	iPP	beta nucleating agent supported carbon nanotube	Notes
S1	99.9wt%	0.1wt%	The β NA supported carbon nanotube was made according to our patent (CN. 200910059258.8)
S2	99.7wt%	0.3wt%	
S3	99.5wt%	0.5wt%	
S4	99.3wt%	0.7wt%	

2.3 characterization

2.3.1 Differential Scanning Calorimetry (DSC) analysis

The DSC test was performed on a TA Q20 differential scanning calorimeter (TA, America) in a nitrogen atmosphere. The calibration of the temperature and heat flow scales at the same heating rate was performed with indium. For the determination of the beta nucleating efficiency and selectivity of the beta-nucleating system used, the sample were quickly heated up to 200 °C and held for 5min prior to crystallization to erase effects of the thermal-mechanical prehistory. Then, the samples were cooled from 200 to 100 °C at a rate of 10 °C /min to obtain the crystallization behaviours. After that, the samples were heated up to 200 °C from 100 °C at a rate of 10 °C /min to obtain the melting behaviours. The samples for DSC tests were taken from the core layer of the injection molded bars.

2.3.2 Wide-angle X-ray diffraction (WAXD) analysis

WAXD measurement was carried out with a D/max-rA X-ray diffractometer at room temperature. The CuK α (wave length=1.542nm) irradiation source was operated at 40 kV and 100 mA. Patterns were recorded by monitoring diffractions from 3 to 50°, and the scanning speed was 3°/min. The samples for WAXD tests were taken from the central part of the injection molded bars.

2.3.3 Mechanical Properties analysis

The notched impact strength was tested on a UJ-40 Izod impact test instrument (Hebei Chengde Material Test Factory, China) according to ASTM D256. Tension of the DDENT specimens was performed on an Instron electrical universal testing machine series IX at 25 °C, with a crosshead speed of 5 mm/min. The load–displacement curves were recorded and the absorbed energy until failure was calculated by computer integration of the loading curves. The tensile test was performed on an AGS-J universal material test machine (Shimadzu Instrument, Japan) according to ASTM D638-82a. The crosshead speed was 50mm/min. The flexural test was performed on an AGS-J universal material test machine (Shimadzu Instrument, Japan) according to ASTM D790. At least five samples were used for each measurement and the average results were reported

2.3.4 MFR analysis

The melt flow rate (MFR) test was performed on an XNR-400 melt flow rate instrument (Chengde test machine factory, P. R. China) according to ASTM D-1238.

2.3.5 Capillary rheology analysis

The capillary rheology test was performed on a Rosand RH7D high pressure capillary rheometer (Malvern instrument manufactory Corporation, UK). Each test was performed at a temperature of 200 °C and a L/D of 16:1, using about 20g dried pellets.

2.3.6 Dynamic rheological analysis (DRA)

The dynamic rheological test was performed on an ARES4400 Advanced Rheology Expanded instrument (TA Corporation, America) at a temperature of 200 °C. The parallel

plates with a diameter of 25mm and a gap height of 2 mm were used for the multi-frequency sweeping. The test specimens were cut from the sheet prepared by compression moulding at 200 °C. The frequency range was 0.025 to 100 rad/s, and the maximum strain was fixed at 5%. These conditions were used to assure that the test was in the linear visco-elastic region. For the temperature sweep, the range was set as 100-200 °C.

2.3.7 X-ray photoelectron spectroscopy (XPS)

The surface analysis of MWCNTs and MWCNT supported β NA were performed on an XSAM800 (Kratos) X-ray photoelectron spectrometer with a base pressure of about 2×10^{-7} Pa. The XPS spectrometer was operated in the FAT (fixed analyzer transmission) mode using Mg K α 1,2 as the X-ray radiation source. The spectrometer energy scale was calibrated using copper plate according to the ASTM E902-88. The C 1s binding energy of the graphite peak was fixed at 284.8eV for the calibration purposes.

2.3.8 Fourier-transform infrared spectroscopy analysis (FTIR)

The samples for FTIR test were MWCNTs and MWCNT supported β NA. The FTIR spectra were recorded from 500 to 4000cm⁻¹ by a 560 FTIR Spectrometer (Nicolet, America)

2.3.9 Scanning electron microscopy analysis (SEM)

For morphology observation, the injection molded samples were fractured in liquid nitrogen after 30-minute immergence. Then the fractured surfaces were sputtered with gold and observed in a JEOL JSM-5900LV SEM instrument, using an acceleration voltage of 20kV.

2.3.10 polarized light microscopy analysis (PLM)

The morphology of the beta nucleating agent chemically supported single carbon fiber filled iPP micro-composites were investigated by a Leica DMIP polarized light microscopy (PLM) equipped with a Linkam THMS 600 hot stage. The micro-composite was heated to 200 °C over a period of 5 min to erase the previous thermal history, followed by a rapid cooling (10 °C /min) to 125 °C, and then isothermally crystallized for 30 min at 125 °C.

2.3.11 Dynamic mechanical thermal analysis

Before the DMA-measurements, the samples were cooled down to the pre-selected temperature in the measurement chamber. All measurements were carried out with a constant strain of 1% and the temperature studied ranged from -60°C to 150°C under a heating rate of $3^{\circ}\text{C}/\text{min}$. In order to measure the storage modulus, loss modulus, loss factor and T_g of the nanocomposites, the measurements were performed at fixed frequency of 10Hz. For each composition, at least two samples were tested and the average values were discussed. The samples for DMTA tests were compression molded at the temperature of 200°C and the pressure of 10MPa.

Chapter 3 Effect of alpha and beta nucleating agents on the fracture behavior of polypropylene-co-ethylene (CPP)

3.1 Introduction

Polypropylene-co-ethylene (CPP) is a versatile semi-crystalline polymer used in a wide variety of applications. The interrelation between structures, especially the crystalline structures, and mechanical behavior of CPP as well as its blends or composites, has been reported in many literatures^[1-9]. The crystallization process of polymer includes two stages, that is, nucleation and crystal growth. Nucleation involves the orientation of the loose coiled polymer chains into proper conformation, while in the process of crystal growth, polymer chains grow on the nuclei in a three-dimensional pattern and in most case, form a spherical crystal cluster which is called a spherulite. Nucleation in polymers may be homogeneous or heterogeneous. Homogeneous nucleation occurs at high degree of super-cooling, while heterogeneous nucleation occurs at relatively low degree of super-cooling and often with the addition of a foreign body called nucleating agents (NAs) which reduces the free energy barrier for nucleation^[10]. It is well known that NA can increase the number of crystallization sites and reduce the spherulite size. Many articles have reported the enhanced physical properties of semi-crystalline polymers such as impact strength and surface gloss when the crystallites size becomes smaller as a result of NA addition.

The essential work of fracture (EWF) method has gained great interest in recent years for its special applicability in studying the fracture performance of ductile polymer products, especially for sheets and films^[11-19]. The EWF concept was first proposed by Broberg^[20] and then developed by Cotterell^[21-23], Mai^[22-27], Reddel^[21] and Karger-Kocsis^[28-35] et al. According to the EWF theory^[22-35], the total energy required to fracture a pre-cracked specimen can be partitioned into the essential work of fracture, W_e and the non-essential work of fracture, W_p . W_e is a surface energy dissipated in the inner fracture process zone (IFPZ), and W_p is a volume energy dissipated in the outer plastic deformation zone (OPDZ). The Deep Double Edge-Notched Tension (DDENT) sample used for EWF tests to show the different energy dissipation zones is presented in Fig. 2.1. For a given thickness, W_e is proportional to the ligament length, l , and W_p is proportional to l^2 . Thus the fracture energy

can be written as:

$$W_f = w_e l t + \beta w_p l^2 t \quad (1)$$

$$w_f = W_f / l t = w_e + \beta w_p l \quad (2)$$

Where w_f is the special total work of fracture, w_e and w_p being the specific essential work of fracture and specific non-essential work of fracture, respectively, l the ligament length, t the specimen thickness and β the shape factor associated with the plastic zone. According to Eq. (2), w_e and βw_p can be obtained from the intercept and slope of the regression line to zero ligaments, respectively.

In order to find out the energy distribution during the fracture process, a method of partition between the specific work of fracture for yielding and for necking and subsequent fracture^[36] is also employed in the present paper, making the peak of the load-displacement curves as the cut-off point, as shown in Fig .3.1. As the composed terms were under plane stress conditions, Eq. (1) can be rewritten as:

$$w_f = w_y + w_n \quad (3)$$

$$w_y = w_{e,y} + \beta' w_{p,y} l \quad (4)$$

$$w_n = w_{e,n} + \beta'' w_{p,n} l \quad (5)$$

where $w_{e,y}$ and $w_{e,n}$, are the yielding and the necking and subsequent fracture related parts of the specific essential work of fracture, respectively; $\beta' w_{p,y}$ and $\beta'' w_{p,n}$, are the yielding and the necking and subsequent fracture components of the non-specific essential work of fracture, respectively.

Till now, EWF method has been successfully used to characterize the fracture properties of polyolefin as well as their blends and composites^[2, 4, 6, 8, 9, 12, 13]. In this paper, we focus on the effect of α and β NAs and their concentration on the fracture properties of CPP. The EWF parameters in the stage of yielding and sequent stage of necking and tearing are also measured to analyze the distribution of fracture energy of nucleated PP.

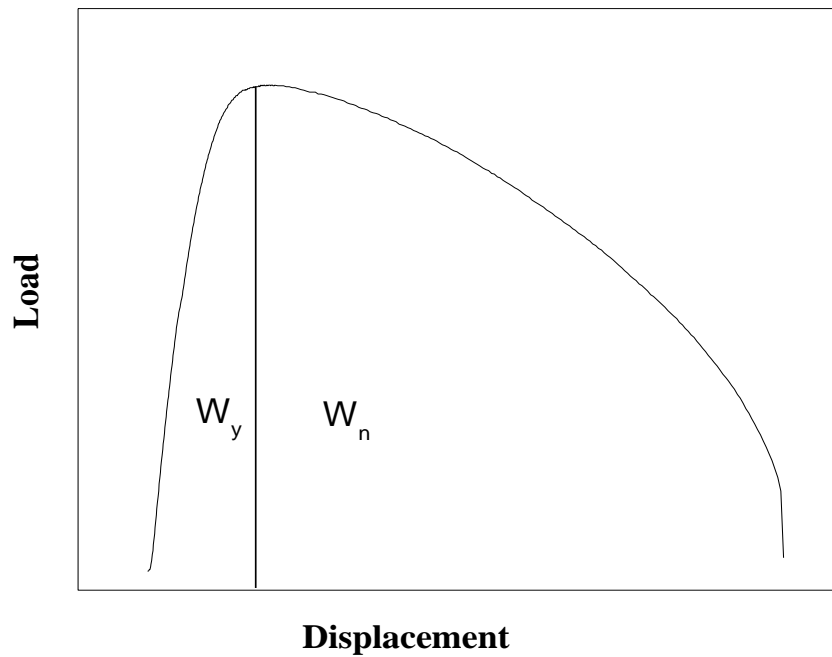


Figure. 3.1 Energy partition of DDENT specimen

3.2 Results and discussion

3.2.1 Load-displacement curve

The load-displacement curves during DDENT tests as a function of ligament length were shown in Fig 3.2. For CPP incorporated with both NAs of different content, the load-displacement curves were self-similar in shape, regardless of the ligament length. The load increased quickly with a slight increase of the displacement before the definite upper point in the initial stage. After the peak, a smooth and slow drop in the load occurred with further increase of the displacement and then the rapid load drop at the end stage of the curves signaling the fracture of the specimens. However, for both types of NAs especially for the β NA nucleated CPPs, the load drop after yielding became faster with increasing amount of NA content.

3.2.2 Fracture parameters

The w_f - l diagrams gave good linear relationship for both type and various content of NAs incorporated CPP samples, as proved by the high linear regression coefficient in Table 3.1. The values of w_e and βw_p , and the results for splitting the essential and non-essential work of fracture as yielding and necking terms were also listed in Table 3.1, which were obtained by plotting w_y and w_n versus l , respectively. From Table 3.1, it was quite clear that the w_e values of CPP incorporated with α NA with different amount were all lower than that of pure CPP, indicating the impaired crack resistance. The w_e value of 0.1wt% α NA nucleated CPP was nearly only a half of that of pure CPP. However, an increase instead of gradual reduction of the w_e values was observed with further increase of α NA amount. When the content of α NA reached 0.5wt%, the w_e values of the nucleated CPP was just 3kJ/m² lower than that of neat CPP. This fact was due to the increase of the crystallinity induced by increase of the NA content^[14]. With the increase of crystallinity, the crystal lattices were arranged more closely, so the crack resistance was improved. This fact was also validated by the crystallinity data obtained from the DSC test listed in Table 3.2. However, the βw_p behaved contrary to w_e with increasing amount of α NA.

Table 3.1 Fracture Parameters obtained from EWF Test for nucleated CPP with α and β NA of different content

NA content (wt %)	content								
	w_f			w_y			w_n		
	w_e (kJ/m ²)	βw_p (MJ/m ³)	R	w_{ey} (kJ/m ²)	$\beta' w_{py}$ (MJ/m ³)	R	w_{en} (kJ/m ²)	$\beta'' w_{pn}$ (MJ/m ³)	R
0	29.84	8.20	0.93	0.59	1.51	0.98	27.68	6.86	0.97
0.1 α	16.29	9.46	0.93	1.05	1.27	0.99	15.23	8.19	0.98
0.3 α	20.57	8.10	0.96	1.93	1.22	0.97	18.32	6.85	0.94
0.5 α	26.54	6.70	0.98	2.24	1.09	0.96	24.29	5.61	0.96
0	29.84	8.20	0.93	0.59	1.51	0.95	27.68	6.86	0.97
0.1 β	25.68	9.54	0.94	3.42	1.57	0.95	24.25	7.74	0.98
0.3 β	37.93	6.98	0.94	5.19	1.07	0.98	31.90	5.99	0.97
0.5 β	40.69	8.30	0.96	6.35	1.21	0.97	34.23	7.06	0.98

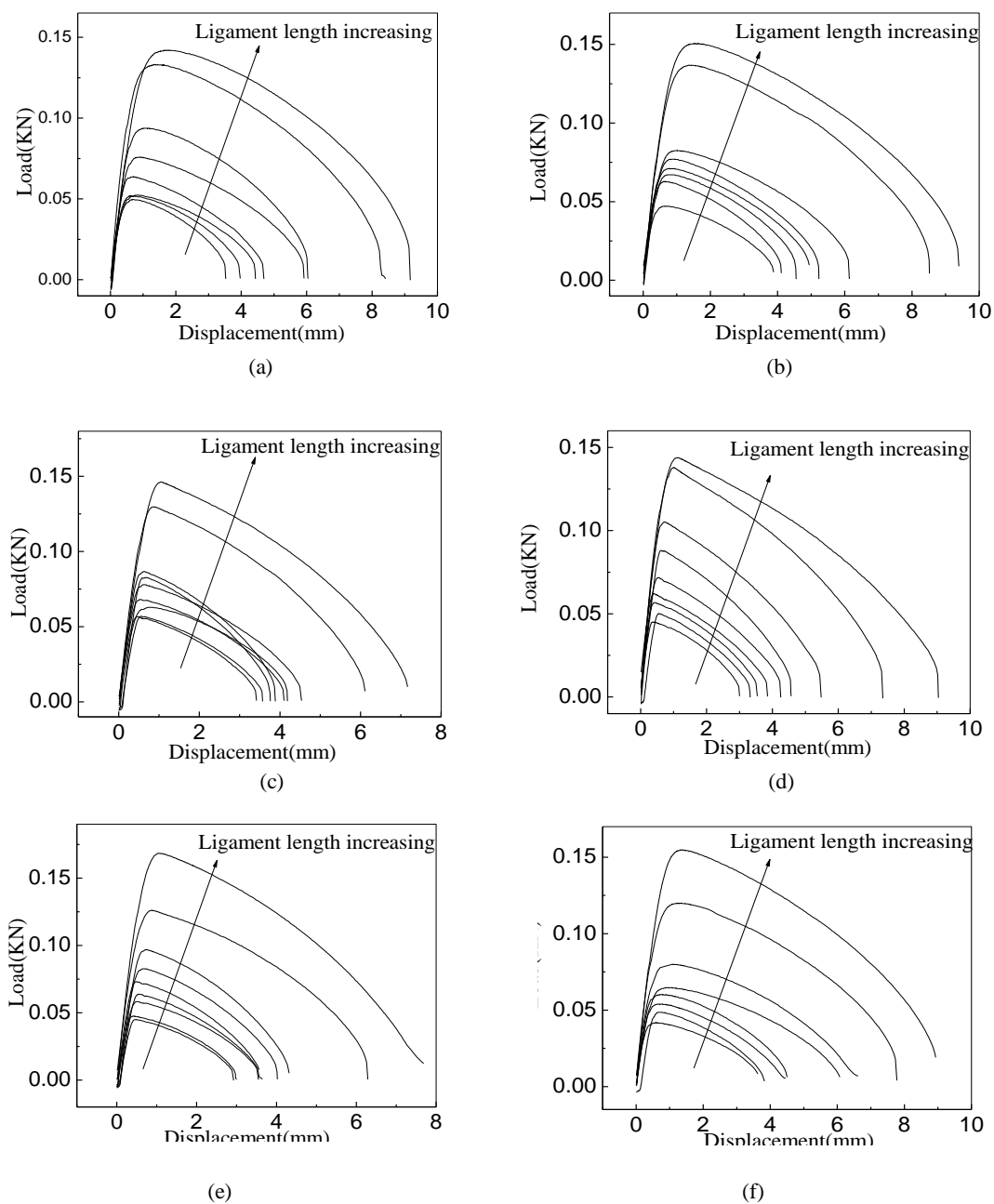


Figure .3.2 A plot of the load versus displacement of CPP incorporated with (a) 0.1wt% α NA(b) 0.1wt% β NA(c) 0.3wt% α NA (d) 0.3wt% β NA (e) 0.5wt% α NA (f) 0.5wt% β NA.

It was shown that the βw_p was the highest at relative low α NA loading (0.1wt%), while decreased with further increasing amount of NA, and nearly 2 MJ/m³ lower than that of neat CPP at 0.5wt% of α NA. Similar trend of variation for both w_e and βw_p with increasing amount of β NAs was observed. But there were some difference worth to be noted between the fracture properties of modified CPP with both NAs, though at the same content. As can be seen, the fracture toughness of 0.1wt% β NA modified CPP was only 4kJ/m² lower than that of pure CPP, which was nearly 10 kJ/m² higher than that of modified CPP with same content of α NA. Then the w_e values increased remarkably with β NA content, which was much higher than that of pure CPP at 0.3 wt% β NA and finally, 10kJ/m² higher than that of neat CPP at 0.5 wt% β NA. Similarly, the fluctuation of the plastic work for β nucleated CPP was also fiercer than that of α NA nucleated CPP. However, at the highest amount of β NA used in this paper, the βw_p value of modified CPP was appreciably higher instead of lower than that of pure CPP for α NA nucleated CPP.

Table 3.2 The crystallinity of CPP modified by α and β NA at different content

content(wt%)	0	0.1 α	0.3 α	0.5 α	0.1 β	0.3 β	0.5 β
crystallinity(%)	34.7	46.4	48.8	49.2	47.3	47.6	48.0

As shown in Table 3.1, the variation of w_{en} and $\beta''w_{pn}$ with increasing NA content for both α and β NAs nucleated CPP was absolutely the same as that of w_e . However, the w_{ey} for both NAs nucleated CPP and $\beta'w_{py}$ for α NA nucleated CPP varied totally different from w_e , as w_{ey} for both nucleated CPP increased with increasing NAs while $\beta'w_{py}$ for α NA nucleated CPP gradually decreased. Only the plastic component before yielding for β NA nucleated CPP showed the same variation as βw_p did. Obviously, the component in the stage of necking and tearing was much higher than that in the stage of yielding, which indicated that the fracture properties were mainly determined by the necking and tearing process.

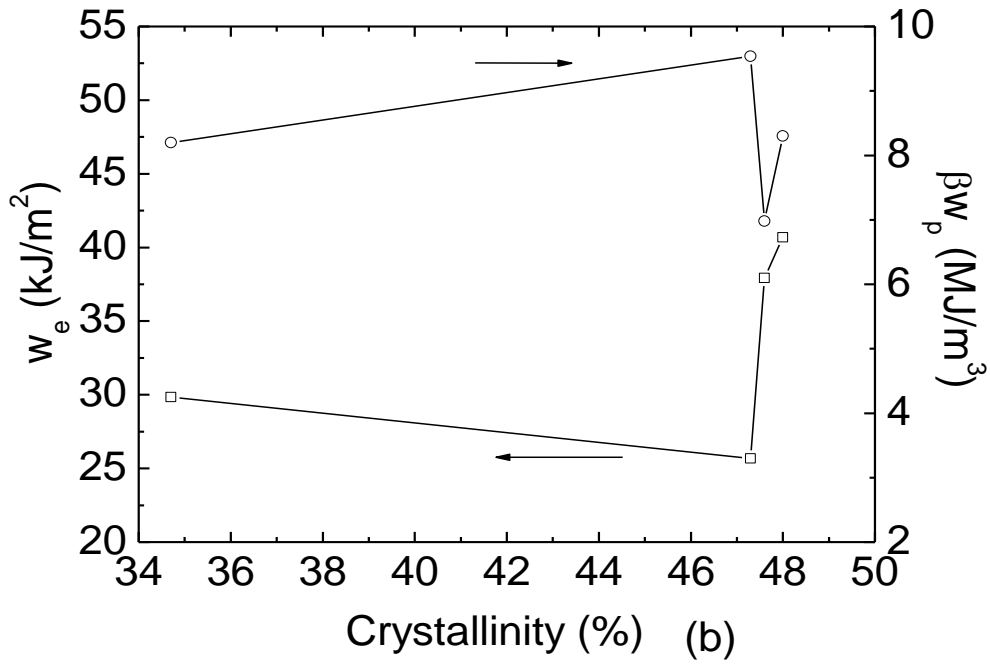
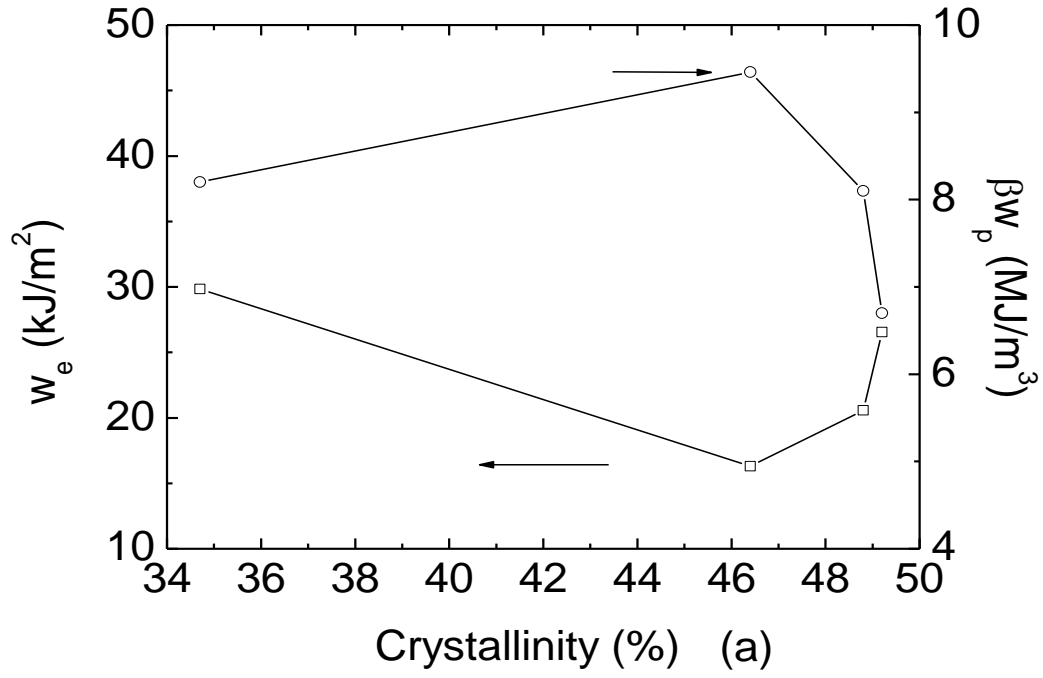


Figure 3.3 Fracture parameters against crystallinity for CPP modified by: (a) α and (b) β NA at different content (\square) w_e (\circ) βw_p

The crystallinity of these samples obtained from the DSC test was listed in Table 3.2 and the dependence of the fracture parameters on crystallinity of the nucleated CPP was summarized in Fig 3.3. The crystallinity of nucleated CPP was calculated by:

$$X_c = \frac{\Delta H}{\Delta H_0} \quad (6)$$

where ΔH_0 was the heat of fusion for 100% crystalline CPP, ΔH was the measured heat of fusion for CPP in the nucleated CPP. The heat of fusion of 100% crystalline α and β CPP were 177.0 J/g and 168.5J/g, respectively^[37].

As shown in Table 3.2 and Fig. 3.3, though the crystallinity for α NA nucleated CPP was higher than that of β NA nucleated CPP with the same content of 0.3wt% and 0.5wt%, the variation of fracture toughness for both NAs nucleated CPP vs crystallinity was similar. However, the down-trend of w_e for α NA nucleated CPP at low crystallinity corresponding to low NA content (0.1 wt%) was more profound than that of β NA nucleated CPP at low crystallinity resulting from low content of β NA (0.1wt%) incorporated, while the up-trend with increasing crystallinity as α NA content increased was far less remarkable than that with increasing crystallinity as β NA content increased. At the same time, the effect of crystallinity on the plastic work of both nucleated CPPs was also similar. As can be seen, the plastic work was the highest at the relative low crystallinity both for 0.1wt% α and β NAs nucleated CPP. Then, the βw_p showed a down-trend with increasing crystallinity in both NAs nucleated CPPs, although a fluctuation was presented for β NA nucleated CPP at the content of 0.3wt%.

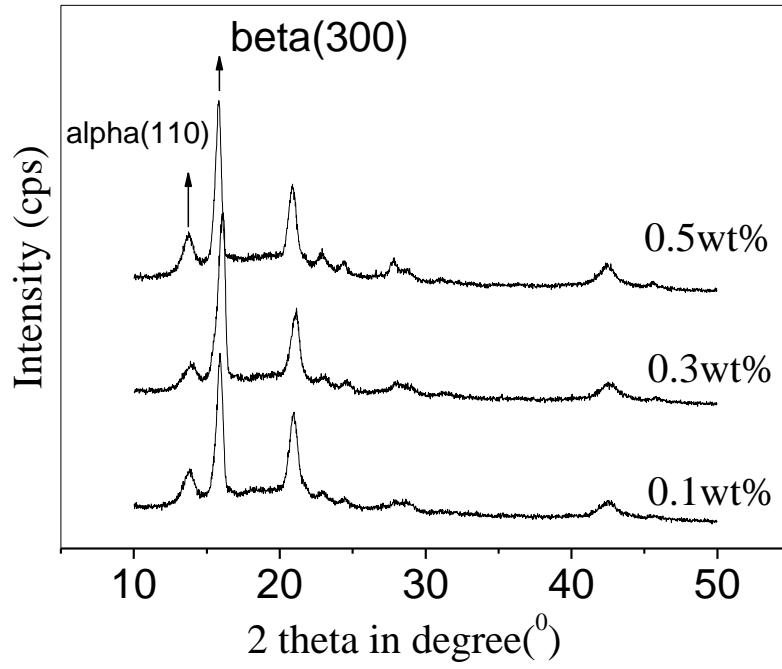


Figure 3.4 Effect of loading content of β type NA on the WAXD patterns of CPP

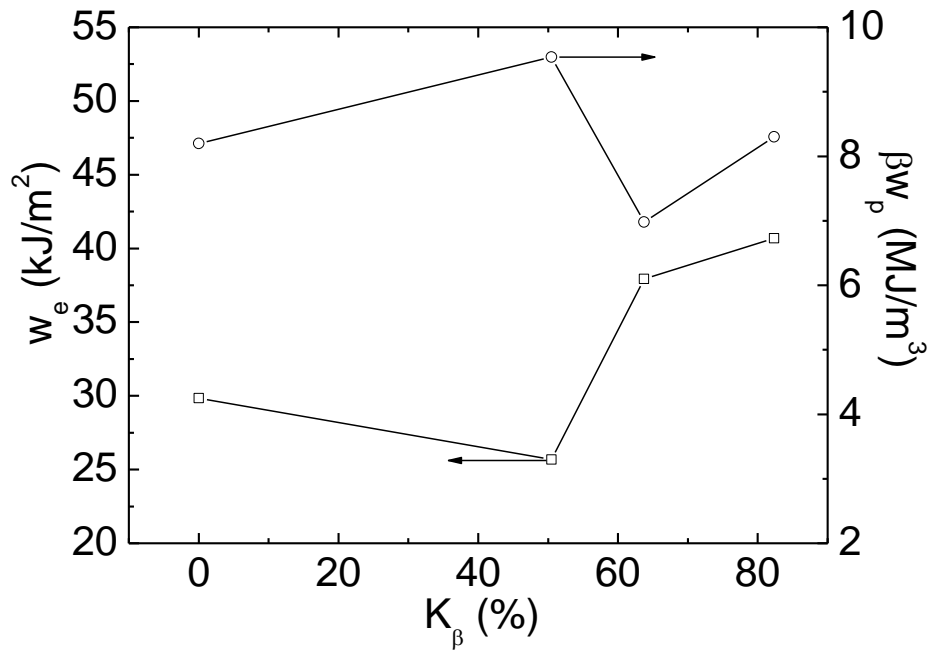


Figure 3.5 Specific work of fracture against K_β for CPP modified by β NA at different content. (\square)

w_e (\circ) βw_p

Table. 3.3 Content of β crystal in β NA modified CPP

NA content (wt %)	$I_{\beta(300)}(\%)$	$I_{\alpha(110)}(\%)$	$I_{\alpha(040)}(\%)$	$I_{\alpha(130)}(\%)$	$K_{\beta}(\%)$
0.1 β	100.00	22.70	11.28	64.02	50.51
0.3 β	100.00	12.55	0	44.37	63.73
0.5 β	100.00	21.43	0	0	82.35

As reported, β NA can induce the transition of crystal from α form to β form, which was also reflected in Table 3.3. The data in Table 3.3 were obtained according to Eq (7)^[38] using the WAXD (shown in Fig 3.4) results. K_{β} was the content of β crystal in nucleated CPP, and I_{β} and I_{α} were the relative intensity corresponding to characteristic diffraction planes of CPP α and β crystal obtained from WAXD tests.

$$K_{\beta} = \frac{I_{\beta(300)}}{I_{\beta(300)} + I_{\alpha(110)} + I_{\alpha(040)} + I_{\alpha(130)}} \quad (7)$$

The crystallization of the NA modified CPP mainly adopted a heterogeneous nucleation process and the growth of β crystals was governed by the number of nuclei existed in the system. The diagrams of fracture parameters as a function of K_{β} of β NA nucleated CPP were presented in Fig 3.5. From the values listed in Table 3, the variation of K_{β} exhibited an evident increasing trend which could also be reflected from the diminishing I_{α} , indicating that elevating amount of NA led to the increasing β content and consequently improved fracture resistance, which was consistent with β -crystal toughening mechanism. The reason why beta-polypropylene crystals can improve the toughness of polypropylene can be attributed to a combined effect of several factors, including the α to β phase transformation induced by mechanical load, enhanced mechanical damping of polypropylene, and the peculiar lamellar morphology of polypropylene^[39].

When the content of NA reached 0.5% the diffraction peaks of α (040) and α (130) in the WAXD pattern was completely depressed, resulting in the prominence of β (300) peak and consequently elevation of K_{β} . For pure CPP, the w_e value was higher than those of β

NA nucleated CPP. With the addition of 0.1% NA, the w_e value of β NA nucleated CPP decreased dramatically compared with that of pure CPP. However, as the NA content increases, the values of w_e increased gradually. This growing trend was coincident with the illustration of Fig 3.3(a). It was worth noting that the w_e value showed an obvious rise, when the NA content exceeds 0.3%, while this kind of dramatic variation appeared as the NA content was higher than 0.1%. The variation trend of βw_p values was also similar to Fig 3.3(a). For the CPP modified by 0.1% NA, its βw_p value reached the climax, whereas, the K_β value was not the highest. With the growing of K_β values, the βw_p value was declining.

3.3 Conclusions

Focusing on the effect of NA of different type and content on the fracture behavior of CPP, the following conclusions were drawn.

- (1) With the addition of NA, the crystallinity of both α and β modified CPP increased remarkably and the β NA successfully induced the transition of CPP crystal from α form to β form.
- (2) The w_e values of CPP added with α NA of different amount were all lower than that of pure CPP. The w_e values increased with further increase of α NA amount. However, the βw_p was the highest at the lowest α NA amount (0.1 wt %), while decreased with further increasing amount. The variation of w_{en} and $\beta''w_{pn}$ with increasing NA content for α NA nucleated PP was absolutely same as those of w_e and w_{ey} did, while the $\beta'w_{py}$ for α NA nucleated PP gradually decreased. The plastic work decreased with increasing crystallinity in α NA nucleated CPP.
- (3) Both w_e and βw_p showed similar trend of variation with increasing amount of β NA. Only the plastic component before yielding for β NA nucleated PP had the same variation as βw_p . While the plastic work decreased first and then recovered close to that of pure CPP, with increasing crystallinity for β NA nucleated CPP. The variation of K_β for NA nucleated CPP was almost same as that of w_e , indicating that elevating amount of NA leading to the increasing of β content and consequently improved fracture resistance. The difference in the variation of βw_p value in CPP filled with β NA may be due to the conversion of crystal form.

3.4 References

- [1]. Wong, S. C.; Mai, Y. W. *Polym Eng Sci* 1999, 39, 356.
- [2]. Mouzakis, D. E.; Gahleitner, M.; Karger-Kocsis, J. *J Appl Polym Sci* 1998, 70, 873.
- [3]. Mouzakis, D. E.; Harmia, T.; Karger-Kocsis, J. *Polym Polym Compos* 2000, 8, 167.
- [4]. Karger-Kocsis, J. *J Macro Sci Phy (B)* 1999, 38, 635.
- [5]. Gong, G.; Xie, B.-H.; Yang, W. *Polym Test* 2005, 24, 410.
- [6]. Gong, G.; Xie, B.-H.; Yang, W. *Polym Test* 2006, 25, 98.
- [7]. Xie, B.-H.; Shen, Y.-X.; Yang, W. *Acta Polym Sci* 2006, 2, 335.
- [8]. Yang, W.; Xie, B.-H.; Yang, M.-B. *J Mater Sci* 2005, 40, 5323.
- [9]. Yang, W.; Xie, B.-H.; Yang, M.-B. *J Appl Polym Sci* 2006, 99, 1781.
- [10]. Nagarajan, K.; Levon, K.; Myerson, A. S. *J Therm Anal Calorim* 2000, 59, 497.
- [11]. Karger-Kocsis, J.; Varga, J. *J Appl Polym Sci* 1996, 62, 291.
- [12]. Hashemi, S. *Polym Eng Sci* 2000, 40, 798.
- [13]. Tjong, S. C.; Xu, S.A.; Mai, Y. W. *Mater Sci Eng* 2003, 347, 338.
- [14]. Mouzakis, D. E.; Gahleitner, M.; Karger-Kocsis, J. *J Appl Polym Sci* 1998, 70, 873.
- [15]. Arkhireyeva, A.; Hashemi, S. *Polymer* 2002, 43, 289.
- [16]. Mouzakis, D.E.; Karger-Kocsis, J. *Polym Bull* 1999, 42, 473.
- [17]. Karger-Kocsis, J.; Ferrer-Balas, D. *Polym Bull* 2001, 46, 507.
- [18]. Marchal, Y.; Oldenhove, B.; Daoust, D. *Polym Eng Sci* 1998, 38, 2063.
- [19]. Karger-Kocsis, J.; Czigany, T. *Polym Eng Sci* 2000, 40, 1809.
- [20]. Broberg, K. B. *Int J Fract* 1968, 4, 11.
- [21]. Cotterell, B.; Reddel, J. K. *Int J Fract* 1977, 13, 267.
- [22]. Mai, Y. W.; Cotterell, B. *Int J Fracture* 1986, 32, 105.
- [23]. Mai, Y. M.; Cotterell, B.; Horlyck, R.; Vigna, G. *Polym Eng Sci* 1987, 27, 804.
- [24]. Mai, Y. W.; Powell, P. *J Polym Sci (B)* 1991, 29, 785.
- [25]. Wu, J.-S.; Mai, Y. W.; Cotterell, B. *J Mater Sci* 1993, 28, 373.
- [26]. Wong, J. S. S.; Ferrer-Balas, D.; Li, R. K. Y.; Mai, Y. W.; MasPOCH, M. L.; Sue, H. J. *Acta Mater* 2003, 51, 4929.
- [27]. Ferrer-Balas, D.; Mai, Y. W. *Polymer* 2001, 42, 2665.
- [28]. Karger-Kocsis, J.; Barany, T.; Moskala, E. *J. Polymer* 2003, 44, 5691.

- [29]. Karger-Kocsis, J.; Barany, T. Polym Eng Sci 2002, 42, 1410.
- [30]. Karger-Kocsis, J.; Moskala, E. J. Polymer 2000, 41, 6301.
- [31]. Karger-Kocsis, J.; Mouzakis, D. E. Polym Eng Sci 1999, 39, 1365.
- [32]. Karger-Kocsis, J. Polym Bull 1996, 37, 119.
- [33]. Karger-Kocsis, J.; Czigany, T.; Moskala, E. J. Polymer 1997, 38, 4587.
- [34]. Karger-Kocsis, J.; Czigany, T.; Moskala, E. J. Polymer 1998, 39, 3939.
- [35]. Karger-Kocsis, J.; Moskala, E. J. Polym Bull 1997, 39, 503.
- [36]. Maspoch, M. L.; Gamez-Perez, J.; Karger-Kocsis, J. Polym Bull 2003, 50, 279.
- [37]. Li, J. X., Cheung, W. L., Jia, D. M. Polymer 1999, 40, 1219.
- [38]. Grein, C. Adv Polym Sci 2005, 188, 43.
- [39]. Varga, J. J Macromol Sci Phys 2002, B41, 1121.

Chapter 4 Structure and properties of peroxide induced controlled rheology polypropylene

4.1. Introduction

Isotactic polypropylene (iPP), a propylene-based polymer produced with transition-metal catalysts ^[1-4], is now becoming one of the most important polymer materials universally used. iPP is well known for its mechanical properties, chemical stability, and low cost. However, its usage is restricted by its relatively high average molecular weight ^[1-2] (MW) and broad molecular weight distribution ^[3-4] (MWD).

Much attention has been focused on adjusting the MW and MWD of iPP to broaden the application and the processing window of iPP to date^[5-6], including the prevalent controlled rheology polypropylene (CRPP) technology, a post-reactor procedure consisting of reactive extrusion of the virgin iPP with organic peroxide^[7-10].

Modification of polypropylene in the so-called "controlled rheology" process is always performed by the addition of certain peroxides such as 2,5-dimethyl-2,5-di(2-ethylhexanoylperoxy) hexane. The peroxide typically is added in the extruder during pelletization after the polymerization process. The peroxide tends to encourage a more-or-less uniform breakdown of the macromolecules of the polypropylene resin under the physical and thermal stress of the extruder. At the first stage of the preparation of peroxide induced CRPP, free radicals come into being from the thermal decomposition of the organic peroxide, then the radicals attack the tertiary carbon atom of main chain, forming macro-radicals. At the second stage, the β scission occurs in the main chain of iPP macromolecules. Due to the equality of being attacked, the longer macromolecular chains are inclined to be broken up easily. In the end, the average molecular weight of the resin is reduced, resulting in a product with a relatively narrow molecular weight distribution. The reduction in the average molecular weight and the improved narrowness of the molecular weight distribution is typically accompanied by an increase in melt flow rate and changes in both the rheological and physical properties as compared with those of a reactor product having a similar melt flow rate. The resulting polypropylene also exhibits improved flowability during the fabrication of the plastic

products.

Commercial polypropylenes, produced in the presence of organic peroxides, are known as controlled-rheology (CR) resins. Although a wide variety of peroxides is available, one specific peroxide, [2, 5-dimethyl-2, 5-di (2-ethylhexanoylperoxy) hexane] as the choice of peroxide, is used throughout the industry to produce CR polymers for its particular decomposition temperature

Tzoganakis et.al investigated systematically the effect of neat polymers^[11-12], polymer blends^[13-14], and processing conditions^[15-16] on the properties of controlled rheology polymers. Extensive studies concerning the kinetic of the processing of the controlled rheology polymers had been carried out by Balke and co-workers^[17-19].

Our previous work^[20-21] has concentrated on the properties of iPP filled with different types of nucleating agent and the crystalline morphology of CRPP. It has been found that the shaped crystalline structure had a major influence on the properties of CRPP. The present paper deals with the effect of peroxide types on the relationship between the structure, especially the crystalline structures and the properties, mainly the rheological and mechanical properties of CRPP.

4.2. Results and discussion

4.2.1 Effect of different peroxides on the capillary rheology properties of peroxides induced polypropylenes

Fig. 4.1 and Fig. 4.2 show the relationship of the shear stress and the shear viscosity against the shear rate of different peroxide induced CRPPs. It indicated clearly that the addition of peroxide increased the shear stress and shear viscosity of the CRPPs in the low shear rate range, especially for the DMDEHPH induced CRPP. The curves of BPO and DCP induced CRPP exhibit almost the same trend. In the low shear rate region, the DMDEHPH induced CRPP is not sensitive to the shear stress, also the higher shear viscosity of the DMDEHPH induced iPP can be seen in Fig. 4.2. The viscosity of the CRPPs is higher than the virgin resin, iPP, due to the formation of the micro crosslinkage in the peroxide induced CRPPs as a result of the non-homogeneous distribution of the

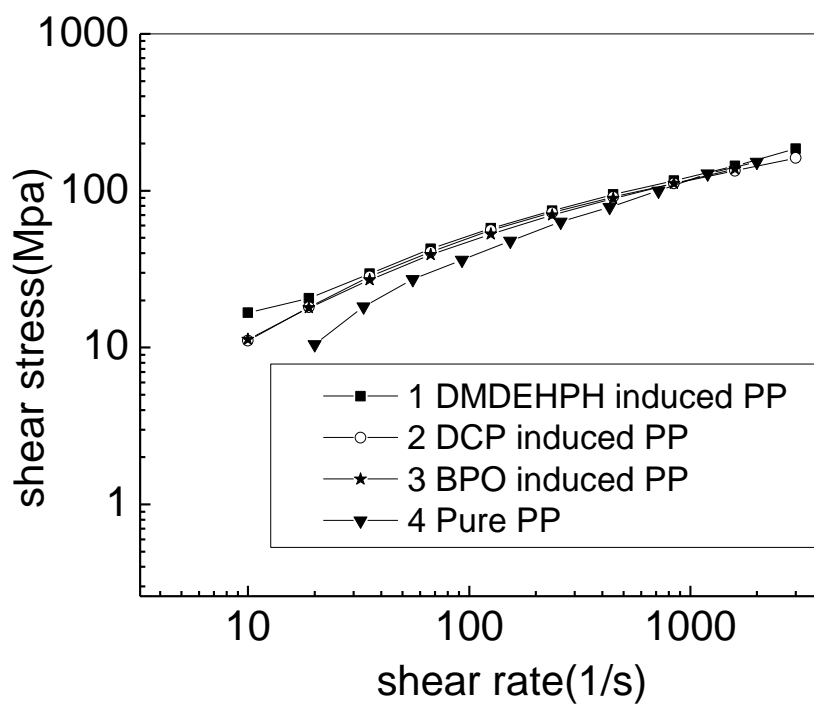


Figure. 4.1. The shear stress against shear rate for different peroxides (0.03wt %) induced CRPP

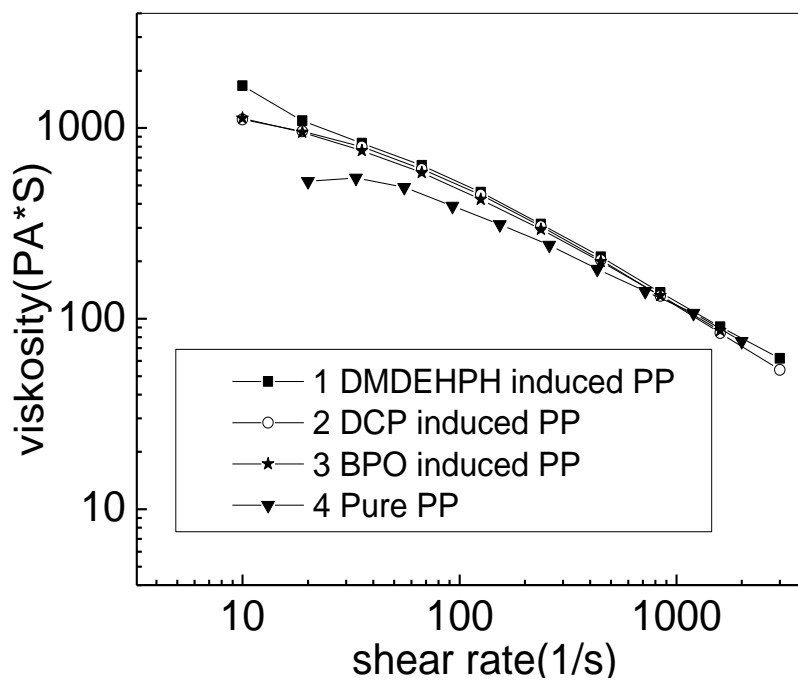


Figure. 4.2. The shear viscosity against shear rate for different peroxides (0.03wt %) induced CRPP.

Peroxide density. The micro crosslinkages were broken up with increasing the shear rate, so the rheological curve of the four samples were shown the same trend in the high shear rate (above 1000/s)

Table. 4.1. MFR and notched impact strength of different peroxides (0.03wt %) induced CRPP

Sample	MFR (g/10min)	Notched impact strength (KJ/m ²)
DMDEHPH induced CRPP	6.44	2.98
DCP induced CRPP	7.59	2.76
BPO induced CRPP	9.54	2.71
Virgin iPP	6.95	2.14

4.2.2 Effect of different peroxides on the MFR and mechanical properties of peroxides induced polypropylenes

Table. 4.2. Tensile properties of different peroxides (0.03%wt) induced CRPP (The crosshead speed was 100mm/min)

Sample	Elastic modulus (MPa)	Elongation at break (%)	Yield stress (MPa)	Elongation at yield (%)
DMDEHPH induced CRPP	1253	578	32.83	7.79
DCP induced CRPP	1156	489	32.12	7.78
BPO induced CRPP	1116	267	33.22	7.84
Virgin iPP	1170	303	31.98	7.76

As is known before, the purpose of CRPP technology is to adjust the molecular weight and molecular weight distribution of normal iPP to broaden its processing conditions and application. Many researches have reported that the decrease of the molecular weight will result in the decrease of the mechanical properties [22-25]. These changes take place due to chain scission of PP chains and degradation of high molecular weight tails in PP chains. But as is shown in Table 4.1, the notched impact strength of these peroxide induced CRPPs is higher than the virgin resin. It seems the produced macromolecules during the peroxide induced reaction process were involved to disperse the notched impact energy and improve

the toughness of CRPPs in some degree.

The tensile properties of these peroxide induced CRPP are shown in Table 4.2. It can be seen that the DMDEHPH induced CRPP shows the highest elastic modulus, elongation at break which means a good balance between the stiffness and the ductility. The tensile yield strength of this sample is also higher than the virgin resin. These facts indicate that the DMDEHPH is a perfect choice in preparing CRPP.

4.2.3 Effect of different peroxides on the crystallize and dynamic rheology properties of peroxides induced polypropylenes

Figs. 4.3 and Fig. 4.4 show the melting and crystallization curves of CRPP prepared with different peroxides and the virgin resin. The calculated crystallinity and the thermal data are listed in Table 4.3. The melting peak temperatures of the CRPPs are slightly higher than the virgin resin. The DSC melting endotherm curves of CRPP is wider than the virgin, indicating the more crystalline structural heterogeneity in the CRPPs. Generally, the increment of the polymer crystallinity is related to a decrease of chain length and so easily forming of crystals. Here, the crystallinity of DMDEHPH induced CRPP is somewhat higher than the other two peroxides induced samples. This might be due to that with the addition of the peroxides, the rearrangement of the newly formed short chain molecular takes place, and more molecular chains in the amorphous phase pack into the crystal patterns, finally increase the crystalline portion of peroxide induced iPP.

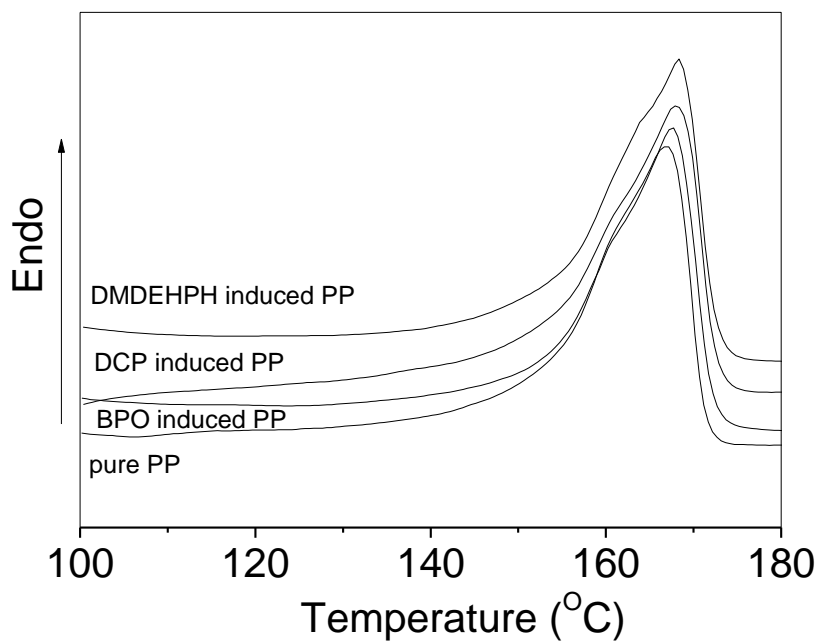


Figure. 4.3. The effect of different peroxides (0.03wt %) on the DSC heating scan of peroxide induced CRPP

Table. 4.3. DSC heating scan of different peroxides (0.03%wt) induced CRPP

Sample	Area(J/g)	Peak(°C)	Onset(°C)	End(°C)	Crystallinity (%)
DMDEHPH induced CRPP	77.88	168.30	155.00	172.60	37.26
DCP induced CRPP	77.48	168.10	154.40	172.50	37.07
BPO induced CRPP	75.51	167.50	154.20	172.10	36.13
Virgin iPP	78.65	166.90	154.00	171.30	36.63

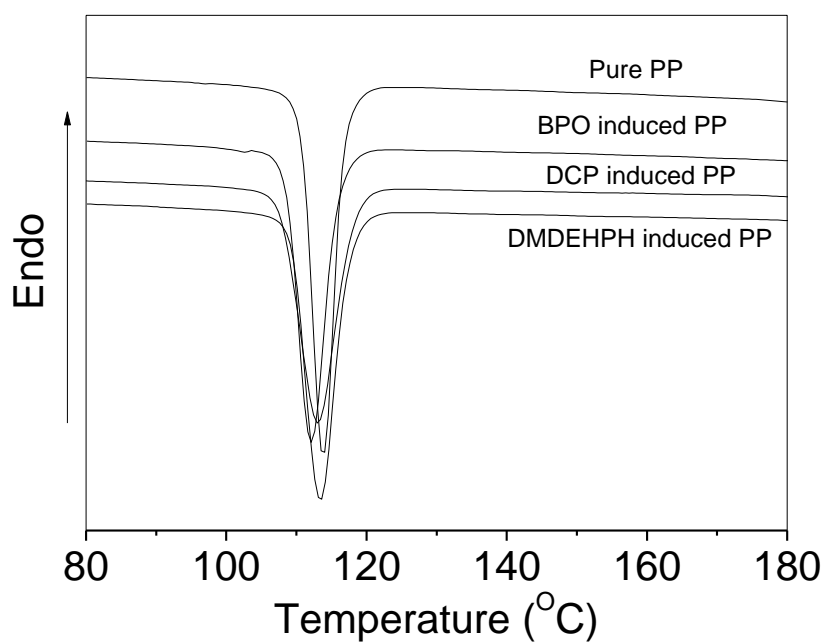


Figure. 4.4. The effect of different peroxides (0.03wt %) on the DSC cooling scan of peroxide induced CRPP

Table. 4.4. DSC cooling scan of different peroxides (0.03%wt) induced CRPP

Sample	Area(J/g)	Peak(°C)	Onset(°C)	End(°C)
DMDEHPH induced CRPP	99.74	113.50	109.40	117.60
DCP induced CRPP	97.83	113.10	107.80	118.20
BPO induced CRPP	92.55	112.10	108.60	116.00
Virgin iPP	92.47	113.90	110.80	116.90

Table. 4.5. PI value of different peroxides (0.03%wt) induced CRPP

Sample	PI
DMDEHPH induced CRPP	1.20
DCP induced CRPP	1.08
BPO induced CRPP	1.22
Virgin iPP	1.67

Similarly, the DSC cooling endotherm curves of CRPP is wider than the virgin as can be seen from Fig.4.4. As for the crystal peak area of three peroxides induced iPPs, DMDEHPH induced iPP is also larger than other two induced iPPs. This fact is consistence with the fact in the melting curves. However, the insensitivity of crystallization temperatures to the peroxide, which can be seen from the cooling endotherm data listed in Table 4.4, is likely to be considered by the fact that the degradation reaction occurs preferentially in the amorphous phase of the polymer.

In addition, in order to obtain more detailed structure information of peroxide induced iPPs, the dynamic rheology measurement was carried out here. According to the theory of Zeichner^[26], the molecular weight distribution can be indirectly estimated by the following equation (2)

$$PI = \frac{10^6}{G^x} \quad (2)$$

The value of PI represents the MWD and G^x can be obtained from the crossing point of storage modulus and loss modulus. The higher PI value represents the broader MWD of sample. The corresponding PI values of the dynamic rheology results based on equation (1) are listed in Table 4.5. It can be easily seen that the PI values of peroxides induce iPPs are lower than the virgin iPP, indicated that the addition of the peroxide can apparently change the MWD of iPP, and finally improved narrowness of the iPP molecular weight distribution.

4.3. Conclusions

Three different peroxides induced CRPPs are explored in this research and the main conclusions are obtained as follow:

The capillary rheology measurement indicates that the DMDEHPH induced CRPP is preferably controllable in a relatively low shear rate range.

DMDEHPH induced CRPP exhibits the highest mechanical properties. DMDEHPH induced CRPP shows the highest crystallinity, which can be used to explain the superior mechanical properties of DMDEHPH induced iPP.

All the three CRPP samples show a lower PI value comparing with the virgin iPP, indicating the improved narrowness of the iPP molecular weight distribution

4.4 References

- [1] Eckstein, A.; Suhm, J.; Friedrich, C.; *Macromol.* 1998, 31, 1335..
- [2] Resconi, L.; Jones, R. L.; Rheingold, A. L.; *Org. Metal.* 1996, 15, 998.
- [3] Fukui, Y.; Murata, M.; Soga, K.; *Macromol. Rapid Commun.* 1999, 20, 637.
- [4] Agarwal, P. K.; Somani, R. H.; Weng, W. Q.; *Macromol.* 2003, 36, 5226.
- [5] Busico, V.; Cipullo, R.; Chadwick, J. C.; *Macromol.* 1994, 27, 7538.
- [6] Gauthier, W. J.; Collins, S.; *Macromol.* 1995, 28, 3779.
- [7] Deroover, B.; Sclavons, M.; Carlier, V.; *J. Polym. Sci., Part A: Polym. Chem.* 1998, 33, 829.
- [8] Kron, A.; Stenberg, B.; Reitberger, T.; *Polym. Degrad. Stab.* 1996, 53, 119.
- [9] Berzin, F.; Vergnes, B.; Dufosse, P.; *Polym. Eng. Sci.* 2000, 40, 344.
- [10] Berzin, F.; Vergnes, B.; Delamare, L.; *J. Appl. Polym. Sci.* 2001, 80, 1243.
- [11] Wang, X. C.; Tzoganakis, C.; Rempel, G. L.; *J. Appl. Polym. Sci.* 1996, 61, 1395.
- [12] Thompson, M. R.; Tzoganakis, C.; Rempel, G. L.; *Polym.* 1998, 39, 327.
- [13] Shearer, G.; Tzoganakis, C.; *Polym. Eng. Sci.* 1999, 39, 1584.
- [14] Dorscht, B. M.; Tzoganakis, C.; *J. Appl. Polym. Sci.* 2003, 87, 1116.
- [15] Barakos, G.; Mitsoulis, E.; Tzoganakis, C.; *J. Appl. Polym. Sci.* 1996, 59, 543.
- [16] Baik, J. J.; Tzoganakis, C.; *Polym. Eng. Sci.* 1998, 38, 274.
- [17] Chan, J. H.; Balke, S. T.; *Polym. Degrad. Stab.* 1997, 57, 113.
- [18] Chan, J. H.; Balke, S. T.; *Polym. Degrad. Stab.* 1997, 57, 127.
- [19] Chan, J. H.; Balke, S. T.; *Polym. Degrad. Stab.* 1997, 57, 135.
- [20] Wang, S. W.; Yang, W.; Xu, Y. J.; Xie, B. H.; Yang, M. B.; Peng, X. F.; *Polym. Test.* 2008, 27, 638.
- [21] Wang, S. W.; Yang, W.; Xie, B. H.; Liu, Z. Y.; Yang, M. B.; *J. Appl. Polym. Sci.* 2008, 108, 591.
- [22] Paul, S.; Kale, D. D.; *J. Appl. Polym. Sci.* 2000, 76, 1480.
- [23] Yoon, L. K.; Choi, C. H.; Kim, B. K.; *J. Appl. Polym. Sci.* 1995, 56, 239.
- [24] Slusarski, L.; Bielinski, D.; Wlochowicz, A.; *Polym. Int.* 1995, 36, 261.
- [25] Naskar, K.; Noordermeer, J. W. M.; *Rubber. Chem. Technol.* 2003, 76, 1001
- [26] Zeichner, G. R.; Patel, P. D.; *Processing of the second World Congress of Chemical Engineering*, 1981.
- [27] Lorenzo, M. L.; Silvestre, C.; *Prog. Polym. Sci.* 1999, 24, 917.

Chapter 5 Crystalline Morphology of β Nucleated Controlled Rheology Polypropylene

5.1. Introduction

The crystalline morphology ^[1-4] and rheological behavior ^[5-7] are two of the most important topics in research of polymer materials. Polypropylene (PP), a typical semicrystalline polymer with rich crystalline morphologies, has gained an important position among polyolefins due to its broad range of applications ^[6-12]. PP is well-known for its mechanical properties, chemical stability and low cost. However, its usage was restricted in certain applications by its relatively high average molecular weight (MW) ^[13] and broad molecular weight distribution (MWD) ^[14-15]. Hence, many efforts were made to control the MW and MWD of PP, and the “controlled-rheology polypropylene”(CRPP) technology ^[14-21] was developed and widely adopted. CRPP can be obtained economically and efficiently by a post reactor procedure which consists of a reactive extrusion of the virgin PP with organic peroxide. The resultant CRPP possesses many superior properties to normal PP, such as high elongation at break, thermal deformation temperature, transparency, surface smoothness, and so on. Additionally, owing to its excellent processability, CRPP is widely used in melt spinning and extrusion of thin films.

Because of its semicrystalline nature, PP chains can organize into different spatial arrangements giving rise to three basic crystalline polymorphs: α -monoclinic, β - trigonal and γ -triclinic phases ^[22-24]. Perfect spherocrystal structure can be formed in PP without any external force. Nucleating agents (NAs) can easily shorten the time of inducing the crystal nucleus for the crystallization process in PP matrix and enhance the overall rate of transformation from the molten state to the crystalline solid state ^[25-30]. Many publications have reported the enhanced physical properties of semi-crystalline polymers, such as impact properties and surface properties, when the size of crystallite becomes smaller as a result of NA addition ^[31-35]. For different kinds of NA modified PPs, the impact strength of β -PP generally exceeds that of α -PP. Varga ^[36] has attributed the superior toughness of β -PP to a combined effect of three factors: the α to β phase transformation induced by mechanical load, the enhanced mechanical damping of β -PP, and the peculiar lamellar

morphology of β -PP.

In our previous work, the crystalline morphology and rheological behavior of PP, PP based blends or composites were studied, respectively ^[37-41]. However, little attention was paid to the effect of CRPP technology on the crystalline morphology of PP. In this paper, the effectiveness of different β NAs, and the effect of DCP and NA content on the crystalline morphology of β NA nucleated CRPP will be discussed.

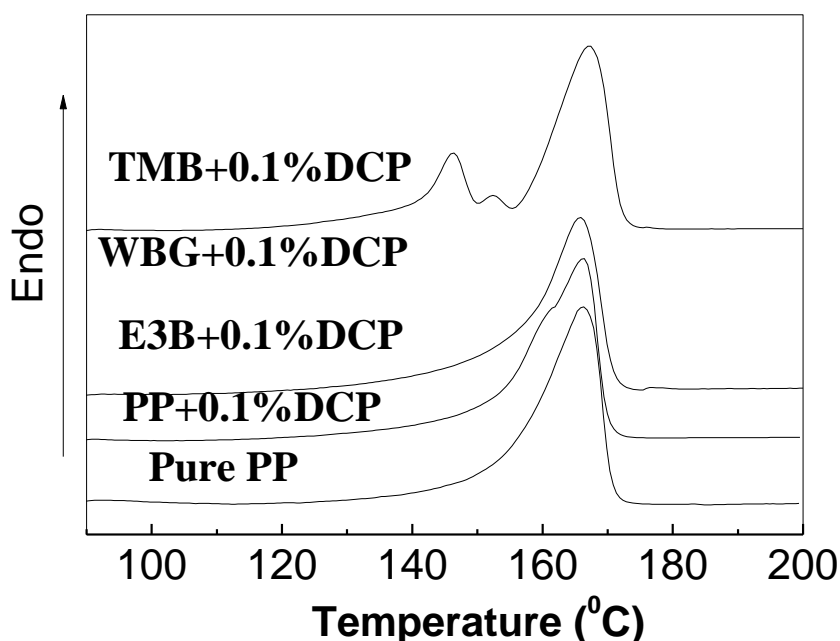


Figure. 5.1. Effect of different β NAs on the DSC heating scan of CRPPs.

5.2. Results and discussion

5.2.1 Effect of NAs on the Crystalline Morphology of CRPPs

Fig. 5.1 shows the effect of β NAs on the DSC heating scan of CRPPs prepared using 0.1wt% DCP with the same β NA content of 0.3wt%. The melting peak of β -crystals of PP can be clearly seen at a temperature around 147 °C for the WBG-II and TMB-5 nucleated samples, indicating significant β -crystals were induced by the NA WBG-II and TMB-5. The multiple melting peaks of β -crystals in these two samples are possibly due to the complexity of the β -crystal structure during the melting process. First, the imperfect β -crystal start to melt with the increase of scanning temperature. Meanwhile, the long chain

molecules pack into adjacent crystals, which increase the thickness of the β -crystal or improve transformation of β -polymorph to α -polymorph. With the temperature increasing further, the perfect β -crystals transform to the α -crystals by recrystallization ^[43-46]. Compared with the WBG-II and TMB-5 nucleated CRPPs, the E3B nucleated system shows no trace of β -crystal in the DSC heating scan. This may be related to the optimum concentration of E3B for creating the trigonal crystal structure in PP. Sterzynski ^[47] reported that the maximum of the β content in the iPP system was achieved at a certain content of E3B concentration, and for lower or higher E3B content, a strong decrease of the β -crystal content

Table. 5.1 DSC results of CRPP (0.1wt% DCP) specimen incorporated with β NA

β nucleating agent(0.3%)	$T_m(^{\circ}\text{C})$	$\Delta H(\text{J/g})$	Crystallinity (%)
Pure PP	166.20	104.20	61.84
PP+0.1wt%DCP	166.30	98.16	58.26
E3B+0.1wt%DCP	165.80	95.50	56.68
WBG- II +0.1wt%DCP	147.02, 166.79	82.09	48.72
TMB-5+0.1wt%DCP	146.32, 152.41, 167.19	91.79	54.47

was observed. The results of the DSC test are listed in Table 5.1.

Compared with the virgin PP, the α melting peak of CRPP without β NA shows no significant change. Nevertheless, the α peak of E3B nucleated CRPP shifts to lower temperature. This is related to the incomplete crystal structure in PP owing to the addition of E3B. The α peaks of the other two NAs nucleated CRPPs move to a little higher temperature, reflecting the increased thickness of α crystal and transformation of the β crystal to α crystal. As regards the extent of the shift of the melting point to higher temperature, TMB-5 is superior to WBG-II, indicating that more β -crystals in the TMB-5 modified PP system were transformed into α -crystals. At the same time, NA can easily shorten the time of inducing the crystal nucleus for the crystallization process, so more crystal nuclei will be created in the limited space of the PP matrix. Finally, the growth rate of crystal nuclei exceeded the total rate of crystallization process, so the total crystallinity index decreased with the addition of NA.

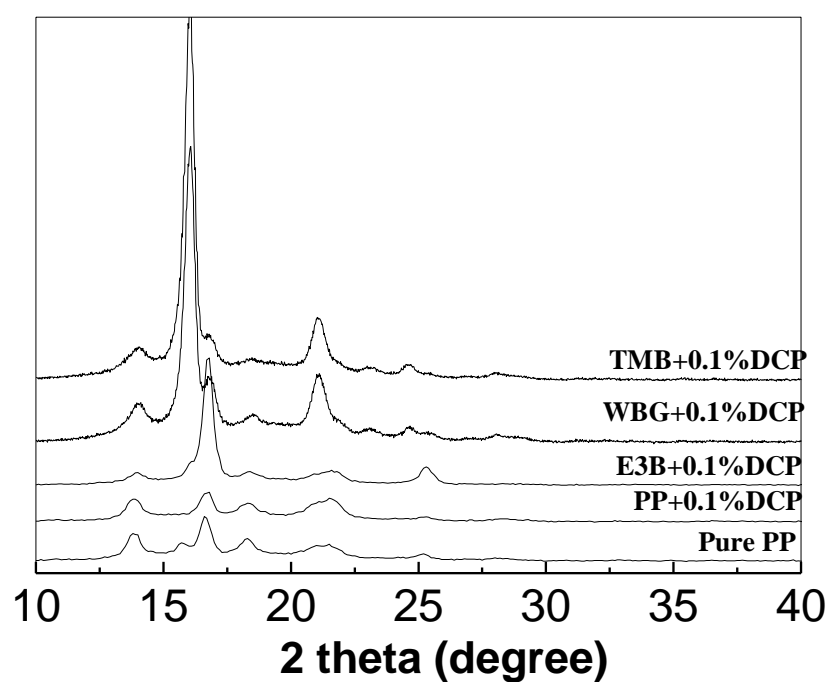


Figure. 5. 2. Effect of different β NAs on the WAXD patterns of CRPPs

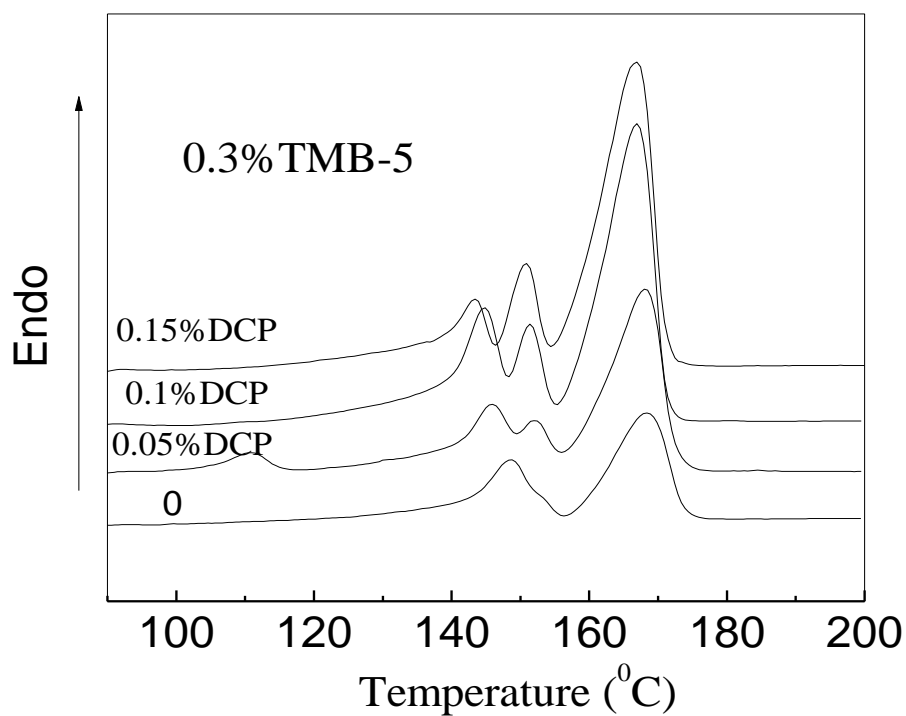


Figure. 5.3. Effect of TMB-5 on the DSC heating scan of CRPPs prepared using different contents of DCP.

Fig. 5.2 shows the effect of types of β NAs on the WAXD patterns of CRPPs. Obviously, WBG and TMB nucleated CRPPs show the characteristic diffraction peak(300), of β -iPP at $2\theta=16.2^\circ$ ^[48]. The higher intensity of (300) peak of TMB-5 nucleated CRPP reflects a higher relative content of β -form in this system. At the same time, the transformation of α -form to β -form owing to the addition of β -NA weakened the diffraction peaks of α -form. The relative content of β -form can be calculated by the well-known Turner-Jones equation^[49].

$$K_{\beta} = \frac{H_{\beta}(300)}{H_{\alpha}(110)+H_{\alpha}(040)+H_{\alpha}(130)+H_{\beta}(300)} \quad (2)$$

Where K_{β} is the relative content of the β -form in the NA nucleated CRPP sample and $H_{\alpha}(110)$, $H_{\alpha}(040)$, $H_{\alpha}(130)$ are the diffraction peak intensities of (110), (040) and (130) crystal planes of α -form in the NA nucleated CRPP sample, respectively. According to equation (2), the relative content of β -form of different NA nucleated CRPPs are 75.28% and 88.82% for WBG-II and TMB-5, respectively. Obviously, TMB-5 shows superiority in inducing β -crystal in CRPP system.

5.2.2 Effect of DCP and TMB-5 content on the crystalline morphology of CRPPs

Fig. 5.3 shows the effect of different content of DCP on the DSC heating scan of CRPP nucleated by TMB-5 (0.3wt %). The two β -crystal melting peaks are also due to the complexity of the β crystal structure during the melting process, as mentioned above, and the broken chain of PP molecular enhanced this process of PP enhanced this process. Xanthos^[50] attributed this fact to the recrystallization and reorganization of the molecules with less entanglement and higher mobility during melting. Peroxide initiated PP degradation has been known as a random chain scission reaction to reduce the number of long chains significantly and result in less entanglement and higher mobility of the molecules. Thus, the recrystallization or reorganization of lower molecular weight samples can occur more easily and faster during melting.

The DSC results from Table 5.2 shows that the crystallinity basically increased with increase of DCP content except for a small decrease at a content of 0.15wt%. Although the

total crystallinity index decreased with the addition of NA, as mentioned above, the crystallinity of β NA nucleated CRPP increased with increase of DCP content. This fact is

Table.5.2 DSC results of PP specimen with different loading contents of DCP incorporated with 0.3wt% TMB-5.

DCP content(%wt)	T _m (°C)	ΔH (J/g)	Crystallinity (%)
0	148.80, 168.30	36.34	21.57
0.05	145.72, 152.11, 168.19	56.48	33.52
0.10	144.73, 151.42, 166.91	85.36	50.66
0.15	143.43, 150.82, 166.90	82.79	49.13

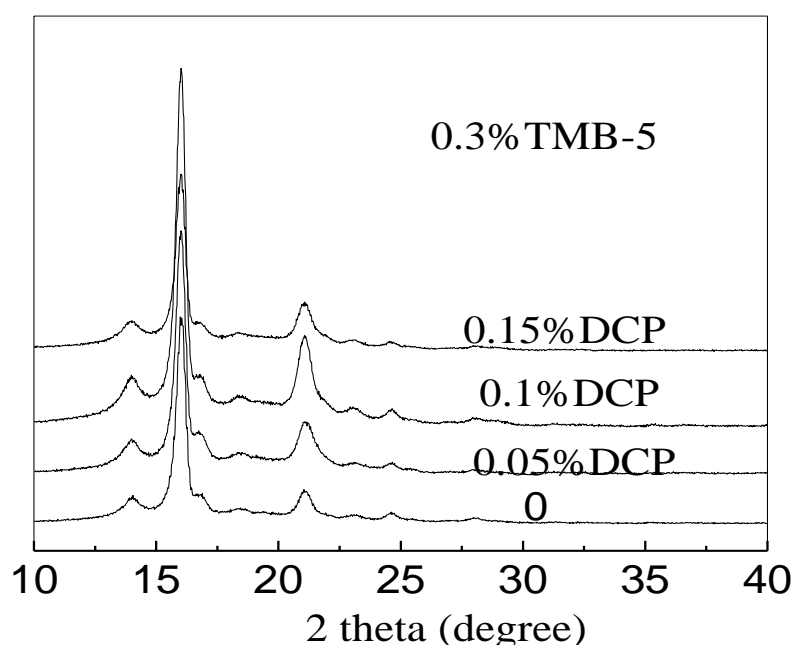


Figure. 5.4. Effect of TMB-5 on the WAXD pattern of CRPP prepared using different contents of DCP.

due to more spaces provided by the broken molecular chains in the CRPP system with increase of the DCP content. Thus, more chains will pack into adjacent crystals easily, and there is enough space for the complete growth of the crystals. The melting peaks of α -crystal shifted to a lower temperature, indicating a thickness reduction of α -crystals. When the DCP content reaches 0.1wt%, there is a critical molecular weight where the molecular chains shorten to a certain level and the number of active sites is optimal. When the content exceeds the critical point, the crystallization of the broken chains will be limited,

or the chains will interact with each other. Finally, crosslinking takes place in CRPP, which is unfavourable for the crystallization process, as there is not enough or even no active sites in the molecular chain to carry out this process.

Fig. 5.4 shows the WAXD patterns of the effect of TMB-5 on CRPP with different DCP contents. The characteristic diffraction peaks of TMB-5 nucleated CRPP prepared using 0.1 wt% DCP is obviously higher than those prepared using other DCP contents in the crystal face of $\alpha(110)$ $\alpha(040)$ $\alpha(130)$ and $\beta(300)$. Combined this fact with the DSC result, the 0.1 wt% DCP content system is suitable to induce complete and high relative β -crystal content.

As the suitable content of DCP for β -crystal was determined as 0.1 wt%, the effect of TMB-5 content on the crystalline morphology was considered at that level. Fig. 5.5 shows the effect of TMB-5 content on the DSC heating curves of CRPP prepared using 0.1 wt% DCP. With the addition of TMB-5, the β melting peak visibly appeared on the DSC curves. The results obtained from the DSC tests are summarized in Table 5.3. It is found that the

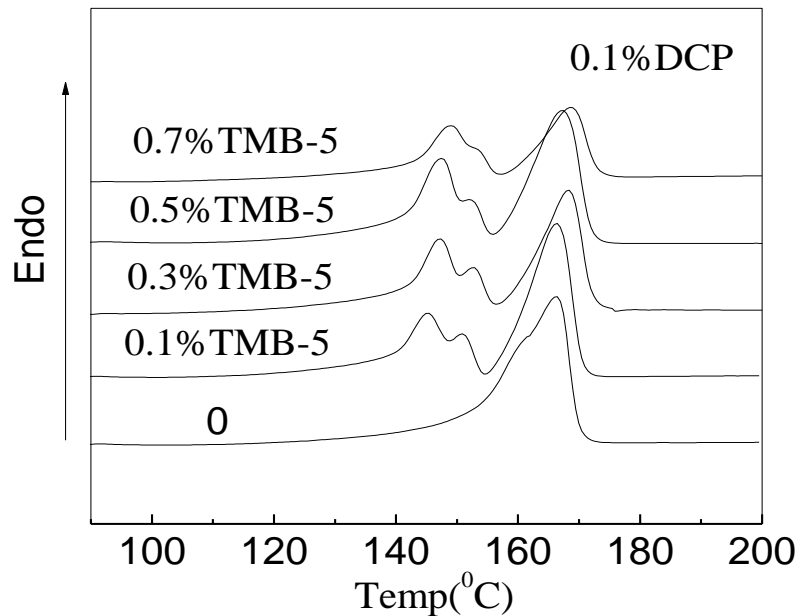


Figure. 5.5. Effect of loading content of TMB-5 on the DSC heating scan of CRPPs.

Table. 5.3 DSC results of CRPP (0.1wt% DCP) specimen incorporated with different loading contents of TMB-5

TMB-5 content (wt%)	T _m (°C)	ΔH(J/g)	Crystallinity (%)
0	166.30	98.16	58.26
0.1	145.20, 150.80, 166.30	100.80	59.82
0.3	147.20, 152.70, 168.30	89.85	53.32
0.5	147.40, 167.20	107.70	63.92
0.7	149.00, 168.70	59.11	35.08

total crystallinity reaches the maximum value at a TMB-5 content of 0.5wt%. Two factors contribute to this: First, the CRPP system is suitable for the high content and complete structure of β -crystals, as mentioned above. Second, the TMB-5 as a nucleating agent in the system is especially active at a content of 0.5wt%. If the NA content exceeds this point, the additional crystal nuclei will take up the limited space in the molten resin and there will not be enough space for them to growth, and the total crystallinity will decrease. Therefore, a TMB content of 0.5wt% is also a critical point for β NA nucleated CRPP.

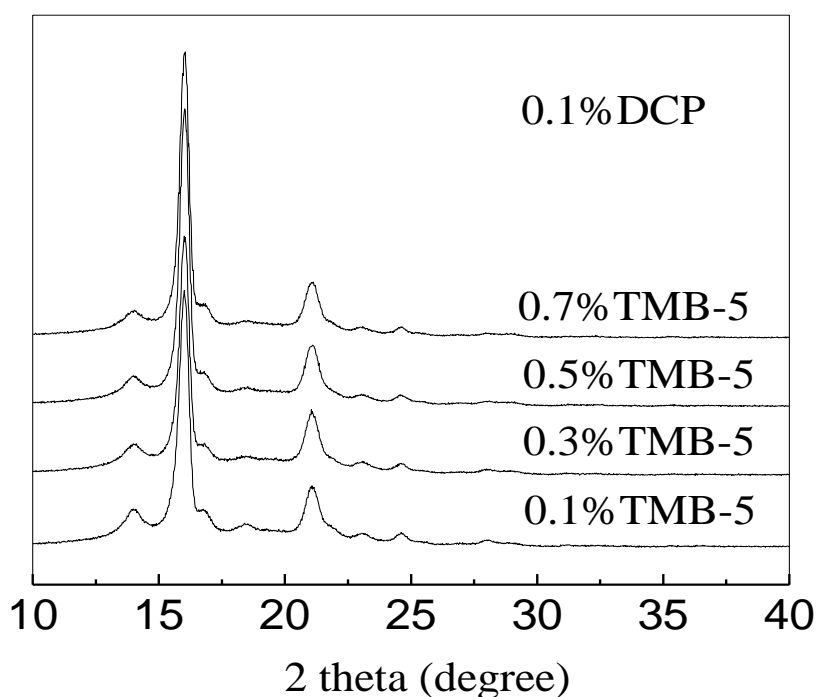


Figure. 5.6. Effect of loading content of TMB-5 on the WAXD pattern of CRPPs.

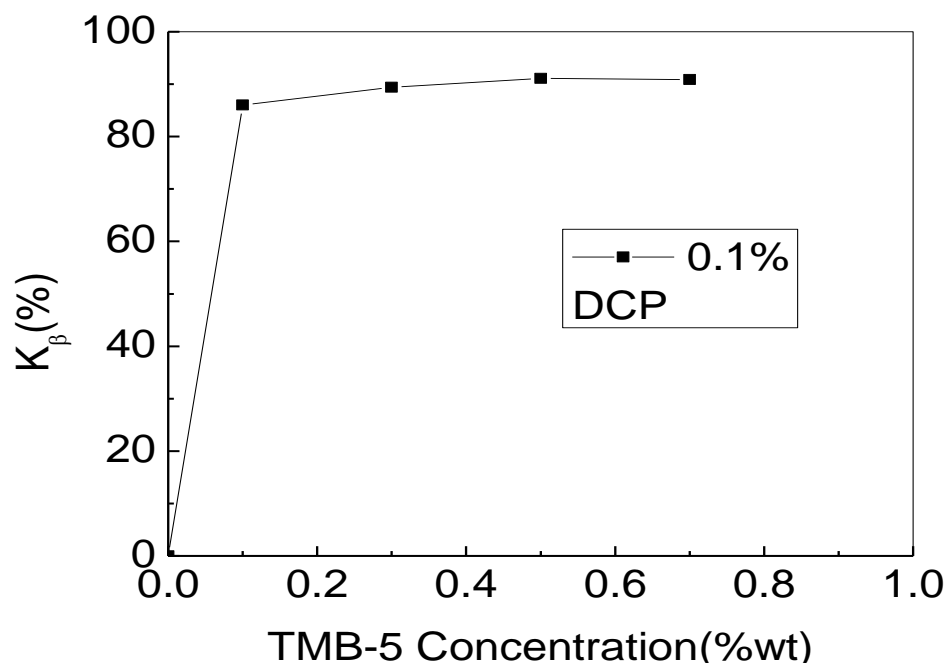


Figure. 5.7. Effect of loading content of TMB-5 on the relative content of β -crystals in CRPPs.

Fig. 5.6 shows the WAXD patterns of TMB-5 nucleated CRPP prepared using 0.1wt% DCP. Evidently, when the NA content reaches 0.5wt%, the intensity of the $\beta(300)$ crystal diffraction peak is significantly higher than that of the other systems, reflecting the highest relative content of β crystals

Fig. 5.7 shows the effect of β NA content on the relative content of β -crystals in CRPP prepared with 0.1wt% DCP. Similarly, with increase of the β NA content, the relative content of β -crystal first increases and then reduces slightly, and the turning point occurs when the NA content reaches 0.5wt%. Due to the crystallization mechanism, only at a certain β NA concentration will complete β -crystals be formed. When the NA content exceed the certain value, the nucleation rate will exceeds the total rate of the crystallization process, so it is too late to form a perfect epitaxial crystallization center for the growth of a complete β -crystal^[51]. At the same time, there is no time for adjusting the PP molecular conformation to meet the requirement for β -crystal formation. Finally, conformational defects arise. Thus, the c axis orderly β -crystal is reduced with the melting point showing a

slight decline, and the α -crystal content increases, leading to a relatively low level of β -crystal content.

5.3. Conclusions

The effects of different β NAs, different DCP content and various β NA content on the crystalline morphology of CRPP were studied in this paper, and the following conclusions were drawn:

(1) The β crystalline melting peaks of WBG-II and TMB-5 nucleated CRPP are clearly shown and shift to a low temperature compared with unnucleated CRPP. The intensity of the β -crystal diffraction peak of TMB-5 modified CRPP is larger than WBG-II.

(2) With the increase of DCP content, the melting temperature of α -crystals increases, and the melting peak of β -crystals is visible in CRPP nucleated with 0.3wt% content of TMB-5. At the critical point of 0.1 wt% DCP, the total crystallinity index of CRPP reaches a maximum value and the relative intensity of diffraction peaks for α and β -crystals are much higher than for other contents.

(3) With increase of the TMB-5 content, the melting peak of β -crystals appears on the DSC heating curves of CRPP prepared using 0.1wt% DCP. With the addition of TMB-5, the maximum value of total crystallinity is reached at a mass fraction of 0.5%. Also, the relative content of β -crystals achieves the maximum value at this point.

5.4 References

- [1] C.deRosa, F. Auriemma, P. Corradini, *Macromolecules*. 29 (1996) 7452-7459.
- [2] G. Kumaraswamy, R.K. Verma, A.M. Issaian, P. Wang, J.A. Kornfield, F. Yeh, B.S. Hsiao, R.H. Olley, *Polymer*. 41 (2000) 8931-8940.
- [3] R.H. Somani, L. Yang, B.S. Hsiao, P.K. Agarwal, H.A. Fruitwala, A.H. Tsou, *Macromolecules*. 35 (2002) 9096-9104.
- [4] S.C. Tjong, J.S. Shen, R.K.Y. Li, *Polym. Eng. Sci.* 36 (1996) 100-105.
- [5] C. Saujanya, S. Radhakrishnan, *Polymer*. 42 (2001) 6723-6731.
- [6] M.J. Solomon, A.S. Almusallam, K.F. Seefeldt, A. Somwangthanaroj, P. Varadan, *Macromolecules*. 34 (2001) 1864-1872.
- [7] G. Barakos, E. Mitsoulis, C. Tzoganakis, *J. Appl. Polym. Sci.* 59 (1996) 543-556

- [6] S.C. Tjong, J.S. Shen, R.K.Y. Li, *Polymer*. 37 (1996) 2309-2316.
- [7] R. Thomann, C. Wang, J. Kressler, R. Mulhaupt, *Macromolecules*. 29 (1996) 8425-8434.
- [8] R. Thomann, J. Kressler, S. Setz, C. Wang, R. Mulhaupt, *Polymer*. 37 (1996) 2627-2638.
- [9] M. Okamoto, P.H. Nam, P. Maiti, T. Kotaka, N. Hasegawa, A. Usuki, *Nano letters*. 1 (2001) 295-298.
- [10] N.V. Pogodina, V.P. Lavrenko, S. Srinivas, H.H. Winter, *Polymer*. 42 (2001) 9031-9043.
- [11] S.C. Tjong, S.L. Liu, R.K.Y. Li, *J. Macro. Sci.* 31 (1996) 479-484.
- [12] S.C. Tjong, S. Bao, *E-Polym.* 31 (1996) 479-484.
- [13] A. Eckstein, J. Suhm, C. Friedrich, R.D. Maier, J. Sassmannshausen, M. Bochmann, R. Mulhaupt, *Macromolecules*. 31 (1998) 1335-1340.
- [14] P.M. Wood-Adams, J.M. Dealy, A.W. deGroot, O.D. Redwine, *Macromolecules*. 33 (2000) 7489-7499.
- [15] A. Nogales, B.S. Hsiao, R.H. Somani, S. Srinivas, A.H. Tsou, F.J. Balta-Calleja, T.A. Ezquerro, *Polymer*. 42 (2001) 5247-5256.
- [16] J.A. Kornfield, G. Kumaraswamy, A.M. Issaian, *Ind. Eng. Chem. Res.* 41 (2002) 6383-6392.
- [17] S.B. Dickson, C. Tzoganakis, H. Budman, *Ind. Eng. Chem. Res.* 36 (1997) 1067-1078.
- [18] X.C. Wang, C. Tzoganakis, G.L. Rempel, *J. Appl. Polym. Sci.* 61(1996) 1395-1404
- [19] J.J. Baik, C. Tzoganakis, *Polym. Eng. Sci.* 38 (1998) 274-281.
- [20] C. Huang, T.A. Duever, C. Tzoganakis, *Polym. React. Eng.* 5 (1997) 1-24.
- [21] M.R. Thompson, C. Tzoganakis, G.L. Rempel, *J. Polym. Sci. Part A: Polym Chem.* 35 (1997) 3083-3086.
- [22] B. Lotz, *Euro. Phys. J.* 3 (2000) 185-194.
- [23] S.C. Tjong, R.K.Y. Li, T. Cheung, *Polym. Eng. Sci.* 37 (1997) 166-172.
- [24] J. Karger-Kocsis, *Polym. Eng. Sci.* 36 (1996) 203-210.
- [25] T. Sterzynski, P. Calo, M. Lambla, M. Thomas, *Polym. Eng. Sci.* 37 (1997) 1917-1927.
- [26] Y. Guan, S.H. Wang, A. Zheng, H.N. Xiao, *J. Appl. Polym. Sci.* 88 (2003) 872-877.
- [27] K. Nagarajan, A.S. Myerson, *Cryst. Growth. Des.* 1 (2001) 131-142.
- [28] B. Pukanszky, J. Moczo, *Macromol Symp.* 214 (2004) 115-134.
- [29] S. Nagasawa, A. Fujimori, T. Masuko, M. Iguchi, *Polymer*. 46 (2005) 5241-5250.
- [30] A. Romankiewicz, T. Sterzynski, W. Brostow, *Polym. Int.* 53 (2004) 2086-2091.
- [31] M. Obadal, R. Cermak, N. Baran, K. Stoklasa, J. Simonik, *Int. Polym. Proce.* 19 (2004) 35-39.

- [32] A. Menyhard, J. Varga, G. J. Molnar, *Therm. Anal. Calor.* 83 (2006) 625-630.
- [33] J. Broda, *J. Appl. Polym. Sci.* 91 (2004) 1413-1418.
- [34] J. Vychopnova, V. Habrova, M. Obadal, R. Cermak, R. Cabla, *J. Therm. Anal. Calor.* 86 (2006) 687-691.
- [35] F. Xiong, R. Guan, Z.X. Xiao, B.L. Xiang, D.P. Lu, *Polym-Plast. Tech. Eng.* 46 (2007) 97-105.
- [36] J. Varga, *J. Macro. Sci. Phys.* 41 (2002) 1121-1171.
- [37] S.W. Wang, W. Yang, G. Gong, B.H. Xie, Z.Y. Liu, M. B. Yang, *J. Appl. Polym. Sci.* 108 (2008) 591-599.
- [38] G. Gong, B.H. Xie, W. Yang, Z.M. Li, W.Q. Zhang, M.B. Yang, *Polym. Test.* 24 (2005) 410-417.
- [39] W. Yang, Z.M. Li, B.H. Xie, J.M. Feng, W. Shi, M.B. Yang, *J. Appl. Polym. Sci.* 89 (2003) 686-690.
- [40] G. Gong, B.H. Xie, W. Yang, Z.M. Li, S.M. Lai, M.B. Yang, *Polym. Test.* 25 (2006) 98-106.
- [41] W. Yang, Z.Y. Liu, G.F. Shan, Z.M. Li, B.H. Xie, M.B. Yang, *Polym. Test.* 24 (2005) 490-497.
- [42] J.X. Li, W.L. Cheung, D.M. Jia, *Polymer.* 40 (1999) 1219-1222.
- [43] A.J. Ryan, J.L. Stanford, W. Bras, T.M.W. Nye, *Polymer.* 38 (1997) 759-768.
- [44] B. Lotz, *Polymer.* 39 (1998) 4561-4567.
- [45] S. Vleeshouwers, *Polymer.* 38 (1997) 3213-3221.
- [46] M. Al-Hussein, G. Strobl, *Euro. Phys. J.* 6 (2001) 305-314.
- [47] T. Sterzynski, P. Calo, M. Lambla., M. Thomas, *Polym. Eng. Sci.* 37 (1997) 1917-1925.
- [48] G. Christelle, *Adv. Polym. Sci.* 188 (2005) 43-104.
- [49] A. TurnerJones, A.M. Aizlewood, D.R. Beckett, *Makromol. Chem.* 75 (1964) 134-158.
- [50] S.H. Ryu, C.G. Gogos, M. Xanthos, *Polymer.* 32 (1991) 2449-2455.
- [51] W. Stocker, M. Schumacher, S. Graff, A. Thierry, J.C. Wittmann, B. Lotz, *Macromolecules.* 31 (1998) 807-814.

Chapter 6 The enhanced nucleating ability of carbon nanotube supported β nucleating agent in isotactic polypropylene

6.1. Introduction

Isotactic polypropylene (iPP), a semi-crystalline polymer with several possible crystal modifications including monoclinic (α), trigonal (β), and orthorhombic (γ) forms ^[1], is widely used in many applications due to its excellent balance between physical properties and low cost ^[2-6]. Among these polymorphs, the β form crystal occurs more rarely than α form crystal because of its lower stability ^[2].

The β crystal of iPP has a trigonal unit cell with parameters $a=b=1.101\text{nm}$, $c=0.65\text{nm}$, containing three isochiral helices. Owing to the different azimuthal orientations of the three helices, the cell of the β phase is frustrated ^[1]. The β phase iPP shows some unique characteristics such as improved impact strength in comparison with the more common α phase ^[7, 8]. Varga attributed the superior toughness of β phase polypropylene (PP) to a combined effect of three factors: the α to β phase transformation, the enhanced mechanical damping and the peculiar lamellar morphology of β phase ^[9].

The β phase can be formed under some special conditions such as addition of β nucleating agent (β NA) into the iPP matrix ^[9-15], directional crystallization in certain temperature gradient ^[16], shearing or elongation of the melt during crystallization ^[17-19]. Among these methods, the introduction of β NA s into iPP is the most reliable method for the preparation of iPP rich in β phase ^[9, 12]. Although several kinds of β NA s have been proposed and patented till now, the compounds of dicarboxylic acid and different Ca compounds has been proved to be a highly selective, thermally stable, and colorless β NA for iPP ^[20]. Grein has pointed out that, if the melting enthalpy of the β phase contributes to 80% or more out of the total enthalpy ^[21], the nucleating agent can be considered as highly active and selective.

It should be noted that although β nucleated iPP shows superior toughness, its yield strength and stiffness are generally much lower than those of non-nucleated iPP or α nucleated iPP ^[22]. Multi-wall Carbon nanotubes (MWCNTs) were widely used in many

areas such as improving the mechanical and electrical properties of polymer based composites due to their unique mechanical and electrical characteristics ^[23-25]. However, due to the nonreactive nature of the carbon nanotube, which have a strong tendency to agglomerate and are very difficult to separate individual nanotubes during mixing with a polymeric material, the preparation of Polymer and MWCNTs composite is generally very difficult.^[26] Different methods have been developed in order to overcome these difficulties. Solution blending, melt blending, and “in situ” polymerization are widely applied techniques to produce nanotube/polymer composites ^[27]. Additionally, the functionalization of the MWCNTs with a number of functional groups has also been used to improve their chemical reactivity and dispersion in polymer materials and can be used as a starting point for further chemical modification ^[28, 29]. Grady et al. observed that octadecylamide-functionalized MWCNTs promoted the growth of β form crystal of PP at the expense of α form crystal ^[30]. However, still some studies showed that MWCNTs can only promoted the formation of α form iPP ^[31].

In this work, a kind of β nucleating agent, calcium pimelate, for PP was supported onto the surface of CNTs and the effect of the supported CNTs on the mechanical properties and morphology of iPP composites were studied. The composites of iPP and MWCNT supported β nucleating agent exhibited excellent impact strength compared with pure isotactic polypropylene and β nucleated isotactic polypropylene without significantly deteriorating the strength and stiffness. The mechanical properties of the composites were correlated with the morphology and the enhanced nucleating ability of the MWCNT supported β nucleating agent.

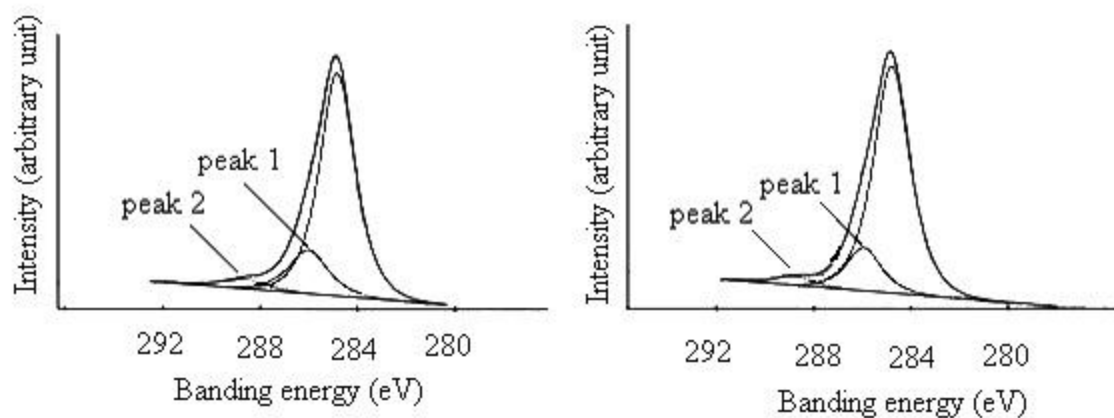
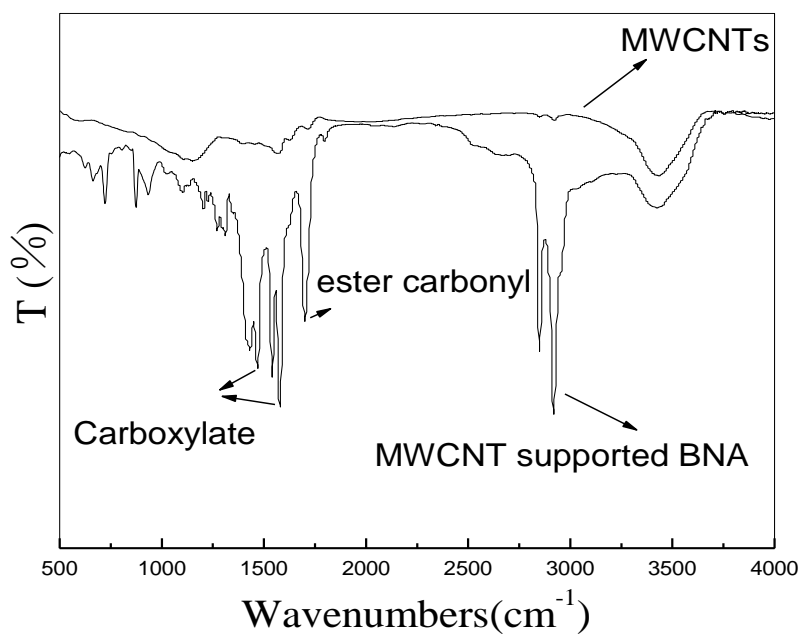


Figure 6.1. XPS spectra of C 1s for MWCNTs (a) and MWCNT supported β NA (b)

Table 6.1. Chemical shift (CS), Relative peak Area, and peak width in C1s Region

Sample	Main peak			Peak1			Peak2		
	B.E. (eV)	area (%)	fwhm (eV)	C.S. (eV)	area (%)	fwhm (eV)	C.S. (eV)	area (%)	fwhm (eV)
CNTs	284.8	78.82	1.69	1.28	17.27	1.89	3.78	3.91	2.09
MWCNT Supported β NA	284.8	81.7	1.76	1.15	15.06	1.69	4.0	3.24	1.82



Figures 6.2. FTIR spectra of MWCNTs and MWCNT supported β NA

6.2. Results and Discussion

6.2.1 Surface analysis

Figure 6.1 shows XPS spectra of C1s for MWCNTs and MWCNT supported β NA, and the fitting results of the curves were shown in Table 6.1. For the MWCNT supported β NA, the peak 1 region was significantly reduced from 17.27% to 15.06%, and the chemical shift of peak 1 was lower than that of MWCNTs sample. According to Wang and Sherwood^[31], the results verified a chemical reaction between β NA and MWCNTs. As the received MWCNTs were chemically treated and hydroxy groups were attached to the tube wall, and the other carboxyl group of calcium pimelate was reactive, the reasonable explanation was that the hydroxy groups reacted with the β NA in the chemical supporting process. In other words, an esterification reaction between β NA and the MWCNTs were performed, and the β NA was chemically supported on the MWCNTs surface.

Figure 6.2 shows the FTIR spectra of MWCNTs and MWCNT supported β NA samples. It showed that an infrared peak appeared at a wavenumber of 1750cm⁻¹, which had been assigned to ester carbonyl group. Also, the peaks at a wavenumber of 1400 cm⁻¹ and 1600 cm⁻¹ had been assigned to carboxylate group. These results further proved that the β NA had been supported on the MWCNT surface.

Table 6.2. Mechanical properties of iPP (Sample P), iPP/MWCNTs (Sample C), β NA nucleated iPP (Sample N) and MWCNT supported β NA modified iPP composites (Sample 1, 3, 5) samples

Samples	Impact strength (kJ/m ²)	Tensile Yield strength (MPa)	Flexural modulus (MPa)
P	3.03	32.05	1282.17
C	5.24	33.14	1407.54
N	7.08	28.18	1078.62
1	7.29	29.87	1231.18
3	14.49	28.51	1138.17
5	22.42	27.63	1133.57

6.2.2 Mechanical properties

Table 6.2 collects the mechanical properties of the samples. As is generally known, pure iPP shows quite low impact strength and the addition of β NA can significantly improve the impact toughness of iPP, which can also be evidenced by the much higher impact strength of β NA nucleated iPP, being more than two times over that of pure iPP. It is interesting that the MWCNTs modified iPP composite shows a simultaneous reinforcing and toughening effect over iPP, which is in accordance with our previous study on the MWCNTs modified iPP composites^[33]. In the presence of MWCNT supported β NA, the iPP composites showed excellent impact strength over pure iPP, beta nucleated iPP and MWCNTs modified iPP composite, up to about 7 times over that of pure iPP and more than 3 times over that of β nucleated iPP. It can also be found that with the increase of the content of MWCNT supported β NA, the impact strength of the composites increased. These results indicated that the MWCNTs showed the potential to promote the formation of β crystals of iPP, and the MWCNTs could cooperate with the β nucleating agent and enhance the nucleating ability of the β nucleating agent, resulting much higher impact toughness of the composites.

Although β nucleated iPP shows high impact strength, the tensile yield strength and the flexural modulus of β nucleated iPP are generally lower than those of non-nucleated or α phase iPP, as can also be seen in Table 6.2. However, with the addition of MWCNT supported β NA, the tensile yield strength of iPP samples increased compared with that of β NA nucleated sample and with the increasing content of MWCNT supported β NA, the yield strength remains at a high level.

The flexural modulus, a signal of the stiffness of materials, for the samples in the presence of MWCNT supported β NA, is much higher than that of β NA nucleated sample. This might be the contribution of the high tensile strength and stiffness MWCNT itself.

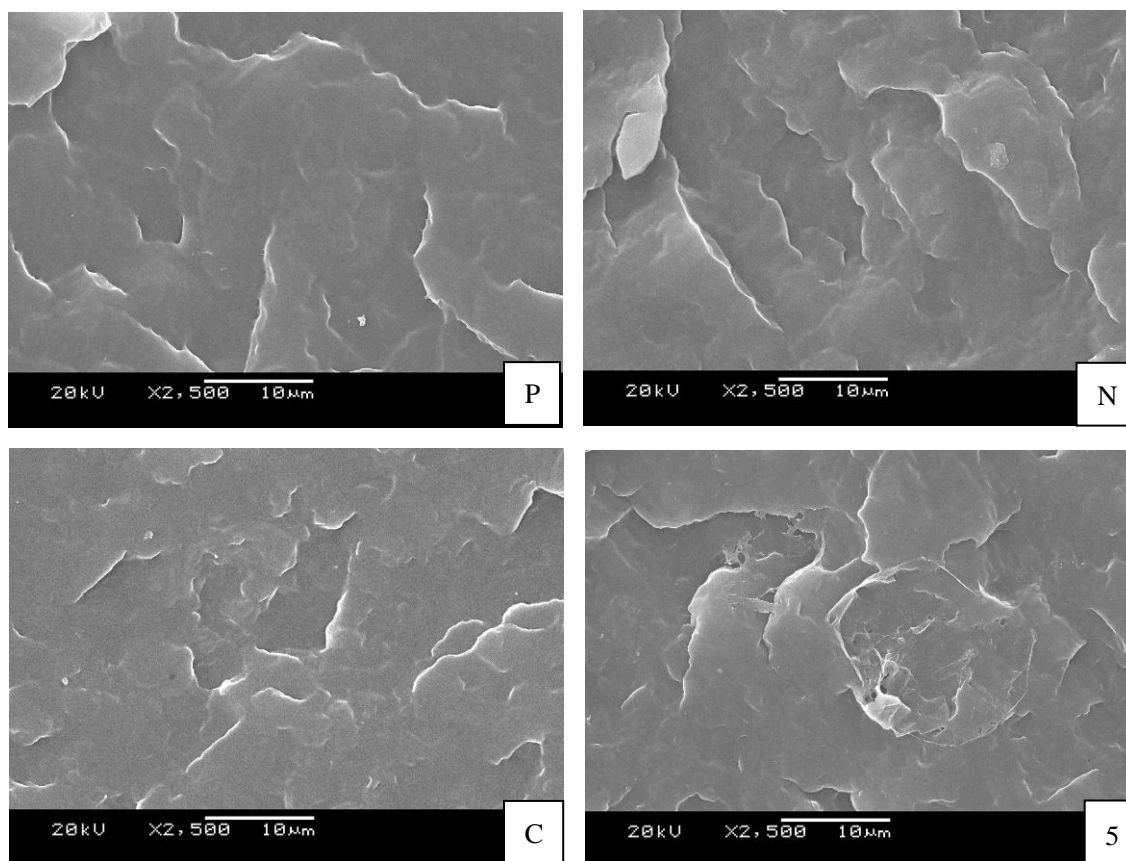
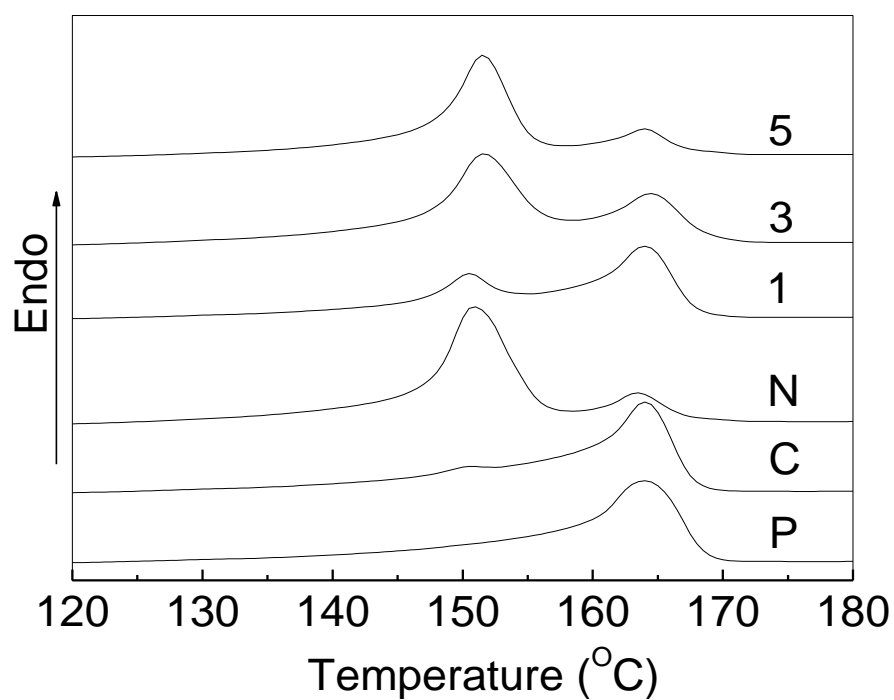


Figure 6.3 SEM photographs of iPP (Sample P), iPP/MWCNTs (Sample C), β NA nucleated iPP (Sample N) and MWCNT supported β NA modified iPP composites (Sample 5)

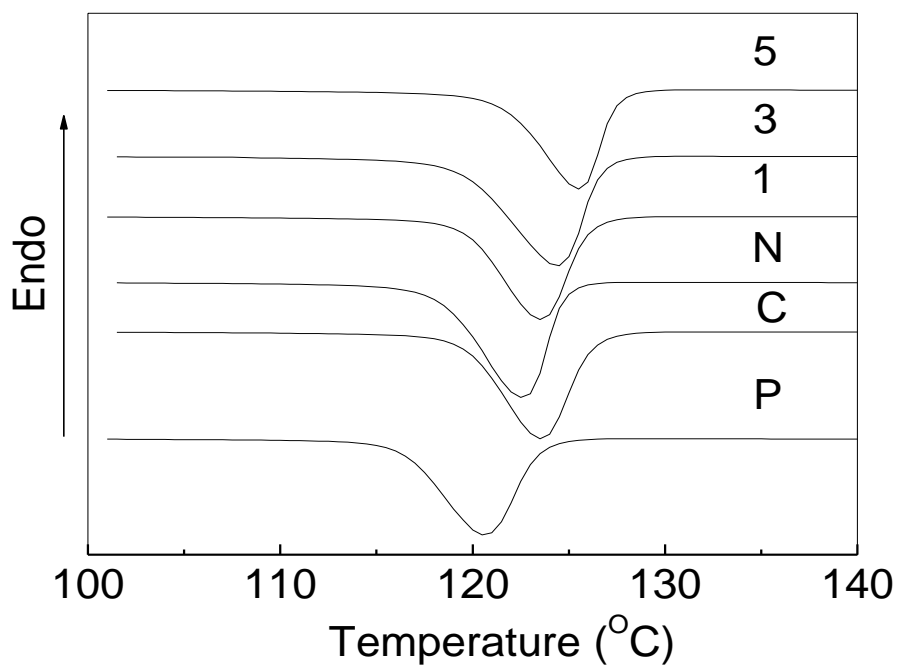
6.2.3 Morphology observation

Figure 6.3 shows the morphology of iPP, iPP/MWCNTs composite, β NA nucleated iPP and MWCNT supported β NA modified iPP composites. In order to avoid the surface damage, no etching procedure was adopted. It can be seen that pure iPP shows an obviously brittle fracture with little indication of plastic deformation. β NA nucleated iPP shows more accidented zones owing to the plastic deformation during the cryogenic fracture in the liquid nitrogen. iPP/MWCNTs composite shows similar plastic deformation as β NA nucleated iPP. MWCNT supported β NA modified iPP composites displays very tough fracture surface, and a ring-shaped morphology appears in the central part of the photo,

which was surrounded by an obvious plastic deformation zone. These observations are in accordance with the mechanical properties of the samples.



(a)



(b)

Figure 6.4. DSC (a) heating and (b) cooling scan of iPP (Sample P), iPP/MWCNTs (Sample C), β NA nucleated iPP (Sample N) and MWCNT supported β NA modified iPP composites (Sample 1, 3, 5) samples

6.2.4 Melting and crystallization behaviours

Figure 6.4(a) gives the DSC heating scan of the samples. As can be seen, β NA nucleated iPP (Sample N) and MWCNT supported β NA modified iPP composites (Sample 1, 3, 5) show two distinct melting peaks at around 151 °C and around 164 °C. The low temperature melting peaks (around 151 °C) in Fig. 6.4.a refer the partial melting of the beta-phase, while the high temperature peaks (around 164 °C) indicate the melting of alpha phase originally presented in the sample and that formed during the beta to alpha recrystallisation. The low temperature melting peaks indicated that the β NA used and the MWCNT supported β NA show the ability to induce the formation of β phase iPP, which can be further verified by the WAXD results. With the content of MWCNT supported β NA increasing, the area under the melting curves of β phase iPP becomes larger, indicating more β phase is induced, which evidences the results of the mechanical properties. The melting curve of iPP/MWCNTs compsite (sample C) also shows a slight melting peak of β

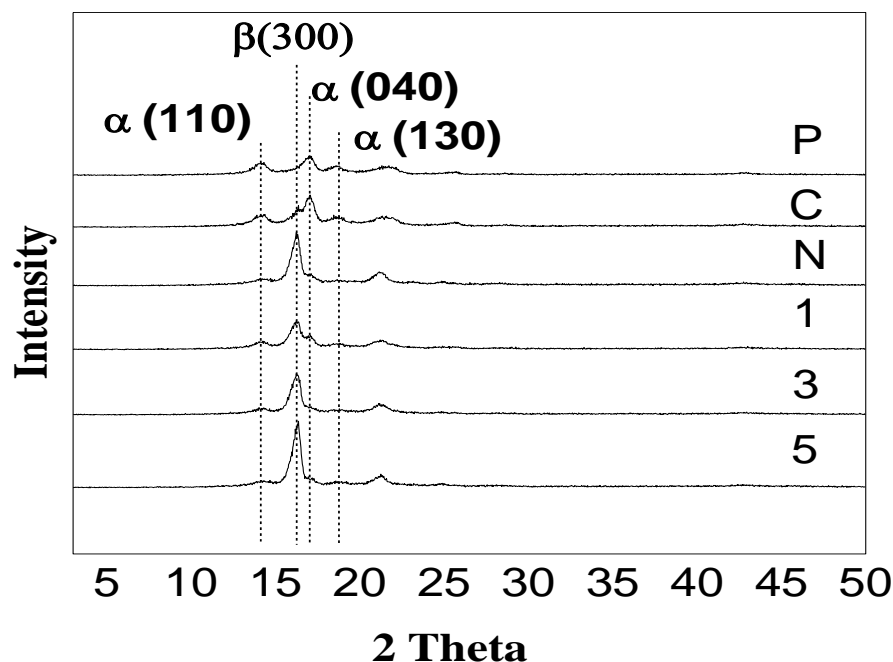


Figure 6.5. WAXD spectra of iPP (Sample P), iPP/MWCNTs (Sample C), β NA nucleated iPP (Sample N) and MWCNT supported β NA modified iPP composites (Sample 1, 3, 5) samples

phase iPP, which affirmed our previous result of low content of MWCNTs has the potential of inducing the formation of β crystal in iPP^[34]. Figure 6.4(b) gives the DSC cooling scan of the samples. It could be seen that the crystallization temperatures (T_c) of all the modified samples were higher than the pure iPP and β NA nucleated iPP, indicating that the crystallization process of the samples were advanced to a higher temperature. With the content of MWCNT supported β NA increasing, the T_c s increased, which was beneficial to reduce the molding cycle of the composites.

Figure 6.5 shows the WAXD curves for all these samples. Comparison of the WAXD patterns revealed that a reflection at 2θ of 16.2° , the characteristic reflection of β phase iPP, occurred for iPP/MWCNTs compsite, β NA nucleated iPP and MWCNT supported β NA modified iPP composites, while pure iPP gave a diffraction pattern characteristic of α phase of iPP. These results were in accordance with the DSC measurements. With the content of MWCNT supported β NA increasing, the intensity of the reflection at 2θ of 16.2° increased, being much higher than that of iPP/MWCNTs compsite (sample C) and β NA nucleated iPP

(Sample N), indicating the enhancement the β nucleating ability of MWCNT supported β NA.

According to the Equation (1) [3]

$$k_{\beta} = \frac{I_{\beta 1}}{I_{\beta 1} + I_{\alpha 1} + I_{\alpha 2} + I_{\alpha 3}} \quad (1)$$

Table 6.4. k_{β} results of iPP (Sample P), iPP/MWCNTs (Sample C), β NA nucleated iPP (Sample N) and MWCNT supported β NA modified iPP composites (Sample 1, 3, 5) samples

Samples	P	C	N	1	3	5
k_{β}	0	0.25	0.75	0.56	0.82	0.84

the relative measurement of beta-modification of iPP can be obtained from the data of the WAXD curves, which was listed in Table 6.4. Here, $I_{\beta 1}$ is the intensity of the (300) reflection of β phase and $I_{\alpha 1}$, $I_{\alpha 2}$ and $I_{\alpha 3}$ are the intensities of the (110), (040) and (130) reflections of α phase, respectively. It could be seen that the k_{β} value increased with the increasing content of MWCNT supported β NA, which agreed well with the mechanical properties and confirmed that the β nucleating ability of β NA for iPP was effectively enhanced with the chemical supporting of β NA onto the surface of carbon nanotube.

6.3. Conclusions

A novel approach to largely improve the impact toughness without significant loss of the stiffness and strength of iPP composites was accomplished. The prepared MWCNT supported β NA can successfully enhance the β nucleating ability of β NA and can induce higher content of β phase of iPP and significantly improve the impact toughness of iPP based composites with little loss of stiffness and strength.

6.4 References

- [1] Lotz B, Wittmann JC, Lovinger AJ (1996) Polymer 37:4979-4992.
- [2] Padden FJ, Keith HD (1959) J Appl Phys 30:1479-1484.
- [3] Turner Jones A, Aizlewood JM, Beckett DR (1964) Makromol Chem 75:134-158.

- [4] Zhou TH, Ruan WH, Rong MZ, Zhang MQ, Mai YL (2007) *Adv Mater* 19:2667-2671.
- [5] Wang SW, Yang W, Gong G, Xie BH, Liu ZY, Yang MB (2008) *J Appl Polym Sci* 108:591-597.
- [6] Wang SW, Yang W, Xu YJ, Xie BH, Yang MB, Peng XF (2008) *Polym Test* 27:638-644.
- [7] Tjong SC, Shen JS, Li RKY (1995) *Scripta Metallurgica et Materialia* 33:503-508.
- [8] Karger-Kocsis J, Varga J, Ehrenstein GW (1997) *J Appl Polymer Sci* 64:2059-2066
- [9] Varga J (2002) *J Macro Sci Phys* 41:1121-1171.
- [10] Varga J, Ehrenstein M (1999) *J Therm Anal Calorim* 56:1047-1057.
- [11] Varga J, Menyhárd A (2007) *Macromolecules* 40: 2422-2431.
- [12] Varga J (1986) *J Therm Anal* 31:165-172.
- [13] Menyhárd A, Varga J (2006) *J Therm Anal* 83:625-630.
- [14] Zhao SC, Cai Z, Xin Z (2008) *Polymer* 49:2745-2754.
- [15] Li J, Cheung W (1998) *Polymer* 39:6935-6940.
- [16] Norton DR, Keller A (1985) *Polymer* 26:704-716.
- [17] Leugering HJ, Kirsch G (1973) *Schmelze Angew Makromol Chem* 33:17-23
- [18] Varga J, Karger-Kocsis J (1996) *J Polymer Sci Part B Polymer Phys* 34:657-670
- [19] Varga J, Ehrenstein GW (1996) *Polymer* 37: 5959-5963
- [20] Varga J, Mudra I, Ehrenstein GW (1999) *J Appl Polym Sci* 74:2357-2368.
- [21] Christelle G (2005) *Toughness of Neat, Adv Polym Sci* 188:43-104.
- [22] Karger-Kocsis J, Varga J (1996) *J Appl Polym Sci* 62:291-300.
- [23] Yu MF, Lourie O, Dyer MJ, Moloni K, Kelly TF, Ruoff RS (2002) *Science* 287:637-640.
- [24] Ruan WH, Huang XB, Wang XH, Rong MZ, Zhang MQ (2006) *Macromol Rapid Commun* 27:581-585.
- [25] Treacy MJ, Ebbesen TW, Gibson JM (1996) *Nature* 381:678-680.
- [26] Vega JF, Martínez-Salazar J, Trujillo M, Arnal ML, Müller AJ, Bredeau S, Dubois Ph (2009) *Macromolecules* 42: 4719-4727.
- [27] Bredeau S, Peeterbroeck S, Bonduel D, Alexandre M, Dubois Ph (2008) *Polym Int* 57: 547-553.
- [28] Boul PJ (1999) *Chem Phys Lett* 310:367-372.
- [29] Stevens JL, Huang AY, Peng H, Chiang IW, Khabashesku VN, Margrave JL (2003) *Nano Lett* 3:331-336.
- [30] Grady BP, Pompeo F, Shambaugh RL, Resasco DE (2002) *J Phys Chem B* 106:5852-5858.

- [31] Bhattacharyy AR, Sreekumar TV, Liu T, Kumar S, Ericson LM, Hauge H, et al (2003) Polymer 44:2373-2377.
- [32] Li JX, Cheung WL (1997) J Vin Addit Techn 3:151-156.
- [33] Yin CL, Liu ZY, Yang W, Yang MB, Feng JM (2009) Colloid Polym Sci 287:615-620.
- [34] Wang TJ, Sherwood PMA (1994) Chem. Mater 6:788-795.

Chapter 7 Superior mechanical properties in carbon nanotube modified polypropylene composites through formation of a beta transcrystalline structure

7.1. Introduction

The transcrystallinity is a kind of common exist crystalline morphology in material research, especially in the polymer/fiber composites. Although the effect of interfacial transcrystalline morphology^[1] on the mechanical properties of polymer / fiber composites remains an issue of contention^[2-5], many researches agree with the improvement of mechanical properties in fiber filled polymers in the presence of transcrystallinity^[6-9]. Wagner reported that the toughness of the polypropylene composites can be improved by careful design of the interfacial transcrystalline region^[10].

Beta transcrystallinity is a kind of transcrystallinity which attracts many attentions in polymer science because of its contribution on high impact resistance of polymer matrix. To explore the formation mechanism of beta transcrystallinity, Varga has investigated the different crystal growth process of beta cylindrite crystals and beta transcrystallinity in isotactic polypropylene (iPP) / carbon fiber (CF) micro-composites ^[11]. He found that the difference exist in the heterogeneous nucleation and self nucleation for transcrystallinity and cylindrite, respectively. Due to the heterogeneous nucleation growth of transcrystalline morphology, the formation of beta transcrystallinity in iPP matrix is difficult under normal conditions ^[12].

Till now, the beta transcrystallinity of PP has been found to be formed by shearing in the micro-composites ^[11] or by using beta nucleating agent (β NA) ^[13-15]. The interfacial morphology of single CF reinforced iPP composites was reported by many researches ^[16-18]. By shearing in the micro-composites melt is a direct-viewing way to investigate the formation of iPP beta transcrystallinity, while the utilization of this method is limited in the micro-composite system and hard to extend to other systems.

It is reported that the enhanced nucleation density contributes to the formation of transcrystalline morphology in the interfacial region of polymer / fiber composites ^[6, 11, 19]. As shown in many reports, nucleating agent (NA) can greatly increase the nucleation density ^[13-15]. If it is perfectly introduced into the fiber/polymer composites, NA can effectively induce the transcrystalline morphology in the composites. Assouline successfully induced the beta transcrystallinity in iPP composites by application of red quinacridone as a beta nucleating agent (β NA), he also explored the kinetics of beta transcrystallization in fiber reinforced iPP composites ^[20].

Wagner ^[10] also demonstrated that the transcrystallinity can be formed at the surface of fiber if appropriate nucleating agents were used to coat the fiber. These agents can nucleate either the α (monoclinic) or β (hexagonal) crystal forms of polypropylene. While, if the combination of β NA and fiber is only via van der Waals force, β NA will flake off easily during the following molding processes, such as extrusion or injection molding.

Chemical modification of fiber surface has been accepted to be a method to improve fiber/matrix adhesion ^[21]. The impact resistance of the matrix can be improved by the

increase of the interaction between filler and matrix ^[22, 23]. By chemically supporting the beta nucleating agent onto the surface of CF or carbon nanotubes (CNTs), the transcrystalline morphology can be induced in CF/PP or CNTs/PP composites. The method of chemical modification has been used in this work, and the beta transcrystalline morphology was affirmed by polarized light microscopy and scanning electron microscopy in beta nucleating agent supported single carbon fiber filled iPP micro-composite and the beta nucleating agent supported CNTs modified iPP composites, respectively. Also, the relationship between the transcrystalline morphology and the impact resistance of β NA supported CNTs modified iPP injection molded samples will be explored.

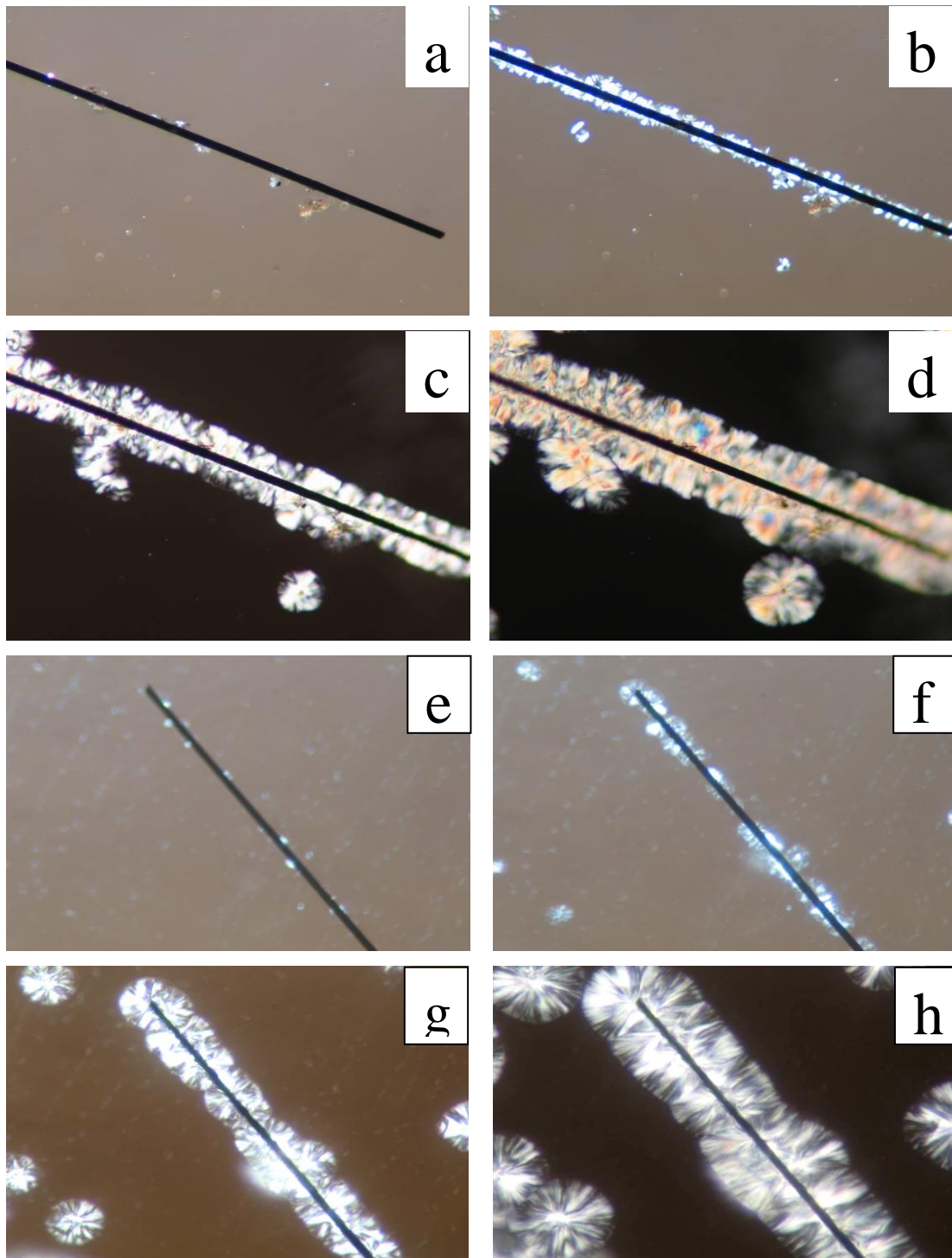


Figure. 7.1 The morphology of beta (a,b,c,d) and alpha (e,f,g,h) transcrystallinity formed during crystallization of beta nucleating agent supported single CF filled iPP micro-composite at 125 °C: (a,e) isothermal crystallizing for 10s; (b,f) isothermal crystallizing for 120s; (c,g) isothermal crystallizing for 240s; (d,h) isothermal crystallizing for 360s

7.2 Results and discussion

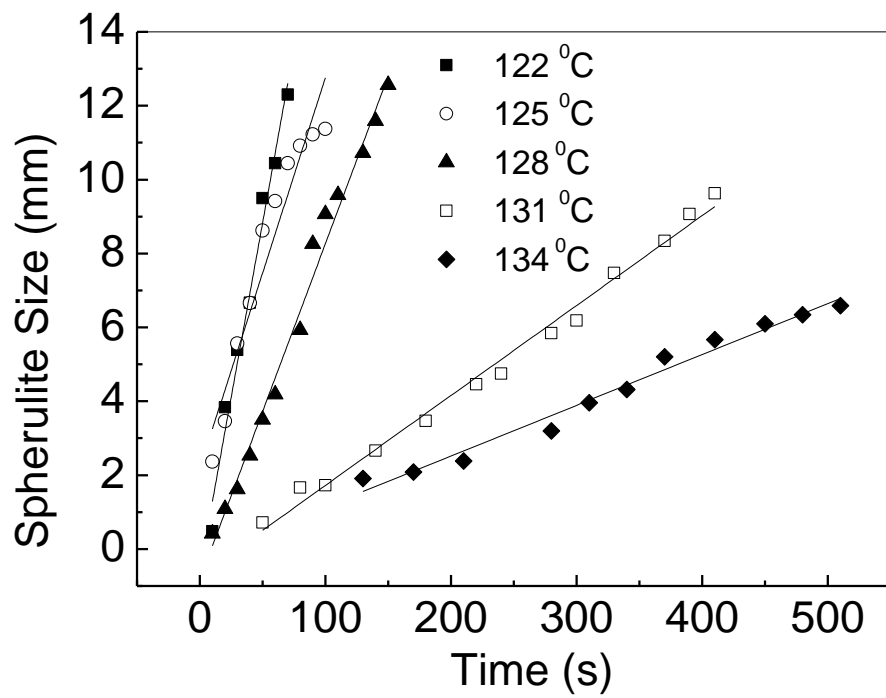
7.2.1 Crystalline morphology development in micro-composites.

Figure 7.1 shows the crystalline morphology of iPP micro-composites in the presence of the beta nucleating agent chemically supported single carbon fiber and virgin carbon fiber without β NA supported, respectively. For each sample, four photographs were taken from 10-360s during the isothermal crystallization process at 125 °C. At the beginning, after 10s isothermal crystallization, there is hardly no heterogeneous nucleation occurred on the carbon fiber surface as shown in Figure 7.1(a). The situation improved after isothermal crystallization for 120s as shown in Figure 7.1(b), a few nucleating points appeared on the surface of the carbon fiber and it started to grow around the carbon fiber surface. While after 240s as given by Figure 7.1(c), the fiber surface was covered by the crystals growing from the heterogeneous nucleation with high nucleation density.

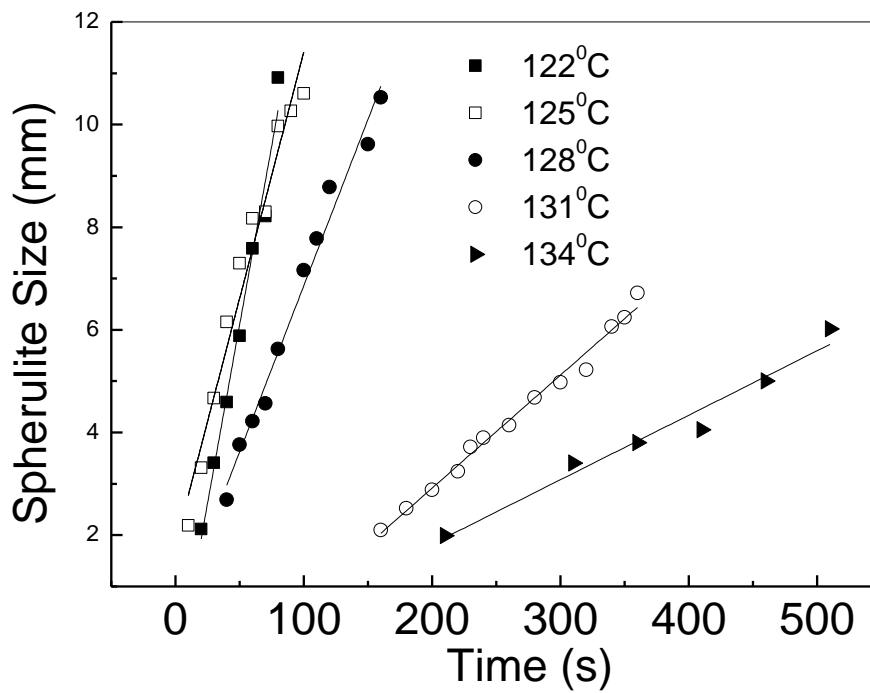
At the interphase region of the micro-composite, the growth of lamellae was restricted in the lateral directions by neighboring entities, and then the growth direction of such surface nucleated crystals was normal to the surface ^[27]. In this way, a transcrystalline morphology finally formed in the micro-composites as can be seen from Figure 7.1(d).

Assouline illustrated that an alpha transcrystalline layer was first promoted on the surface of fiber ^[20]. Figure 7.1 (e-h) shows a typical alpha transcrystallinity in iPP/single CF micro-composites obtained at the same condition of Figure 7.2(a-d). Compared with Figure 7.1 (e-h), the alpha layer was not very obvious in Figure 7.1(a-d). Furthermore, the growth of crystals on the single CF surface reflects a beta form transcrystallinity, which has a negative radial texture compared with the alpha one.

A number of studies have shown that the beta transcrystallinity of iPP can be formed under a certain temperature region of 130 °C or certain condition such as melt shearing. In this work, the beta transcrystalline morphology formed easily at 125 °C. The special interfacial morphology was attributed to crystalline structure transition induced by the β NA supported single CF.



(a)



(b)

Figure 7.2 Relationship between temperature and spherulite size of iPP (a) and iPP induced by β NA supported CF (b).

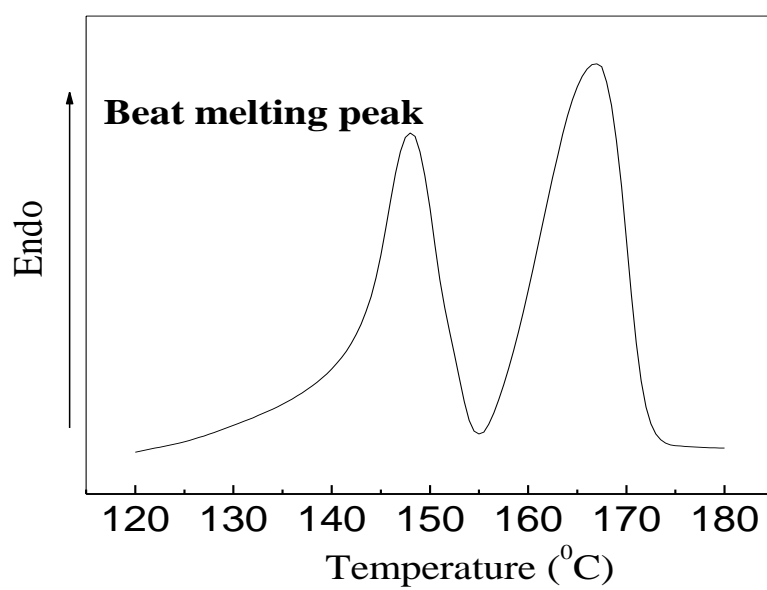
Moreover, the dynamic of crystal growth at different temperature was investigated by performing the PLM tests to get the results of spherulite size at different time. The spherulite size increased with extending time at the fixed temperature, as can be seen from Figure 7.2. There existed a fluctuate of the data point at the temperature of 125⁰C for the sample of iPP induced by β NA supported single CF. The variation of the spherulite size confirmed that a crystalline structure transition taken place at this temperature, that is the formation of transcrystallinity. The slope and Y-intercept results calculated from the curves were shown in Table 7.1. The slope of the curves for iPP filled by β NA supported single CF were higher than the pure iPP, which indicated that the growth of the crystals were accelerated by filling of β NA supported single CF. By a comparison of the size of crystal at the beginning, the filling of β NA supported single CF can reduce the size of the crystal because of the grain refinement.

Table 7.1 The slope and Y-intercept results calculated from the curves of Figure 6.2.

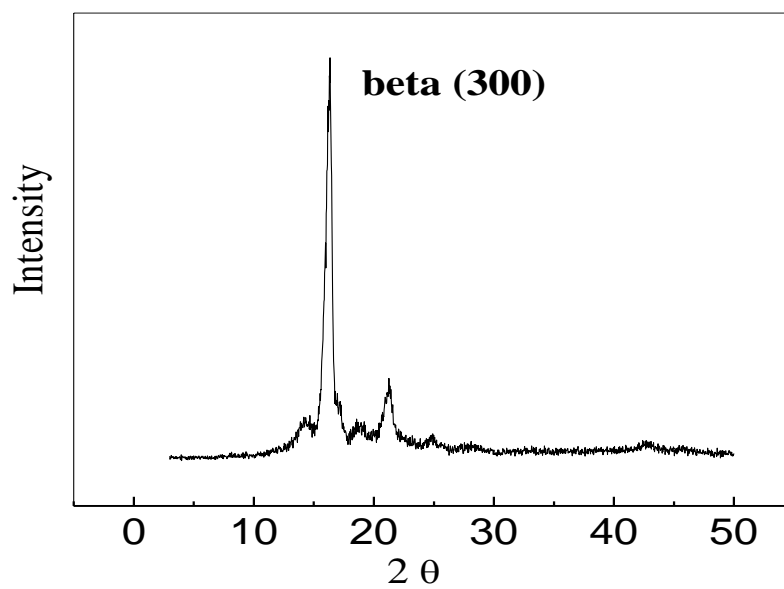
Type	T(⁰ C)	122	125	128	131	134
Pure iPP slope		0.14	0.10	0.07	0.02	0.01
β NA supported single CF filled iPP slope		0.19	0.11	0.10	0.02	0.01

7.2.2 Crystalline structure validation.

To validate the crystalline morphology in the micro-composites, DSC and WAXD tests were performed on the interphase region of the micro-composites near beta nucleating agent chemically supported carbon fiber. The results were given in Figure 7.3. As can be seen from Figure 7.3(a), in the melting curve of the micro-composite, a significant endothermic peak appears at 148 °C, which was assigned to the melting of beta crystals of iPP [15, 25]. Fig.7.3 (b) shows that a diffraction peak appears at the 2 theta angle of 16.30, which was assigned to the (300) diffraction of beta crystals of iPP [28]. Both results further



(a)



(b)

Figure. 7.3 β NA supported single CF filled iPP micro-composite (a) Melting behaviour (b) WAXD

curve

proved the transcrystalline morphology induced by the beta nucleating agent chemically supported carbon fiber was beta transcrystallinity of iPP.

7.2.3 Crystalline morphology in injection samples.

The beta transcrystallinity have been induced in the beta nucleating agent supported single CF filled iPP micro-composites, the next step is how to enlarge its application and extend to other system besides micro-composites. Figure 7.4 (a-d) shows the etched fracture surface of β NA chemically supported MWCNTs modified iPP injection samples. The typical sector texture in Figure 7.4(a-d) indicates that the β NA chemically supported MWCNTs successfully induced beta crystals in the matrix ^[11]. It should be pointed out that in Figure 7.4 (a-d) carbon nanotube was across the sector texture and the crystal growth direction was perpendicular to the nanotube surface, especially at the near core layer of the samples in Figure 7.4(d).

Due to the morphology and growth mechanism of the crystals, it is reasonable to illustrate that the beta transcrystallinity had formed in the interphase region of modified iPP injection molded samples. The parallel caves in the Figure 7.4(a) assumed to be the β NA supported MCNTs, which have induced the beta transcrystallinity, flaked off during the later processing. As the length of the MWCNTs have a wide distribution, short MWCNTs prefer to appear in the skin layer during the injection molding process.

For comparison, the etched surface of virgin without β NA supported MWCNTs modified iPP injection samples were shown in Figure 7.4(e-h). Although the sector texture can also be seen from Figure 7.4(e) as a result of the exist β NA, the MWCNTs in the iPP matrix showed a random distribution. No sector texture was founded near the caves of the skin layer in Figure 7.4(e), as well as no nanotube transfixes the crystals in Figure 7.4(f) and Figure 7.4(g). Further more, in the near core layer as shown in Figure 7.4(h), the nanotube even showed a bended morphology which indicated that the nanotube seems to be expelled by the near crystals instead of transfixing it. So no beta transcrystalline morphology was formed in the MWCNTs without chemically supported β NA modified iPP injection molded samples.

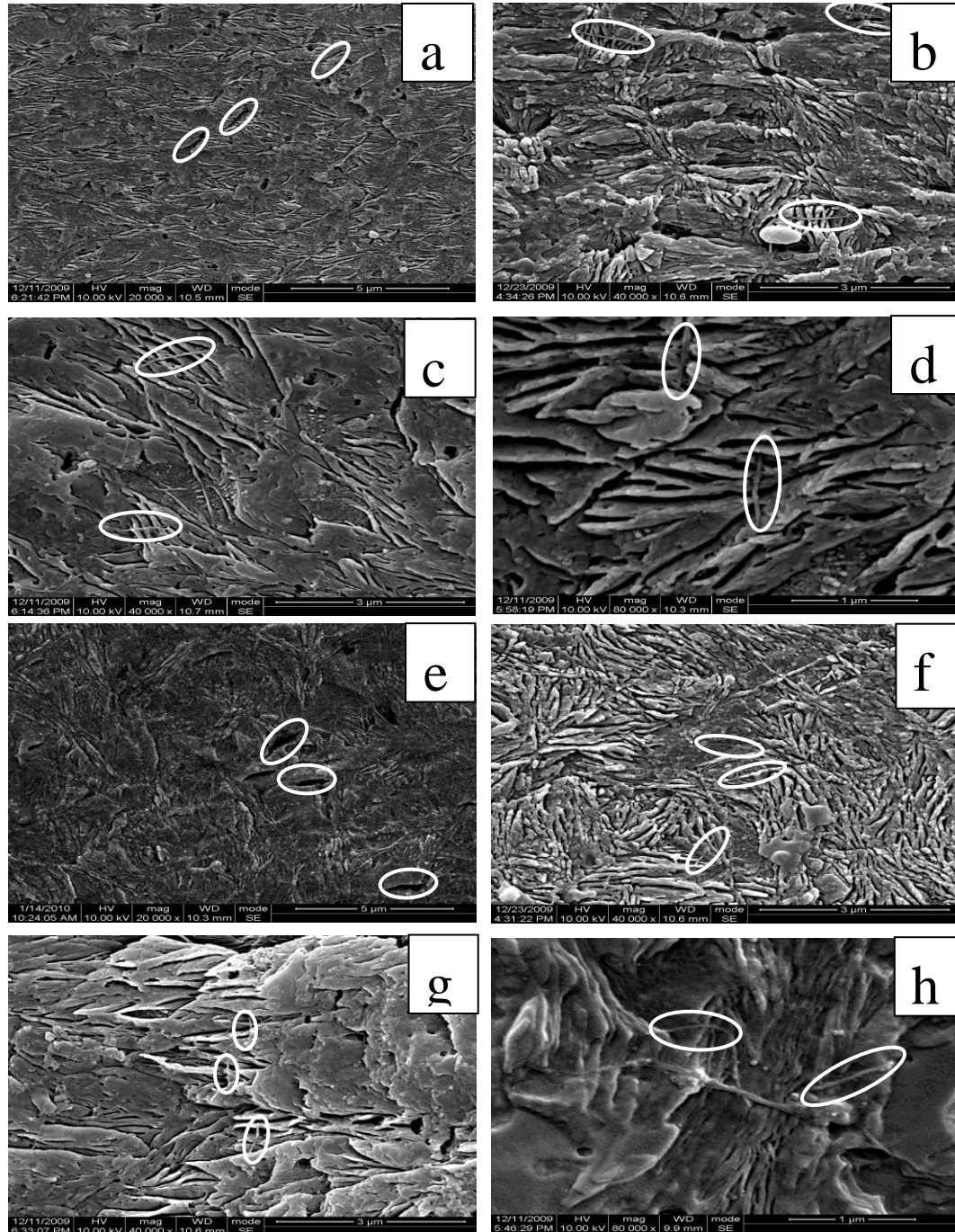


Figure 7.4 SEM images of β NA chemically supported (a, b, c, d) and unsupported (e, f, g, h) MWCNTs modified iPP composites. The samples were perpendicular to the flow direction. (a,e) 0 μ m (b,f) 200 μ m (c,g) 800 μ m (d,h) 2000 μ m from the skin to core layer of the injection molded samples.

7.2.4 Relationship between crystalline morphology and mechanical properties.

It has been reviewed that the nanometer scale may not always be able to significantly influence the performance of the finally products ^[23]. In our previous work, the impact strength of β NA supported MWCNTs modified iPP was seven times that of pure iPP and three times that of β NA modified iPP samples. This result has been attributed to the enhanced nucleating ability of β NA supported CNTs ^[15]. Now, it can be further conformed that the enhanced nucleating ability was attribute to the formation of beta transcrystalline morphology in the interphase region of β NA supported MWCNTs modified iPP injection molded samples. The transcrystallinity can greatly improve the impact resistance of modified iPP samples, which was in accordance with the previous work ^[6-9,15].

7.3 Conclusion

The beta transcrystalline morphology can be formed in both iPP/single fiber micro-composites and β NA supported CNTs modified iPP injection molded samples. The seven times improvement of impact resistance of β NA supported CNTs filled iPP injection molded samples were attributed to the formed interfacial beta transcrystallinity.

7.4 References

- [1] Quan, H.; Li, Z. M.; Yang, M. B.; Huang, R. *Compos. Sci Technol.* 2005, 65, 999.
- [2] Klein, N.; Marom, G.; Pegoretti, A.; Migliaresi, C. *Composites* 1995, 26, 707.
- [3] Stern, T.; Teishev, A.; Marom, G. (1997). *Compos. Sci Technol.* 2000, 57, 1009.
- [4] Son, S. J.; Lee, Y. M.; Im, S. S. *J. Mater. Sci.* 2000, 35, 5767.
- [5] Nuriel, H.; Klein, N.; Marom, G. *Compos. Sci Technol.* 1999, 59, 1685.
- [6] Amash, A.; Zugenmaier, P. *Polymer* 2000, 41, 1589.
- [7] Amash, A.; Zugenmaier, P. *Polym. Bull.* 1998, 40, 251.
- [8] Zafeiropoulos, N. E.; Baillie, C. A.; Matthews, F. L. *Composites Part A.* 2001, 32, 525.
- [9] Pompe, G.; Mader, E. *Compos. Sci Technol.* 2000, 60, 2159.
- [10] Wagner, H. D.; Lustiger, A.; Marzinsky, C. N.; Mueller, R. R. *Compos. Sci Technol.* 1993, 48, 181.
- [11] Varga, J.; Karger-kocsis, J. *Polymer* 1995, 36, 4877.
- [12] Vendramini, J.; Bas, C.; Merle, G.; Boissonnat, P.; Alberola, N. D. et al. *Polym Compos.* 2000, 21, 724.
- [13] Bai, H. W.; Wang, Y.; Zhang, Z. J.; Han, L.; Li, Y. L.; Liu, L.; Zhou, Z. W.; Men, Y. F. *Macromolecules* 2009, 42,

6647.

- [14] Abraham, T. N.; Wanjale, S. D.; Báány, T.; Karger-Kocsis, J. *Composites Part A*. 2009, 40, 662.
- [15] Wang, S. W.; Yang, W.; Bao, R. Y.; Wang, B.; Xie, B. H.; Yang, M. B. *Colloid. Polym. Sci.* 2010, 288, 681.
- [16] Gresó, A.-J.; Phillips, P.-J. J. *Adv. Mater.* 1994, 25, 5.
- [17] Thomason, L.; Rooyen, A. A. J. *Mater. Sci.* 1992, 27, 889.
- [18] Mobbs.; S. Y. *Nature, Phys. Sci.* 1971, 234, 12.
- [19] Joseph, P. V.; Joseph, K.; Thomas, S.; Pillai, C. K. S.; Prasad, V. S.; Groeninckx, G.; Sarkissova, M. *Composites. Part. A*. 2003, 34, 253.
- [20] Assouline, E.; Pohl, S.; Fulchiron, R.; Gerard, J. F.; Lustiger, A.; Wagner, H. D.; Marom, G. *Polymer* 2000, 41, 7843.
- [21] SalehiMobarakeh, H.; AitKadi, A.; Brisson, J. *Polym. Eng. Sci.* 1996, 36, 778.
- [22] Zhou, T. H.; Ruan, W. H.; Rong, M. Z.; Zhang, M. Q.; Mai, Y. L. *Adv. Mater.* 2007, 19, 2667.
- [23] Hu, G. H.; Hoppe, S.; Feng, L. F.; Fonteix, C. *Chem. Eng. Technol* 2007, 62, 3528.
- [24] Li, J. X.; Cheung, W. L. J. *Vin. Addit. Techn.* 1997, 3, 151.
- [25] Varga, J.; Menyárd, A. *Macromolecules* 2007, 40, 2422.
- [26] Olley, R. H.; Bassett, D. C. *Polymer* 1982, 3, 1707.
- [27] Sukhanova, T. E.; Lednicky, F.; Urban, J.; Baklagina, Y. G.; Mikhailov, G. M.; Kudryavtsev, V. V. J. *Mater. Sci.* 1995, 30, 2201.
- [28] Wang, S. W.; Yang, W.; Xu, Y. J.; Xie, B. H.; Yang, M. B.; Peng, X. F. *Polym. Test* 2008, 27, 638.

Chapter 8 Effect of filler on the structure and properties of polypropylene blends

8.1 Introduction

The crystallization behaviours are characterized with the nucleation and crystal growth rates. Based on Norimasa's research^[1], the crystal growth rate remarkably decreases with the molecular weight, while the primary nucleation rate shows the opposite dependence. Molecular weight dependence of overall crystallization rate seems to be very complicated. In this part, a controlled molecular weight distribution iPP blends will be obtained, and it will be modified by β NA, carbon nanotube, as well as β NA supported MWCNTs. The structure and properties relationship of the modified iPP will be investigated.

8.2 Results and discussions

8.2.1. The selection of the isotactic polypropylenes proportion

In this part, all the samples were prepared according to the Table 2.2 and processed in the micro-compounder at the temperature of 200°C with a screw speed of 70r/min.

Table. 8.1 The DSC results of the iPP blends with different proportion.

Number	Heating peak(°C)	Cooling peak(°C)
1	163.55	113.56
2	165.89	112.47
3	159.81	113.20
4	162.38	115.23
5	160.48	113.24
6	160.44	113.47
7	167.97	113.74

The DSC results of the samples were collected in the following Table 8.1. Taking the cooling peak temperature into account, the highest cooling peak temperature can be found at sample 4. This fact indicated that the molecular structure of iPP blend is at a favourite state for crystallization. For the melting peak temperature, the sample 4 was under a middle

state, which shows that the higher molecular part and the lower one were all take a certain part in the two iPP blend.

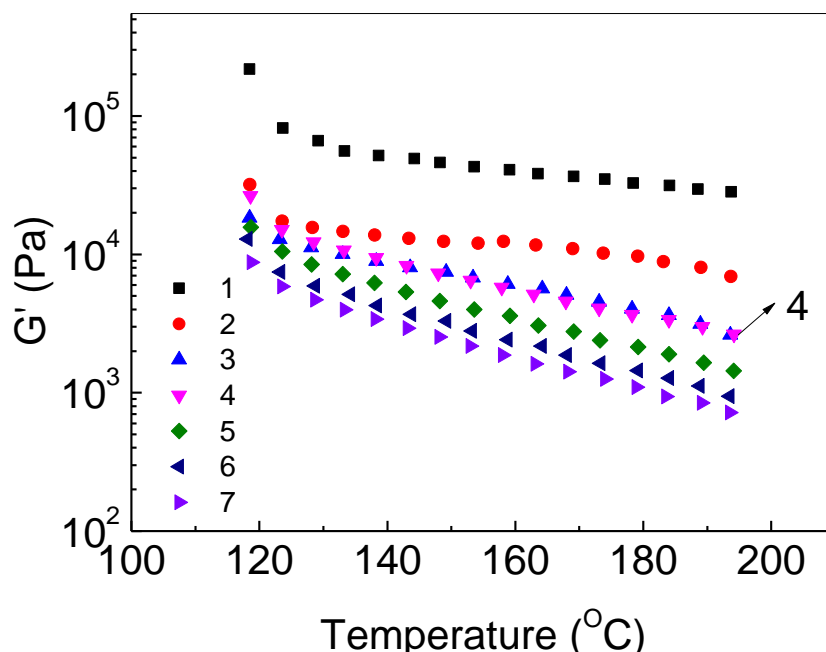


Figure 8.1. The dynamic rheological result of storage module vs temperature for different iPP blends

The temperature sweep of the dynamic rheological test shows a cooling curve for the blends of two different isotactic polypropylenes. From the high temperature to low temperature, the storage modulus tends to be higher as a result of the solidification and crystallization induced by the cooling process. For different blends, they show the same trend. While, it is interesting to find out that for the sample 4, which contains 50 % weight percent of low molecular weight isotactic polypropylene, the cooling curve is almost coincide with sample 3, which contains 30 wt% of low molecular weight isotactic polypropylene. Based on the DSC result, we deduce that there maybe a crystalline morphology structure change when the low molecular weight isotactic polypropylene reached a half part in the blends.

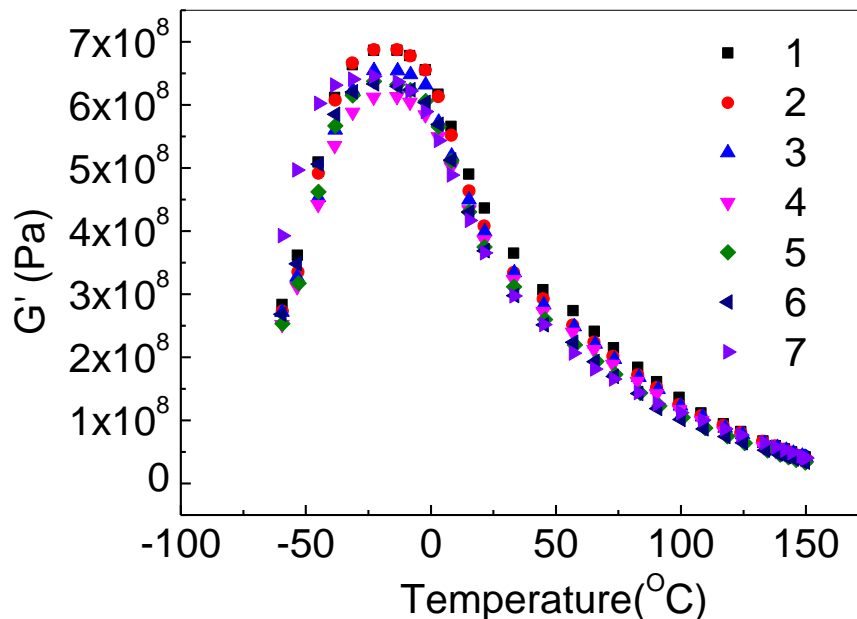


Figure 8.2 The dynamic mechanical thermal analysis result of storage module vs temperature for different iPP blends

It is obviously that the variation of storage modulus with the temperature shows an irregular tendency, especially after the sample 4, which stands for the 50 weight percent of low molecular weight isotactic polypropylene. As can be seen from Figure 8.2, the curve of sample 7 is much higher than sample 4 at relatively low temperature, from -50°C to 0 °C. This fact indicates that with increase of the low molecular weight proportion, the molecular structure of iPP blends tend to complex and hard to be controlled. While, at high temperature, the trend of the curves tends to be regular, this may be due to the increase of the mobility of the molecular chains at higher temperature, and finally result in a uniform composition at the temperature of 150 °C. Based on the dynamic rheological analysis, the sample 4 is worth to be investigated as a result of its irregular structure.

According to the above tests and analysis, the results indicated that sample 4 shows an irregular molecular structure, and the DSC result indicates that the structure is benefit for the crystallization process. Thus it was selected in the next stage to investigate the relationship between structure and properties of modified iPP blends.

8.2.2. The selection of processing parameters

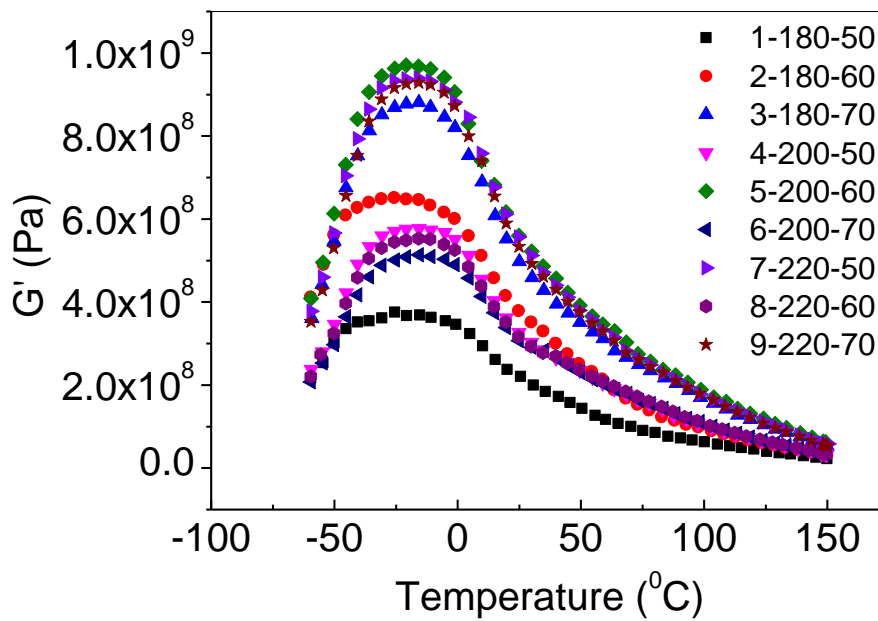
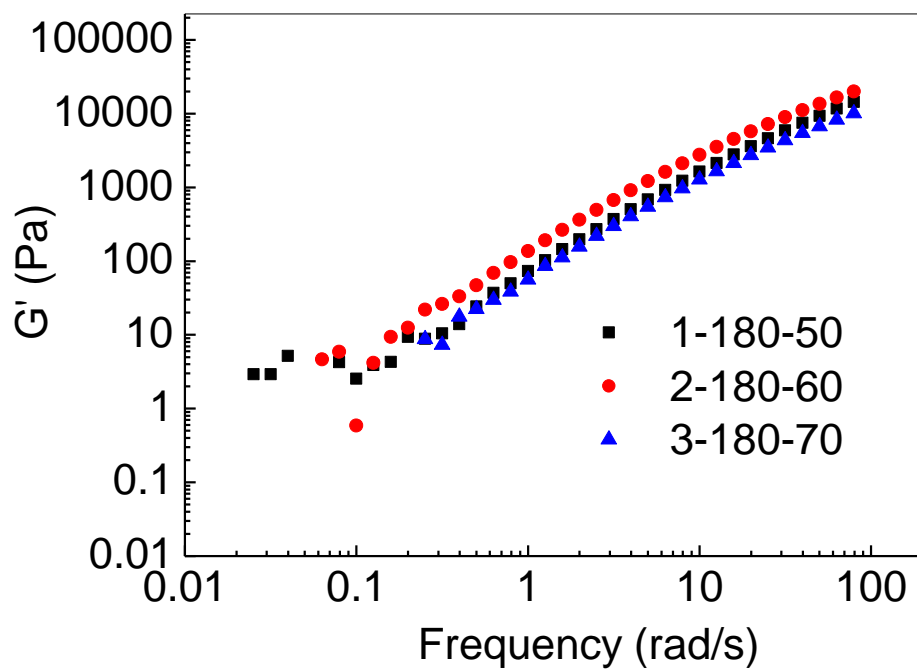


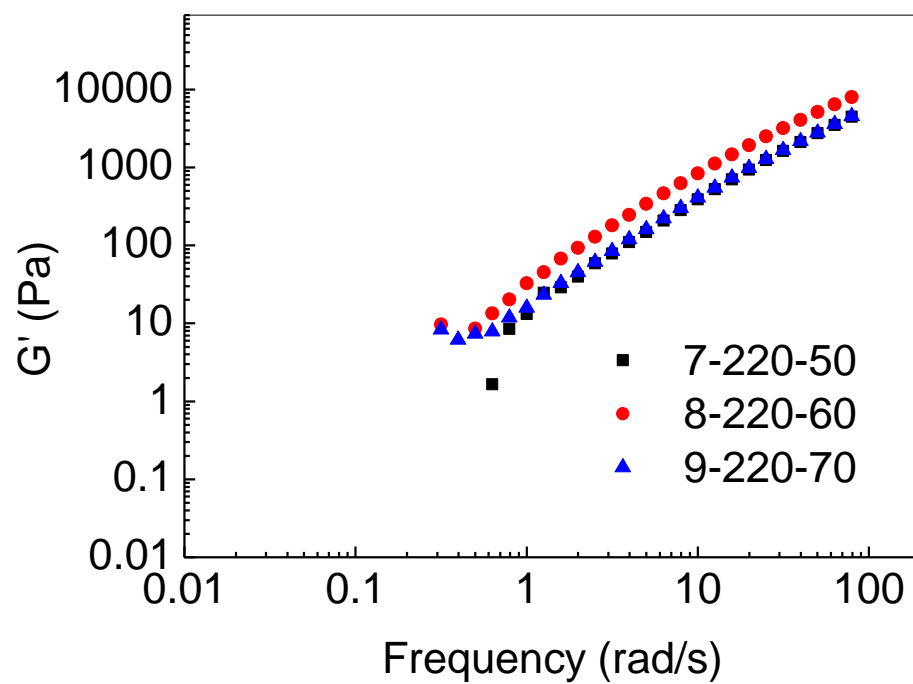
Figure 8.3 The dynamic mechanical thermal analysis result of storage module vs temperature for the effect of different processing parameters of iPP blends.

In this part, three different temperatures 180⁰C, 200⁰C, 220⁰C as well as three different screw speed 50 r/min, 60 r/min, 70 r/min were selected for detect the most suitable processing parameter for iPP blends.

According to the Figure 8.3, the curve of sample 5 shows the highest storage module. The increase of the storage module reflects the decrease of the molecular chain mobility. For the fixed iPP blends, the increase of the storage module was due to the already formed network or tangle point which will be the starting point for the nucleation process of iPP blends crystallization[2-4].

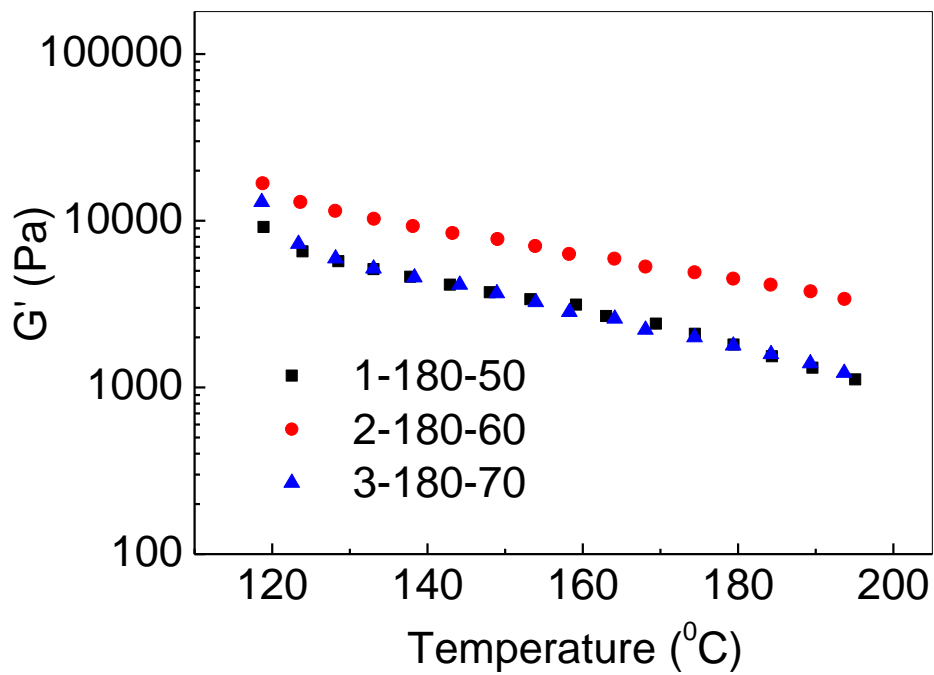


(a)

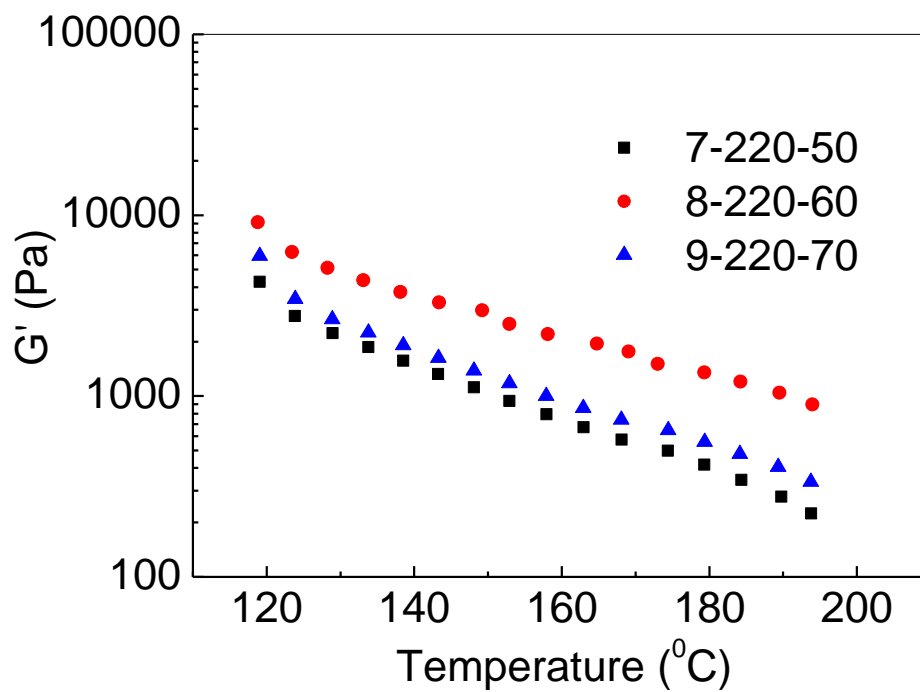


(b)

Figure 8.4 The dynamic rheological result of storage module vs frequency for the effect of different processing parameters on iPP blends.



(a)



(b)

Figure 8.5 The dynamic rheological result of storage module vs temperature for the effect of different processing parameters on iPP blends.

Separate tests were also performed to make sure the selection of the processing parameter 5. Figure 8.4 shows the dynamic rheological tests under the frequency sweep at 200°C, the samples selected were prepared at different temperature and different screw speed. It is quite obviously that even processed at different temperature, when it was fixed at the screw speed of 60r/min, the samples shows the highest storage module than the others. This result was consistent with the dynamic mechanical thermal analysis result of Figure 8.3.

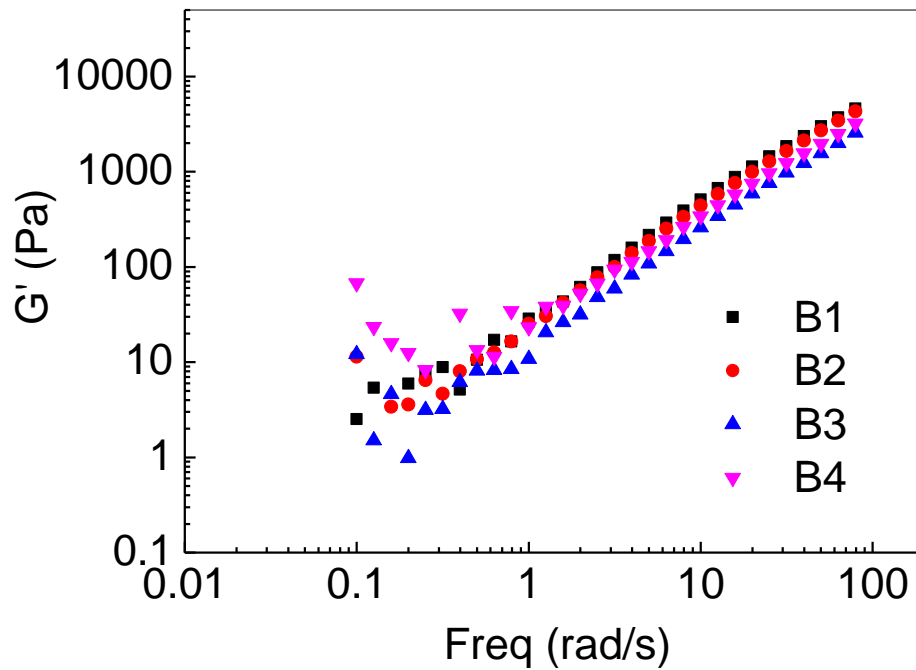
The temperature sweep tests were performed to validate the already got conclusion. As shown in Figure 8.5, it also shows the same trend compared with the frequency sweep. For the samples prepared at the screw speed of 60r/min, its storage modules show the highest value, which was related to block of the already formed crystal structure. It was because of the already formed network or tangle point successfully performed as the nucleating point during the crystallization process.

The results of DSC heating and cooling sweeps were consistent with the dynamic result as shown in Table 8.2. Just seen from the peak temperature, the cooling peak at the sample of parameter 5 shows the highest value, which indicated that it can be crystallized easier than other samples, which may be due to the already formed network or tangle point as we deduced from the dynamic results^[5-7].

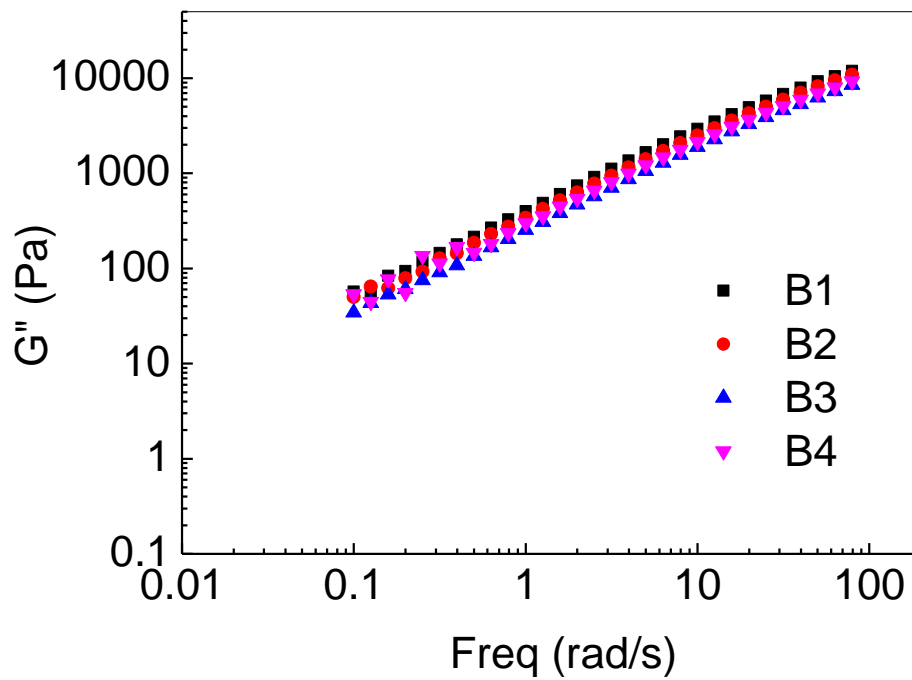
Table 8.2 The DSC results of the samples of different processing parameters

Number	Heating peak(°C)	Cooling peak(°C)
4-200-50	161.39	114.32
5-200-60	162.38	115.14
6-200-70	161.43	114.46

8.2.3. The structure and properties of beta nucleating agent modified polypropylene blends

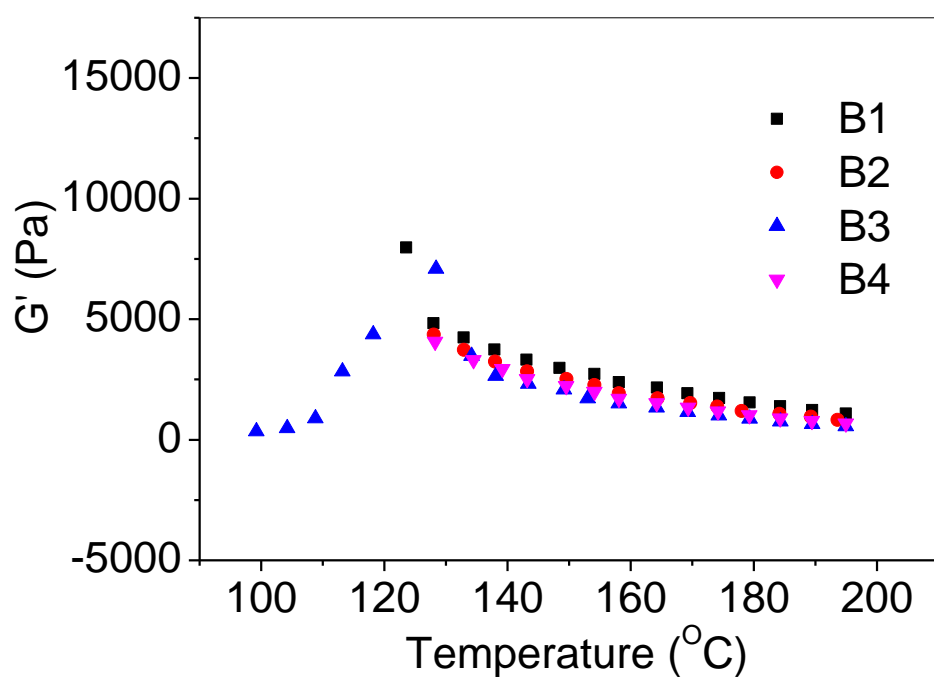


(a)

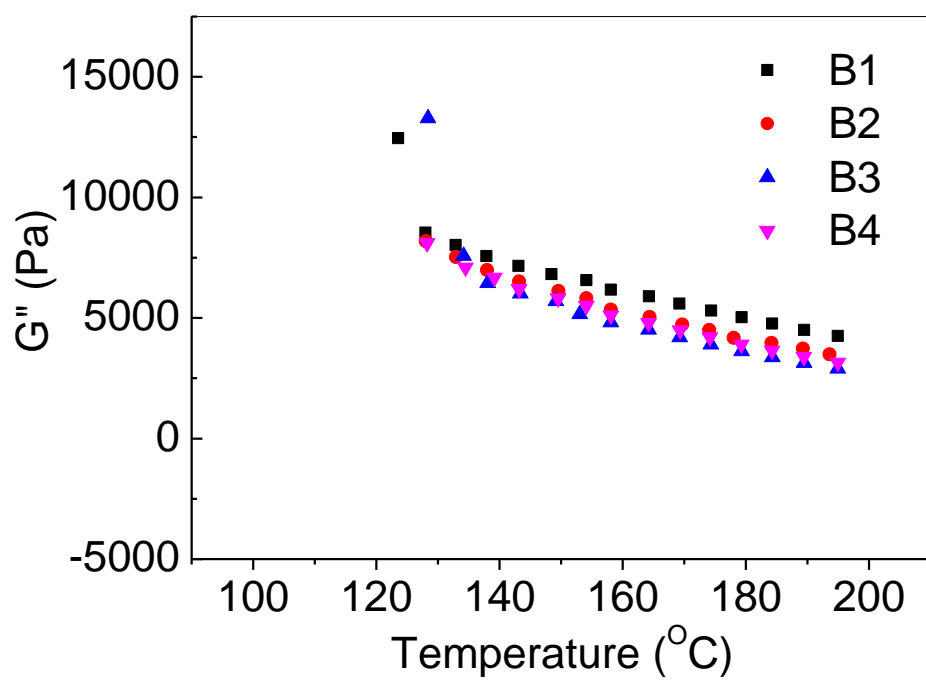


(b)

Figure 8.6 The dynamic rheological result of storage module (a) and lose modules (b) vs frequency for different β NA content modified iPP blends



(a)



(b)

Figure 8.7 The dynamic rheological result of storage module (a) and lose modules (b) vs temperature for different NA content modified iPP blends

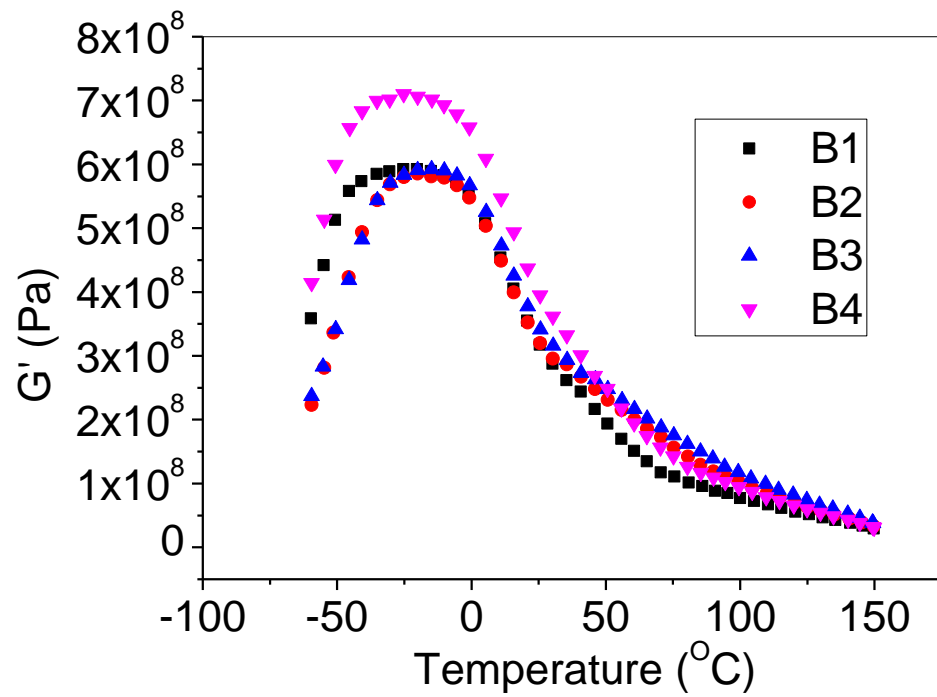
As shown in the Figure 8.6, the storage modules of different content of β NA modified polypropylene verified with increase of the frequency. In the low frequency region, as a result of the existence of low molecular weight content, the viscosity of the matrix decreased, as well as the irregular fluency. While in the high frequency region shows a regular tendency. It is worth mention that, as well as the increase of the nucleating agent content, the storage modules show an obviously turning point at the sample 3. The storage module of sample 4 is higher than sample 3. The lose modules of different content nucleating agent modified polypropylene show the same tendency. As we have previously mentioned, there exist a turning point of the nucleating agent content in β NA modified polypropylene matrix^[8-11]. Now we can conform that the same trend exists in the polypropylene blends, and the turning content in this research is 0.5wt%.

The temperature sweep of dynamic rheology measurement can be used to simulate the crystallization process of polymer at the constant strain, the result of different content NA modified polypropylene was shown in the Figure 8.7. The storage module was improved with increase of the temperature, which was due to the crystallization process occurred in the low temperature region. With the increase of the NA content, the storage modules decreased, and the turning point appears at the content of 0.5wt%. The lose module shows the same trend as the storage modules

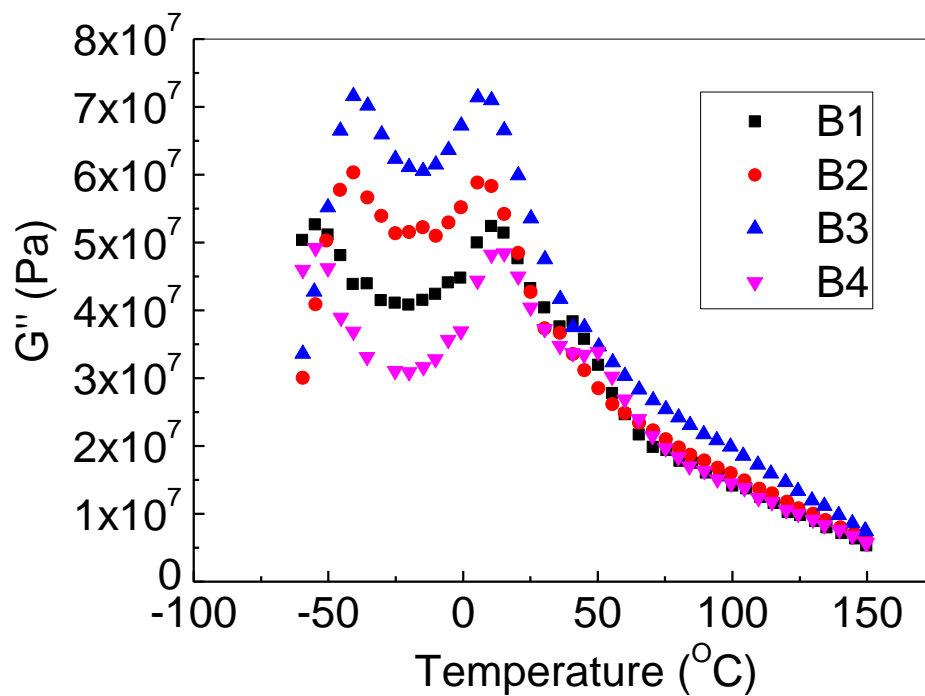
Table 8.3 The DSC results of the samples modified by different β NA content.

Number	Beta Heating peak(°C)	Alpha Heating peak(°C)	Heating Enthalpy(J/g)	Cooling peak(°C)	Cooling Enthalpy(J/g)
B1	152.48	168.64	85.42	122.60	85.77
B2	151.94	167.92	84.31	123.65	84.46
B3	151.84	167.95	83.81	124.21	84.45
B4	151.08	167.68	81.31	124.87	81.80

The crystallization process at the normal condition without the constant strain was investigated by the DSC method. As shown in the Table 8.3, with increase of the NA content, the melting peak of alpha and beta crystals of polypropylene were all show a little



(a)



(b)

Figure 8.8 The dynamic mechanical result of storage module (a) and lose modules (b) vs temperature for different NA content modified iPP blends

decrease. The turning point of melting enthalpy was at the content of 0.5wt%. The cooling peak temperature increased with the content of the NA in polypropylene blends, which was accordance with the heterogeneous nucleation process ^[12-15]. The turning point of cooling enthalpy was also appears at the NA content of 0.5wt%. This fact agrees with the dynamic rheology measurement. All the fact proved that the content of 0.5wt% is a critical point for the NA modified polypropylene blends.

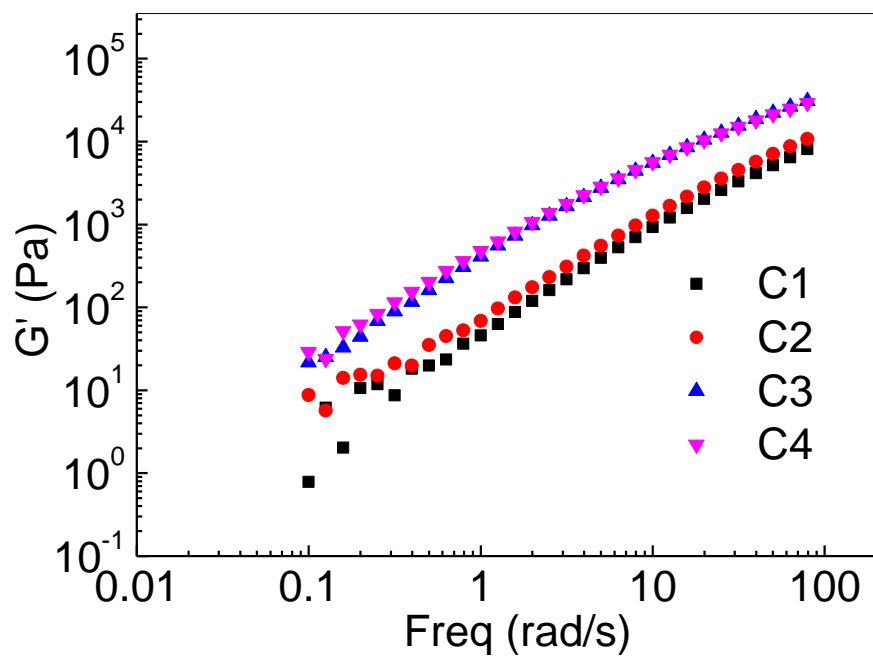
As shown in the Figure 8.8, the change of the storage modules displays three stages. At the lower temperature region, with increase of the NA content, there is no effect on the storage modules before the NA content of 0.5wt%. While after that, the storage modules show an obviouse change. This fact can be explained by the already formed crystalline structure in the NA modified polypropylene. In the temperature region of 0-50⁰C, all the samples show the same trend and finally in the higher temperature there is no difference exist in the storage modules. With increase of the NA content, the lose modules increased, which can be explained by the different crystal structure of beta crystal compared with alpha one. The lowest lose modules displays at the NA content of 0.5wt%.

8.2.4. The structure and properties of carbon nanotube modified polypropylene blends

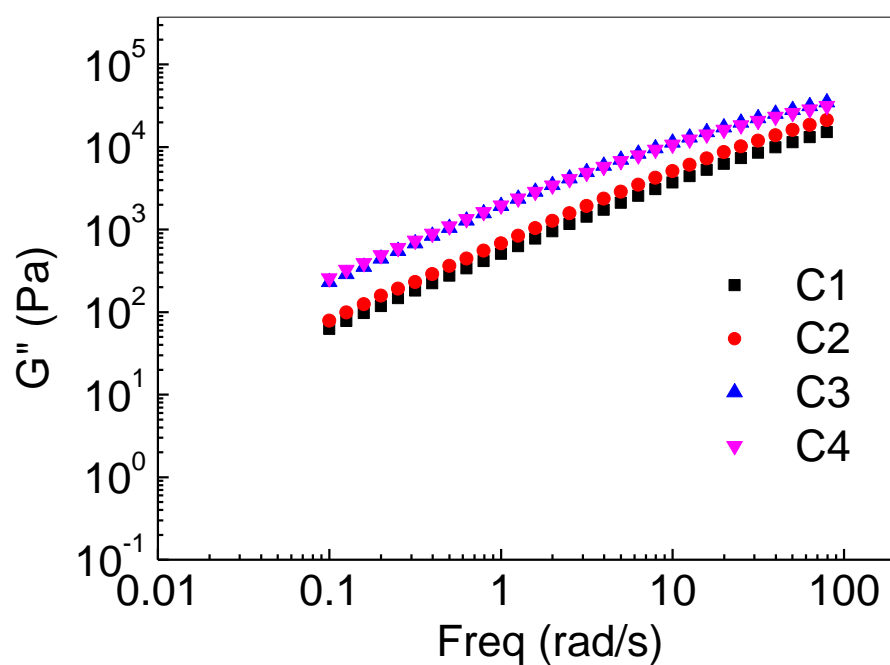
In order to compare with the effect of NA, the carbon nanotube was developed to modified polypropylene as a reference system. Most of the studies agree with the induction of alpha crystal in the carbon nanotube modified polymer system, though some agreed that the low content of carbon nanotube can promote the appearance of beta crystal in polypropylene matrix ^[16-20]. In this study, the carbon nanotube was mainly used to induce the alpha crystal in iPP blends. For the normal crystallization process of iPP blends, the

Table 8.4 The DSC results of the samples of different carbon nanotube content.

Number	Melting peak(°C)	Melting Enthalpy(J/g)	Crystallizaiton peak(°C)	Cooling Enthalpy(J/g)
C1	165.2	85.46	123.29	91.09
C2	164.53	83.59	125.45	89.4
C3	165.39	84.81	126.82	88.1
C4	166.06	88.9	128.43	90.12



(a)



(b)

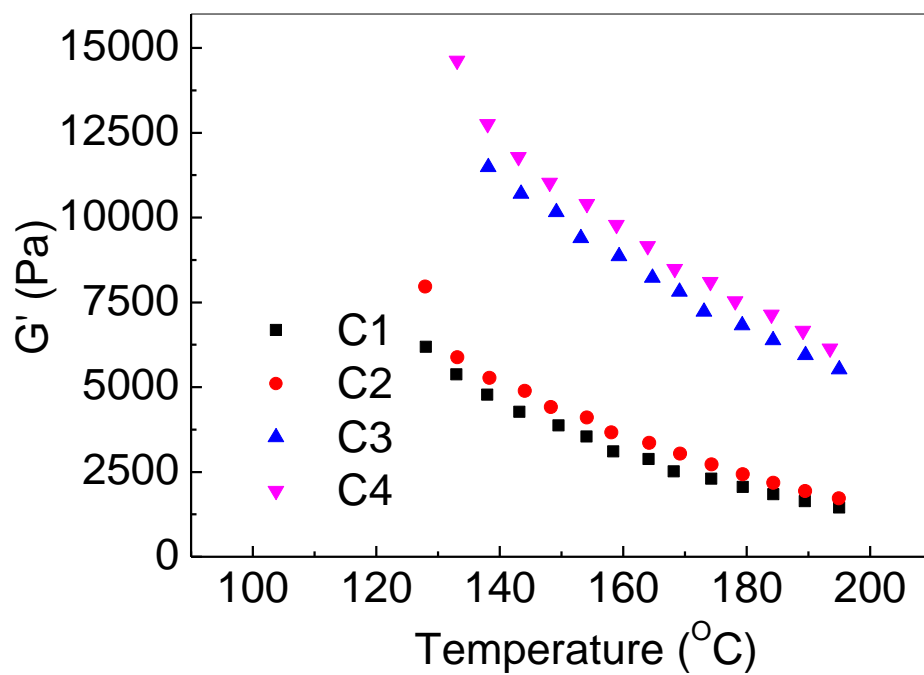
Figure 8.9 The dynamic rheological result of storage module (a) and lose modules (b) vs frequency for different carbon nanotube content modified polypropylene blends

heating peak temperature increase with the carbon nanotube as can be seen in the Table 8.4. The melting enthalpy increases with the carbon nanotube content. The cooling point which indicates the crystallization ability of iPP increased with the carbon nanotube content. The cooling enthalpy shows little change.

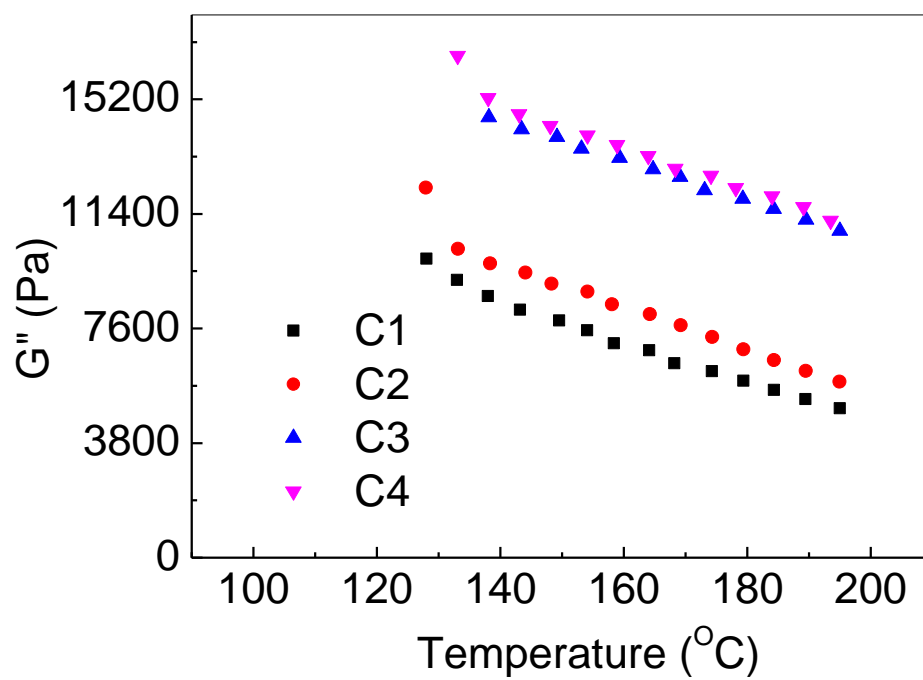
Based on the relationship between storage modules and frequency as shown in Fig 8.9, the carbon nanotube can successfully increase the storage modules of modified iPP blends, which was much different from the NA modified iPP blends. There is no critical point in this system, and the storage modules increased with the improvement of the carbon nanotube content all the time. This fact reflects the different effect of beta and alpha crystal on the structure and properties of polypropylene, as the carbon nanotube can induce alpha crystal in the modified iPP blends. For the loss modules, there is a sharp increase of the loss modules at the content of 0.5wt%, while the same trend can be seen in the storage modules.

The results of temperature sweep of dynamic rheology measurement shows in the Figure 8.10. With increase of the carbon nanotube content, the storage modules increased with decrease of the temperature. The change tendency of carbon nanotube modified polypropylene blends shows an obviously different trend compare with the NA modified iPP blends. Between the low and high content, there exist a turning region, which does not change the trend but obviously change the degree of the tendency.

As the alpha crystal is the normal crystalline morphology in the normal crystallization condition, the carbon nanotube shows no effect on the change of crystalline morphology of iPP blends. For the dynamic mechanical properties in Figure 8.11, increase with the content of carbon nanotube, the storage modules shows almost no change, which was because of the stiffness of the carbon nanotube. For the loss modules vs temperature result, a conclusion can be drawn that the single carbon nanotube modified polypropylene shows little effect on the properties of iPP blends.

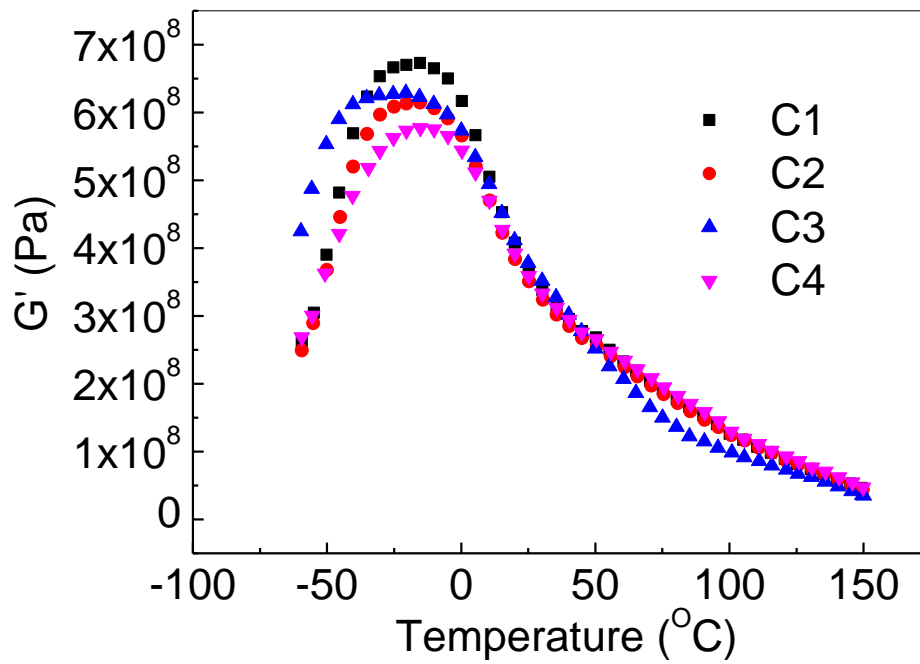


(a)

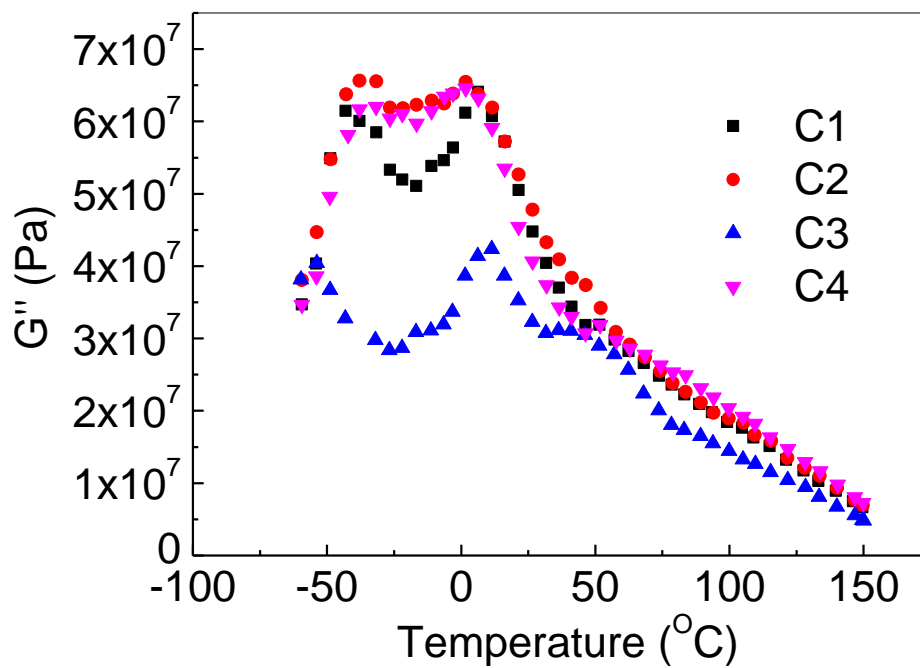


(b)

Figure 8.10 The dynamic rheological result of storage module (a) and lose modules (b) vs temperature for different carbon nanotube content modified polypropylene blends



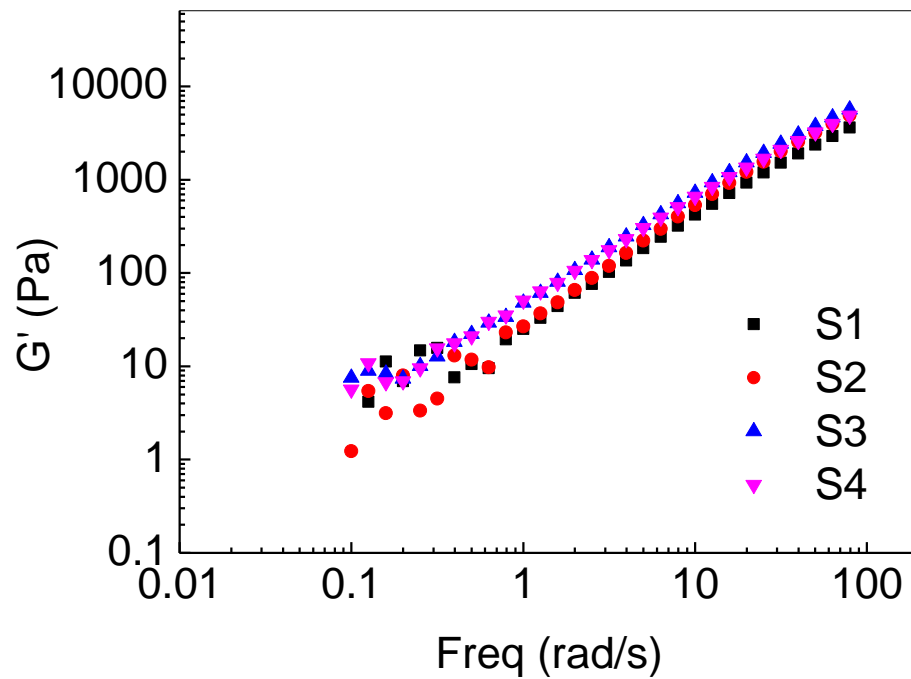
(a)



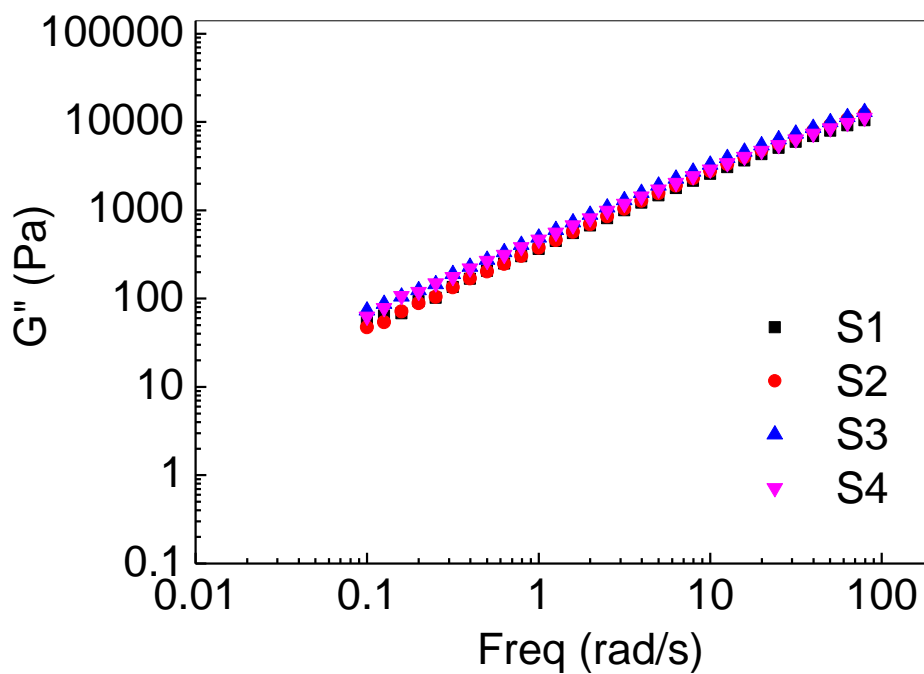
(b)

Figure 8.11 The dynamic mechanical result of storage module (a) and lose modules (b) vs temperature for different carbon nanotube content modified polypropylene blends

8.2.5. The structure and properties of beta nucleating agent supported carbon nanotube modified polypropylene blends



(a)



(b)

Figure 8.12 The dynamic rheological result of storage module (a) and lose modules (b) vs frequency for carbon nanotube supported β NA modified iPP blends

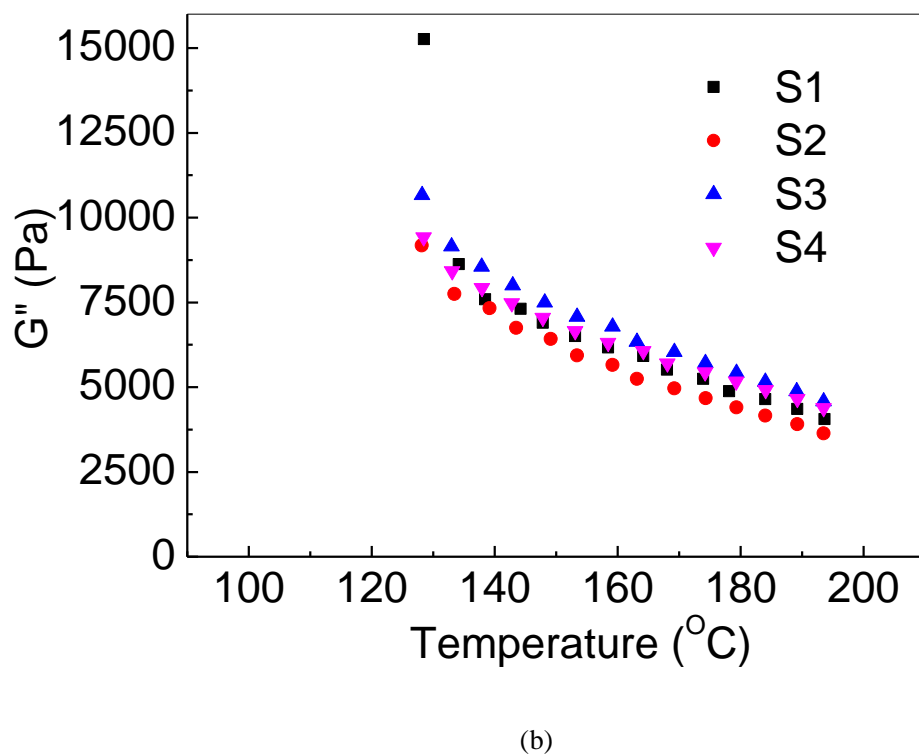
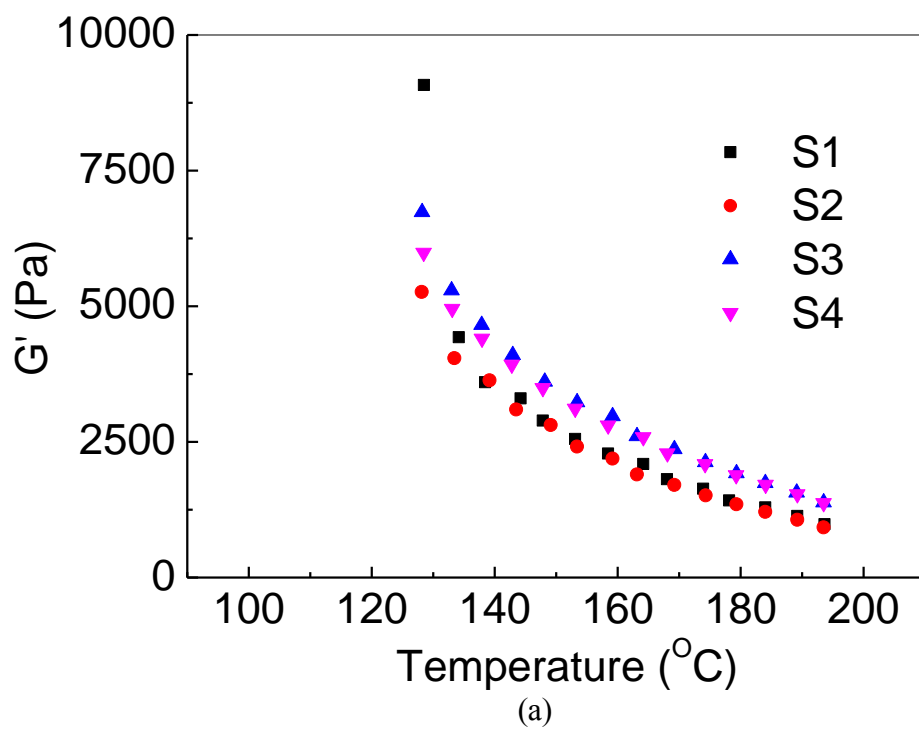


Figure 8.13 The dynamic rheological result of storage modules (a) and lose modules (b) vs temperature for carbon nanotube supported β NA modified iPP blends

In this part, the β NA supported carbon nanotube will be introduced into the iPP blends, and the structure and properties of β NA supported CNTs modified iPP blends will be investigated based on the same portion arrangement of carbon nanotube and NA separately.

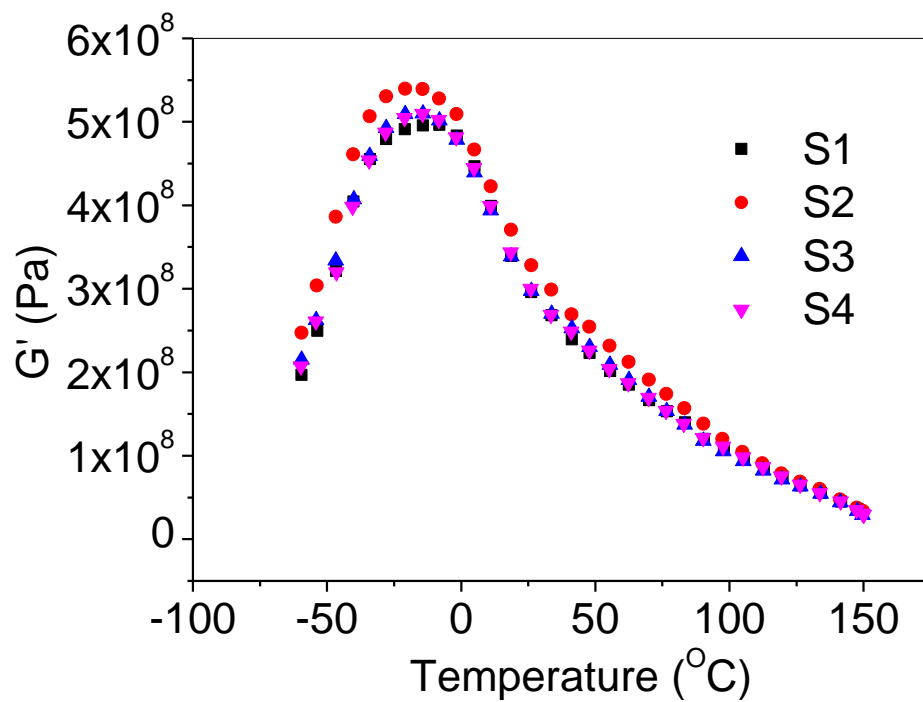
For the result of storage modules vs frequency, excepted for the low frequency region fluctuate as a result of the low molecular weight portion, the storage modules increase with the content of the β NA supported CNTs. For the single NA modified iPP, there exist a turning point of 0.5wt%, while based on the same crystallization process of beta crystal induction, the supported system modified iPP blends show the same trend at the content of 0.5wt%. This fact can be explained that the supporting process has no decrease effect on the inducing ability of beta crystal in iPP blends. This was accordance with the result we have previously published [21].

The change of the loss modules shows little variation, which indicated that there is little reduce of the modules in the β NA supported carbon nanotube modified iPP blends system. This is also the aim of the supported system modified iPP blends and can be used to verify the universality of the already got conclusion.

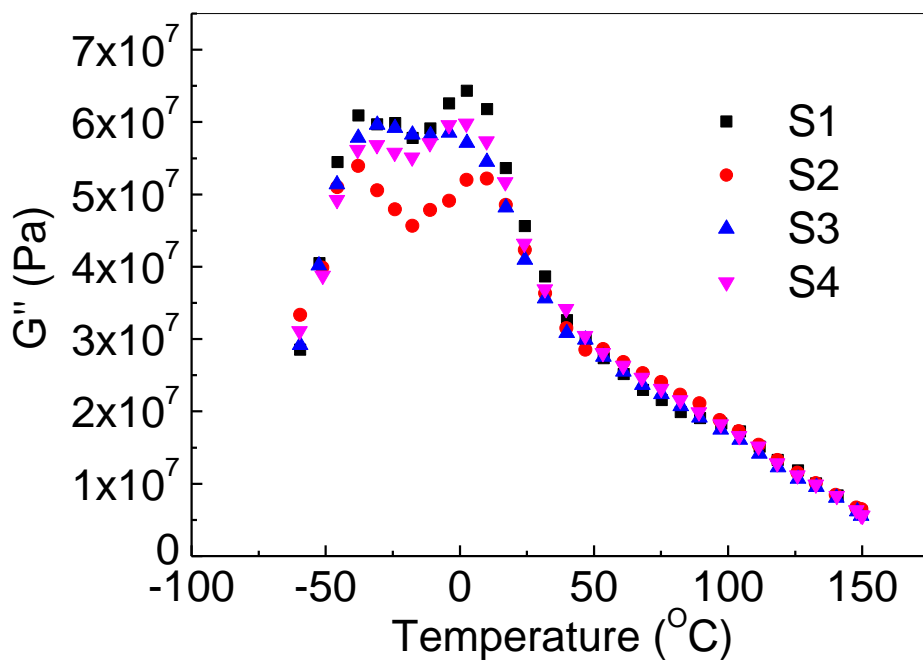
Based on the temperature sweep result as shown in Figure 8.13, the storage modules increase with the decrease of the temperature. At the same time, there is also a turning point at the content of 0.5wt%, and the tendency is more obviously. The variation of the loss modules compared with the storage modules is more flat. There is no fluctuate point exist which indicated that the good induction ability of β NA supported CNTs modified iPP blends.

Table 8.5 The DSC results of the samples under different β NA supported CNTs content.

Number	Heating peak(°C)	Enthalpy(J/g)	Cooling peak(°C)	Enthalpy(J/g)
S1	151.44	84.1	124.59	85.56
S2	151.21	85.4	125.25	85.85
S3	151.04	84.14	125.9	85.44
S4	151.15	81.45	125.65	83



(a)



(b)

Figure 8.14 The dynamic mechanical result of storage module (a) and lose modules (b) vs temperature for carbon nanotube supported β NA modified iPP blends

There is almost no change in the heating peak temperature of different content of β NA supported CNTs modified iPP blends as shown in Table 8.5. The melting enthalpy shows a turning point at 0.5wt%. For the cooling process, there is almost no change in the cooling peak temperature, while the enthalpy of cooling shows a shape change at the turning point of 0.5wt%. This fact indicated that the different content of β NA supported CNTs has almost no effect on the peak temperature of modified iPP blends; while sharply change its enthalpy.

It is interesting to find out that there is almost no change of the storage modules for the different content of β NA supported CNTs modified iPP blends as shown in Figure 8.14, except at the low temperature, a little fluctuate exist at the content of 0.3wt%. For the lose modules, a turning point exist at the content of 0.5wt% and it was only exit in the low temperature.

8.3 Conclusion

The conclusion can be draw as follow,

First of all, based on the melting and cooling behaviours, dynamic mechanical and rheological properties analysis, the suitable aproportion for the iPP blends is 50wt%:50wt%.

Then, based on the melting and cooling behaviours, dynamic mechanical and rheological properties analysis, the suitable processing parameters is 200°C and the srcew speed is 200rpm.

The beta nucleating agent can successfully induce beta crystal in modified iPP blends and the turning point of the properties appears at the content of 0.5wt%. Carbon nanotube mainly induce alpha crystal in modified iPP blends, and for the properties of carbon nanotube modified iPP blends, there is no turning point because of its dominant alpha crystalline morphology. The β NA supported carbon nanotube shows good induction ability than the single β NA or single carbon nanotube, there is also a turning point exist at the content of 0.5wt%

8.4 References

- [1] N. Okui, S. Umemoto, R. Kawano and A. Mamun. Lecture Notes in Physics, 2007, 714, 391.
- [2] C. Hadinata, D. Boos, C. Gabriel, E. Wassner, M. Rullmann, N. Kao, M. Laun, Journal of Rheology, 2007, 51, 195
- [3] K. Yang, R. Ozisik, Polymer, 2006, 47, 2849
- [4] K. Koyama, Nihon Reoroji Gakkaishi, 2006, 34, 267
- [5] E. Bilotti, H. R. Fischer, T. Peijs, Journal of Applied Polymer Science, 2008, 107, 1116
- [6] Y.F. Zhang, Z. Xin, Journal of Polymer Science Part B-Polymer Physics, 2007, 45, 590
- [7] W.D. Lee, S. S. Im, Journal of Polymer Science Part B-Polymer Physics, 2007, 45, 28-
- [8] H. Tsuji, H. Takai and S. K. Saha, Polymer, 2006, 47, 3826
- [9] F. Perrin-Sarazin, M. T. Ton-That, M. N. Bureau and J. Denault, Polymer, 2005, 46, 11624
- [10] A. Menyhard, J. Varga, A. Liber and G. Belina, European Polymer Journal, 2005, 41, 669
- [11] H. Bai, Y. Wang, B. Song and L. Han, Journal of Applied Polymer Science, 2008, 108, 3270
- [12] D.G. Georgieva, M. E. Kuil, T. H. Oosterkamp, H. W. Zandbergen and J. P. Abrahams, Acta Crystallographica Section D-Biological Crystallography, 2007, 63, 564
- [13] H. Tsuji, H. Takai and S. K. Saha, Polymer, 2006, 47, 3826
- [14] J.H. Chen and Y. D. Chiou, Journal of Polymer Science Part B-Polymer Physics, 2006, 44, 2122
- [15] M. Avella, S. Cosco, M. L. Di Lorenzo, E. Di Pace, M. E. Errico and G. Gentile, European Polymer Journal, 2006, 42, 1548
- [16] A.R. Bhattecharyya, T.V. Sreekumar, T. Liu, S. Kumar, L.M. Ericson, Polymer, 2003, 44, 2373
- [17] M.K. Seo, J.R. Lee, S. Park, J Mater Sci Eng A, 2005, 404, 79
- [18] Wu DF, Sun YR, Wu L, Zhang M, J Appl Polym Sci, 2008, 108, 1506
- [19] G.W Lee, S Jagannathan, H.G. Chae, M.L. Minus, S. Kuma, Polyme, 2008, 49, 1831
- [20] D. Bikiaris, A. Vassiliou, K. Chrissafis, K.M. Pataskevopoulos, A. Jannakoudakis, A. Docoslis Polym Degrad Stab, 2008, 93, 952
- [21] S.W. Wang, W. Yang, R.Y. Bao, B. Wang, B.H. Xie, M.B. Yang, Colloid and Polymer Science, 2010, 288, 681

Chapter 9 conclusion

Polypropylene is one of the most important general used plastic materials. Different kinds of nucleating agents were added to the polypropylene as well as the controlled rheology polypropylene matrix. Mechanical properties as well as fracture behaviour, crystalline morphology was discussed. The effect of different kinds of nucleating agent, different nucleating agent content on the crystalline structure and mechanical properties of polypropylene was further explored. A kind of filler called fiber supported nucleating agent was introduced to the modification of polypropylene, and the impact resistance of fiber supported nucleating agent modified polypropylene greatly increased. The mechanism of the large increased impact resistance was attributed to the formation of beta transcrystalline morphology in the fiber supported nucleating agent polypropylene matrix.

With the addition of NA, the crystallinity of both α and β modified CPP increased remarkably and the β NA successfully induced the transition of CPP crystal from α form to β form. The w_e values of CPP added with α NA of different amount were all lower than that of pure CPP. The w_e values increased with further increase of α NA amount. However, the βw_p was the highest at the lowest α NA amount (0.1 wt %), while decreased with further increasing amount. The variation of w_{en} and $\beta''w_{pn}$ with increasing NA content for α NA nucleated PP was absolutely same as those of w_e and w_{ey} did, while the $\beta'w_{py}$ for α NA nucleated PP gradually decreased. The plastic work decreased with increasing crystallinity in α NA nucleated CPP. Both w_e and βw_p showed similar trend of variation with increasing amount of β NA. Only the plastic component before yielding for β NA nucleated PP had the same variation as βw_p . While the plastic work decreased first and then recovered close to that of pure CPP, with increasing crystallinity for β NA nucleated CPP. The variation of K_β for NA nucleated CPP was almost same as that of w_e , indicating that elevating amount of NA leading to the increasing of β content and consequently improved fracture resistance. The difference in the variation of βw_p value in CPP filled with β NA may be due to the conversion of crystal form.

To explore the structure and properties of CRPP, three different peroxides were used. The capillary rheology measurement indicates that the DMDEHPH induced CRPP is preferably controllable in a relatively low shear rate range. DMDEHPH induced CRPP exhibits the highest mechanical properties. DMDEHPH induced CRPP shows the highest crystallinity, which can be used to explain the superior mechanical properties of DMDEHPH induced iPP. All the three CRPP samples show a lower PI value comparing with the virgin iPP, indicating the improved narrowness of the iPP molecular weight distribution.

The effects of different β NAs, different DCP content and various β NA content on the crystalline morphology of CRPP were studied. The β crystalline melting peaks of WBG-II and TMB-5 nucleated CRPP are clearly shown and shift to a low temperature compared with unnucleated CRPP. The intensity of the β -crystal diffraction peak of TMB-5 modified CRPP is larger than WBG-II. With the increase of DCP content, the melting temperature of α -crystals increases, and the melting peak of β -crystals is visible in CRPP nucleated with 0.3wt% content of TMB-5. At the critical point of 0.1wt% DCP, the total crystallinity index of CRPP reaches a maximum value and the relative intensity of diffraction peaks for α and β -crystals are much higher than for other contents. With increase of the TMB-5 content, the melting peak of β -crystals appears on the DSC heating curves of CRPP prepared using 0.1wt% DCP. With the addition of TMB-5, the maximum value of total crystallinity is reached at a mass fraction of 0.5%. Also, the relative content of β -crystals achieves the maximum value at this point.

A novel approach to largely improve the impact toughness without significant loss of the stiffness and strength of iPP composites was accomplished. The prepared MWCNT supported β NA can successfully enhance the β nucleating ability of β NA and can induce higher content of β phase of iPP and significantly improve the impact toughness of iPP based composites with little loss of stiffness and strength.

The beta transcrystalline morphology can be formed in both iPP/single fiber micro-composites and β NA supported CNTs modified iPP injection molded samples. The seven times improvement of impact resistance of β NA supported CNTs filled iPP injection molded samples were attributed to the formed interfacial beta transcrystallinity.

Based on the melting and cooling behaviours, dynamic mechanical and rheological properties analysis, the suitable proportion for the iPP blends is 50wt%:50wt%, the suitable processing parameters is 200°C and the screw speed is 200rpm. The beta nucleating agent can successfully induce beta crystal in modified iPP blends and the turning point of the properties appears at the content of 0.5wt%. Carbon nanotube mainly induce alpha crystal in modified iPP blends, and for the properties of carbon nanotube modified iPP blends, there is no turning point because of its dominant alpha crystalline morphology. The β NA supported carbon nanotube shows good induction ability than the single β NA or single carbon nanotube, there is also a turning point exist at the content of 0.5wt%

Acknowledgements

First and foremost I would like to express my best gratitude to my supervisors Prof. Guo-hua HU, and Prof. Ming-bo YANG. Their creative ideas of research, patient guidance and consistent encouragement push and inspire me to finish my PhD study. I also would like to express my great appreciation to Dr. Sandrine HOPPE and Prof. Wei Yang for providing much help and suggestions during my PhD study.

I am greatly thankful to my mates both in Chinese and French groups, Prof. Bang-hu XIE, Jian-min FENG, Zheng-ying LIU, Bo YIN, Yan-mei LI, who kindly helped me a lot during my PhD study. Thank my friends Guan GONG, Gui-fang SHAN, Xue-gang TANG, Chao-lu YIN, Rui-ying BAO, Yuan-ming ZHAI, Yu WANG, Lin ZHOU, Ya-jun XU, Li XIANG, Ben WANG, Man LUO, Xiao XIAO, Jin-biao BAO, Zheng-hui LI, Pin LV, Yuan FANG, Xiao-bo SONG, Jin-bai ZHANG, Fei MAO so much, and they have great contributions to my wonderful life both in China and France.

This study could not been finished without the generous financial support from the National Natural Science Foundation of China (Grant No. 50503014, 50533050, 20734005, 50973074), Program for New Century Excellent Talents in University (NCET-08-0382), Doctoral Research Foundation granted by the National Ministry of Education, China (Grant No. 20060610029) ,the Opening Project of The Key Laboratory of Polymer Processing Engineering, Ministry of Education, China and the Special Funds for Major Basic Research (Grant No: 2005CB623808). Thank China Scholarship Council for supporting my studying in France. Finally, I would like to express my great appreciation to my parents for their understanding and encouragement which support me to finish my PhD study.

List of articles published during the thesis

1. **Shi-Wei Wang**, Wei Yang*, Guan Gong, Bang-Hu Xie, Zheng-Ying Liu, Ming-Bo Yang*, Effect of α and β nucleating agents on the fracture behavior of polypropylene-co-ethylene(CPP), Journal of Applied Polymer Science, 2008, 108(1):591-597
2. **Shi-Wei Wang**, Wei Yang*, Ya-Jun Xu, Bang-Hu Xie, Ming-Bo Yang, Xiang-Fang Peng , Crystalline morphology of β nucleated controlled rheology polypropylene , Polymer Testing, 2008, 27 : 638-644.
3. **Shi-Wei Wang**, Wei Yang*, Rui-Ying Bao, Ben Wang, Bang-Hu Xie, Ming-Bo Yang, The enhanced nucleating ability of carbon nanotube-supported β -nucleating agent in isotactic polypropylene, Colloid and Polymer Science , 2010, 288:681-688.
4. **Shi-Wei Wang**, Sandrine Hoppe*, Mingbo Yang, Effect of nucleating fillers on the structure and properties of Polypropylene blends, Polymer-Plastics Technology and Engineering, in press.
5. Jie Li, **Shi-Wei Wang**, Wei Yang*, Bang-Hu Xie, Ming-Bo Yang, Mechanical, Thermal Characteristics and Morphology of Polyamide 6/Isotactic Polypropylene Blends in the Presence of β Nucleating Agent, Journal of Applied Polymer Science, 2011, 121, 554-562.
6. Jie Li, **Shi-Wei Wang**, Ke-Jun Zhan, Wei Yang*, Bang-Hu Xie, Ming-Bo Yang, Effect of Carbon Nanotube-supported β Nucleating Agent on the Thermal Properties, Morphology and Mechanical Properties of Polyamide 6/Isotactic Polypropylene Blends, Journal of Applied Polymer Science, doi: 10.1002/app.35137

**AUTORISATION DE SOUTENANCE
DU DOCTORAT DE L'UNIVERSITE DE LORRAINE**

o0o

VU LES RAPPORTS ETABLIS PAR :

Monsieur BOUQUEY Michel, Professeur, ECPM-Université de Strasbourg,

Monsieur LIU Xiao-Bo, Professeur, University of Electronic Science and Technology of China.

L'Administrateur Provisoire de l'Université de Lorraine, autorise :

Monsieur WANG Shi-Wei

à soutenir devant un jury de l'UNIVERSITE DE LORRAINE, une thèse intitulée :

"Controlling the structure and properties of toughened and reinforced isotactic polypropylene"

en vue de l'obtention du titre de :

DOCTEUR DE L'UNIVERSITE DE LORRAINE


Intitulé du doctorat : **"Génie des Procédés et des Produits"**

Fait à Vandoeuvre, le **2 Avril 2012**

Pour l'Administrateur Provisoire par délégation,

Le Chargé de Mission,

François LAURENT



TITRE

Contrôle des structures et des propriétés d'un polypropylène isotactique

RESUME

En tant que polymère de grande diffusion, les applications du polypropylène isotactique (PP) sont limitées par sa faible résistance au choc. D'après la relation structure – propriétés, sa résistance au choc peut être améliorée en contrôlant sa structure. Dans ces travaux, différents types d'agents nucléants ont été utilisés pour promouvoir la formation des cristaux de type bêta et de mélanges de deux PP de masses molaires différentes. Les propriétés mécaniques, le comportement à la rupture, et la morphologie cristalline ont été étudiés. Les influences du type et de la teneur en peroxyde et agent nucléant sur la morphologie cristalline et les propriétés mécaniques ont aussi été explorées. Un agent nucléant supporté sur des nanotubes de carbone multi-parois (MWCNT) a été utilisé pour modifier la structure cristalline du PP, ce qui a permis d'augmenter sa résistance au choc 7 fois comparée à celle du PP vierge et 3 fois comparée à celle du PP cristallisé en phase bêta. Cette importante augmentation en résistance au choc peut être attribuée à la formation des trans-cristaux de type bêta qui est favorisée par l'agent nucléant supporté sur les MWCNT.

MOTS-CLES

Polypropylène, agent nucléant, polypropylène à rhéologie contrôlée, résistance au choc.

TITLE

Controlling the structure and properties of toughened isotactic polypropylene

ABSTRACT

As a commodity polymer, the applications of isotactic polypropylene (PP) are limited by its low impact strength. Based on the structure-property relationship, its impact strength could be improved by controlling its structure. In this study, different kinds of nucleating agents were used to promote the formation of beta crystals of PP as well as mixtures of two PPs of different molar masses. The mechanical properties, fracture behaviour, and crystalline morphology were investigated. The effects of the type and content of the peroxide and nucleating agent on the crystalline structure and mechanical properties of the PP were also explored. A multi-walled carbon nanotube (MWCNT) supported nucleating agent was introduced to modify the crystalline structure of PP and the impact strength of the resulting PP was 7 times that of the pure PP and more than 3 times that of β nucleated PP. The large increase in the impact strength was attributed to the formation of beta transcrystalline morphology which was promoted by the MWCT supported nucleating agent.

KEY WORDS

Polypropylene, nucleating agent, controlled rheology polypropylene, impact resistance.